12-2010

Human Decomposition Ecology at the University of Tennessee Anthropology Research Facility

Franklin Edward Damann
fedamann@gmail.com

To the Graduate Council:

I am submitting herewith a dissertation written by Franklin Edward Damann entitled "Human Decomposition Ecology at the University of Tennessee Anthropology Research Facility." I have examined the final electronic copy of this dissertation for form and content and recommend that it be accepted in partial fulfillment of the requirements for the degree of Doctor of Philosophy, with a major in Anthropology.

Walter Klippel, Major Professor

We have read this dissertation and recommend its acceptance:

Lee M. Jantz, Arpad A. Vass, Steven Wilhelm

Accepted for the Council:

Carolyn R. Hodges

Vice Provost and Dean of the Graduate School

(Original signatures are on file with official student records.)

To the Graduate Council:

I am submitting herewith a dissertation written by Franklin Edward Damann entitled "Human Decomposition Ecology at the University of Tennessee Anthropology Research Facility." I have examined the final electronic copy of this dissertation for form and content and recommend that it be accepted in partial fulfillment of the requirements for the degree of Doctor of Philosophy, with a major in Anthropology.

Walter E. Klippel, Major Professor

We have read this dissertation
and recommend its acceptance:

Lee Meadows Jantz

Arpad Vass

Steven Wilhelm

Accepted for the Council:

Carolyn R. Hodges
Vice Provost and Dean of the Graduate School

(Original signatures are on file with official student records.)

HUMAN DECOMPOSITION ECOLOGY AT THE UNIVERSITY OF TENNESSEE ANTHROPOLOGY RESEARCH FACILITY

A Dissertation Presented for the
Doctor of Philosophy
Degree
The University of Tennessee, Knoxville

Franklin Edward Damann
December 2010

ACKNOWLEDGMENTS

Firstly, I would like to thank the members of my Doctoral Committee for strengthening the research though mentorship, and most importantly accepting the work. A majority of the laboratory work would not have been accomplished if not for the support of Aphantree Tanittiasong who provided daily bench work, Alice Layton of the UT Center for Biotechnology who provided next-generation sequencing, Anita Biernacki of Microbial Insights who provided DGGE results, and a special thank you to Danielle Henning-McLoud, Program Manager for Research and Development in Forensic Anthropology of the National Institute of Justice, without her support of the research and grant management skills this work would not have occurred. To those that have helped in one fashion or another, providing guidance, advice, and laughs along the way: Stephanie Young, Derek Benedix, Brad Adams, Megan York, Tom and Mary Holland, John Byrd, David Carter, Miranda Jans, Odile Lorielle, Mike Coble, and all members of the AFDIL staff and administration for allowing an anthropologist into your laboratories. To Cam and Bud who provide the unconditional support, especially when this book report was the furthest from our minds. And lastly, to Ambrose Bierce for providing a most fitting definition:

> Edible, adj., Good to eat, and wholesome to digest, as a worm to a toad, a
> toad to a snake, a snake to a pig, a pig to a man, and a man to a worm.

In light of the incredible assistance received throughout this work, it should be mentioned that the results of the analyses and conclusions reached including the mistakes are solely those of the author.

ABSTRACT

The University of Tennessee Anthropology Research Facility (ARF) is well known for its unique history as a site of human decomposition research in a natural environment. It has been integral to our understanding of the processes of human decomposition. Over the last 30 years 1,089 bodies have decomposed at this 1.28 acre facility, producing a density of 850 corpses per acre of land. This project evaluated the abiotic and biotic characteristics of the soil exposed to various levels of human decomposition in order to determine the effect on the physicochemical properties and the indigenous bacterial communities.

Specifically, 75 soil samples were taken to determine abiotic properties. A biological matrix was generated for the 40 samples inside the facility based on sequencing of the 16S rDNA gene. The identified taxonomy was evaluated for differences among decomposition bins and taxa.

Results of the abiotic soil properties demonstrated few differences among the predefined bins of decomposition density. Significant differences were observed between samples inside the facility to the negative control, and to those samples taken below actively decomposing corpses. When taken together, the abiotic data demonstrated a temporal shift away from control, with the greatest deviation at 18 to 24 months. After which time, the samples became more similar to control samples.

Similarly, the biotic data remained concordant with the abiotic data, but demonstrated significant differences between the areas of high decomposition to those with no history of decomposition. The high decomposition bins were marked by high levels of chemoorganotrophic and sulfate-reducing bacteria, and a reduction in Acidobacteria, indicating a

change in the community of underlying bacteria in response to carcass enrichment and ammonification of the soil.

Thirty years of decomposition research at the ARF has forced a shift in the underlying bacterial community in response to the enrichment of the soil with increased nitrogen and carbon-containing compounds. The baseline data presented in this work provides a control dataset for further exploration regarding the biogeochemical relationships among microbial organisms, soil characteristics, and cadaver decomposition. Within this relationship exists the potential for developing new models relating to postmortem interval estimation and clandestine grave location.

PREFACE

A portion of this project was supported by Award No. 2008-DN-BX-K165 awarded by the National Institute of Justice, Office of Justice Programs, U.S. Department of Justice. The opinions, findings, and conclusions expressed in this presentation are those of the authors and do not necessarily reflect those of either the Department of Justice or the Department of Defense.

TABLE OF CONTENTS

LIST OF TABLES

LIST OF FIGURES

CHAPTER 1: INTRODUCTION

The ecology of human decomposition is a complex series of occurrences that are driven by biotic and abiotic processes. Among the postmortem biotic processes, the associated microbial communities are significant modulators. Enteric microbes initiate putrefaction, which are then replaced by edaphic microorganisms during late stage decomposition, eliciting micro- and macroscopic destruction of soft and bone tissue. Microbially-mediated human decomposition is a significant biologic function that facilitates the transformation of a once living organism to a resource of energy and nutrients that become available to the surrounding landscape.

In general terms of organic decomposition, biologic modification in the terrestrial landscape is accomplished primarily by edaphic fungi and bacteria. Their activity accounts for approximately 90% of the mobilization of carbon and nitrogen in an ecosystem (Swift et al. 1979); in fact, decomposition is second only to photosynthesis for the cycling of nutrients and energy in an ecosystem (McGuire and Treseder 2010). It is no wonder that "microbes are essential in the decay and recycling of materials important to life (e.g., carbon, nitrogen, etc.) by transforming the detritus of human society" (Prostgate 2000:244) – including ourselves.

The traditional paradigm of decomposition and nutrient cycling comes from reviews of litter decay in soil science and basic ecology texts (Burges 1967; Swift et al. 1979; Ricklefs 1997; Paul 2007), while less attention had been placed on functions inherent to carcass decay. Awareness of carcass enrichment of soil and its relationship to microbiology and ecosystem function has increased in recent years (Putman 1978a; Putman 1978b; Towne 2000; Hopkins et al. 2000; Dent et al. 2004; Carter et al. 2007; Benninger et al. 2008; Carter et al. 2010).

Functionally, decomposition of organic material by microbes occurs primarily by catalysis, where complex macromolecules are broken down into simple organic structures, and by the leaching of those reduced compounds into the surrounding environment. Microbial activity is highly specialized for recycling sequestered organic debris. In order to do so, each species contains a suite of genes for carrying out specific functions. In any ecosystem containing multiple species and, by extension, multiple species-specific functions, interactions among the inhabitants of any microbial community will occur by mutualism, commensalism, or competition. One example of microbial interaction takes place in the human gut microbiome, where two different species interact through mutualism in order to acquire an appropriate nutrient source. In this scenario the amino acid arginine, which is present in many foods of the human diet is transformed by enzymes of *Enterococcus faecalis* to ornithine. Only then can *Escherichia coli* convert ornithine to putrescine, which can then be used by both *E. faecalis* and *E. coli* (Wilson 2008). This interaction is of particular note as putrescine is one of many volatile organic compounds released during corporal decomposition (Gill-King 1997; Vass et al. 2002, 2008). The level of interaction and type of competition for access to the available resource will ultimately drive the level of microbial biodiversity.

Decomposition in the terrestrial setting not only involves the enteric organism, but also includes the diverse communities of the surrounding soil matrix, where microbial activity is highly instrumental in the breakdown of organic material (McGuire and Treseder 2010). In this relationship soil receives minerals and nutrients released from a carcass that then become reincorporated as living biomass or released into the atmosphere as carbon dioxide (CO_2) (Putman 1978a), and other volatile organic compounds (Vass et al. 1992; 2002; 2004; 2008). The cadaver-soil interface has a highly complex ecology, and should be an important area of

investigation for identifying potential changes in microbial diversity as the edaphic and enteric organisms use the same resource.

At the cadaver-soil interface there is an enormous quantity of bacterial species. An adult human is estimated to have 10^{14} prokaryotic cells primarily located in the gastrointestinal tract, oral cavity, vagina, and skin (Wilson 2008). Amazingly, this measure is an order of magnitude greater than the number eukaryotic cells throughout the entire body. If these numbers of bacteria were not enough to categorize, a single gram of soil has been estimated to have approximately 10^{9} prokaryotic cells (Paul 2007), keeping in mind that this number excludes fungi, nematodes, and other microorganisms with saprophytic activity. Given these estimates, there is no instrumentation today that can fully encapsulate the true diversity and complexity that exists at the interface of a decomposing human cadaver in the terrestrial landscape.

Despite the incredible variation in microbial species that exists at the soil-cadaver juncture, Carter and colleagues (2007) discussed cadaver decomposition processes in the terrestrial setting, and described the breakdown of a corpse as a complex hub of heterogeneous activity, where the mobilization of nutrients occurs through a localized pulse of water, carbon, nitrogen, phosphorus and energy into the surrounding ecosystem. The authors (Carter et al. 2007) suggested that the biogeochemical processes inherent to cadaver decomposition are delineated in both time and space, and that the rich quality of a carcass associated with the changing edaphic parameters will affect the underlying microbial community.

Benninger et al. (2008) followed this work by evaluating ecological parameters of soil below actively decomposing carcasses, where pigs (*Sus scrofa*) were used as the model organism. They found significant changes in the soil solution soon after death, only to have the affected soil mimic control soils 60 to 80 days postmortem, reflecting the ephemeral pulse of nutrients and

energy suggested by Vass et al. (1992) and again recently by Carter and colleagues (2007). Recognition of this fact suggests that it may be possible to identify microbial markers of human decomposition in the landscape, as the structure of the microbial population is sensitive to the changing nutrient source.

In the terrestrial setting, the interface of the soil and cadaver microenvironment is a complex ecosystem where the quality of the substrate to be decomposed significantly effects the rate of decomposition; the resource being decomposed will select the microbial community (Moorhead and Sinsabaugh 2006). When the body is understood to be a rich nutritional substrate, then it follows that specific identifiable enteric anaerobic and facultative-anaerobic bacteria of putrefaction should be succeeded by aerobic microbes from the immediate surrounding grave site as the chemistry of the nutrient source (i.e., the body) changes over time (Evans 1963; Carter et al. 2007; Parkinson 2009). The transition from primarily endogenous microbes to those of the surrounding environment should be consistent across the landscape.

At this point in time, microbial structure and biodiversity at human cadaver decomposition sites has only recently been investigated (Parkinson 2009). Little else is known about microbial community structure's relationship to the changing human decomposition ecosystem, and how the shifting community structure can be used and applied as a spatial and temporal biomarker of forensic investigation; thereby, requiring additional systematic investigation.

CHAPTER 2: RESEARCH GOALS AND OBJECTIVES

This research project evaluates the composition of the soil and microbial communities associated with human decomposition in the terrestrial setting at the University of Tennessee Anthropology Research Facility (ARF). Over the last 30 years the ARF has been a site for studies of human decomposition, and as a result has become one of the most active and highly concentrated "cemeteries" in the United States. Congruent with this history, the ARF soils may have become saturated with a specific community of microbes that are involved in the specific processes associated with human decomposition.

To that end, this research evaluates the microbial communities and associated soil characteristics of human decomposition at the ARF. In so doing, the following goals are achieved:

1. Complete a baseline survey of the current abiotic environmental and edaphic features across the University of Tennessee ARF in order to better understand and establish patterns of human decomposition ecology.
2. Complete a baseline survey of the current microbial community and diversity indices of the ARF soil in order to better understand and establish patterns of human decomposition ecology.
3. Explore the relationships between the abiotic and biotic data obtained from the ARF soil in order to assess the causal relationships between microbial structure and environment.

4. Evaluate a cross-sectional sampling of soil taken below decomposing human corpses of varying times since death in order to identify changes in soil dynamics as a result of time-dependent changes of human decomposition.

By evaluating human decomposition in a broad ecological context this research seeks to develop an understanding of the trends in temporal and spatial variation in the edaphic characteristics and microbial diversity of a decomposing human corpse. In so doing, the forensic anthropologist acquires baseline data for developing new tools to refine postmortem interval estimations and locating clandestine graves.

CHAPTER 3: BACKGROUND AND LITERATURE REVIEW

From an organism's death to its discovery, a finite amount of time elapses. During the postmortem continuum, a corpse is engaged in a complex web of cultural, physicochemical, and biological reactions that either preserves or destroys a body; a dichotomy that is driven by the interrelationship of a corpse, its decomposition ecology, and time.

Integral to this relationship is the microbially-mediated mobilization of nutrients bound to once living organisms into the surrounding ecosystem, so that they may be recycled as living biomass (Swift et al. 1979; Putman 1978), or they may escape altogether as inorganic constituents and be preserved through fossilization (Behrensmeyer 1984); such are the tenets of taphonomy.

Taphonomy

Defined by Efremov in his 1940 publication: *Taphonomy: A New Branch of Paleontology*, Efremov explained that taphonomy is the study of the transition (in all its details) of animal remains from the biosphere into the lithosphere. The incorporation of taphonomic studies to issues germane to forensic sciences can be understood through a rather shallow history, with the study being formalized in paleontology in the 1940s, and parallel development in archaeology and paleoecology (Gifford 1981), and eventually being fully adopted by forensic sciences in 1997 with the publication of *Forensic Taphonomy: The Postmortem Fate of Human Remains* (Haglund and Sorg 1997).

As a paleontologist, Efremov applied an ecological understanding toward the mechanisms and conditions that precipitated preservation, and conversely the loss of organisms in the paleontological record. In effect, Efremov acknowledged Darwin's "incompleteness of the

geological chronicle" from 81 years earlier by stating that the greatest difficulty in paleontological reconstruction is the incomplete character of the material and causality of its preservation in the rock (Efremov 1940). The loss of information by way of taphonomic processes biases our conclusions in the historical sciences.

Highlighting the link between recovered fossils and interpretation, Behrensmeyer correctly pointed out "the earliest bird might have been mistakenly identified as a reptile, were it not for the fortuitously preserved impression of feathers in limestone" (Behrensmeyer 1984:558). Continuing this line of reasoning, Martin (1993) explained that everything we know about primate evolution from the fossil record today is drawn from approximately 3% of the total estimated richness of primate species.

Interested in the biasing effects of skeletal assemblage formation, archaeologists were early adopters of the taphonomy concept. With this model they were able to better understand accumulation and modification of the archaeological record (Bonnichsen and Sorg 1989). Most notably was Brain's (1981) rebuttal of Dart's 1957 publication on the Osteodontokeratic culture of Australopithicines at Makapansgat. Through actualistic and ethnographic research, Brain provided an alternate hypothesis of bone fractures, suggesting that the observable effects were actually caused by the pressure of overlying rocks and earth in limestone caves, rather than the intentioned scavenging activity of hominids to procure nutrients (Brain 1981).

More recently, Dominguez-Rodrigo and Barba (2006) offered a reinterpretation of carnivore tooth marks on remains of the FLK Zinj assemblage, suggesting that the frequencies reported by Blumenschine (1995) were artificially high, and that many of the reported tooth marks were in fact taphonomic effects of saprophytic fungi. In this example, the subject (archaeological bone)

was viewed in the larger ecological context, rather than the narrower carnivore-hominid dichotomy.

The adoption of taphonomy in the forensic sciences can be marked by the publication of *Forensic Taphonomy: The Postmortem Fate of Human Remains* (Haglund and Sorg 1997). With this publication taphonomy entered the forensic science vocabulary, becoming a recognized field of forensic investigation. Like all new paradigms though, there were a number of taphonomic studies in the forensic sciences that led up to this publication. A review of articles published in the *Journal of Forensic Sciences* from 1975 to 2005 identified a number of taphonomy-related projects (Rodriguez and Bass 1983, 1985; Willey and Snyder 1983; Mann et al.1990; Vass et al. 1992); interestingly though, none of these publications used "taphonomy" as a keyword, but included phrases such as "human decomposition" and "time since death".

Forensic anthropologists have come to understand taphonomic consideration as the interpretation of all events that affect remains between death and discovery (Ubelaker 1997), indicating that decomposition is a subset of taphonomy. Within this framework, taphonomy is often invoked to differentiate natural from human-induced markers on tissue, estimating time since death, and describing the destructive properties of various taphonomic processes.

To that end, the taphonomy concept has been used to differentiate perimortem trauma from postmortem damage (Ubelaker and Adams 1995), and natural from cultural modification of remains (Holland et al. 1997). Taphonomy has also been used for estimating time since death, where timed events are relative and related to the succession of specific taphonomic processes (Bass 1984, 1997; Haglund 1997a; Sledzik 1998; Love and Marks 2003, Klippel and Synstelein 2007), and the decay of biochemical evidence (Castellano et al. 1984; Perry et al. 1988; Gill-King 1997; Parsons and Weedn 1997), bone macrostructure (Willey and Heilman 1987; Willey

and Snyder 1989; Haglund 1997b; Klippel and Synstelein 2007) and bone microstructure (Hackett 1981; Hedges et al. 1995; Jans et al. 2004). The power of taphonomic interpretation lies in the ability to separate that which is man-made from myriad natural biogeochemical processes inherent to decomposition.

Factors affecting the rate of human decomposition

In the terrestrial landscape natural human decomposition follows a sigmoidal curve, indicating rapid mass loss followed by periods of less change (Carter et al. 2007), which contrasts with the decomposition rates of plants and fecal material where percent mass loss is constant over time (Olson 1963; Putman 1983; Coleman et al. 2004). Natural decomposition however is often the exception rather than the rule, since cadaver decomposition lies at the nexus of four influential modulators that include: (1) the quality of the resource being decomposed, (2) cultural determinants, (3) environmental determinants, and (4) the potential decomposer community. Each modulator contains a suite of possible factors that affect preservation / destruction, as well as the rate of decomposition.

Resource quality. Resource quality is inversely proportional to the ratio of carbon and nitrogen, where the amount of carbon is expressed per single nitrogen atom; a high ratio indicates a poor-quality resource, and vice versa. A high-quality resource implies increased availability of carbon and nitrogen mobilization in the ecosystem (Swift et al. 1979). For example, plant material contains a carbon: nitrogen ratio of 100, whereas cow manure is 18 (Carter et al. 2007). In this example, cow manure is the higher quality resource. For a human cadaver the carbon: nitrogen ratio is 5.5 (Carter et al. 2007), creating the expectation that the rate of decomposition is greater for a human cadaver than plant material, which is consistent with percent mass loss curves for the rate of decomposition between cadavers and plants. That said,

intra-species variation also contributes to the decomposition rate as not all members of the same species enter the burial environment in a similar manner. Factors that an individual organism contributes to accelerating or decelerating the rate of decomposition have been identified previously, and include the presence or absence of clothing (Mann et al. 1990; Aturaliya and Lukasewycz 1999), and an individual's age, weight, and health status (Mann et al. 1990; Campobasso et al. 2001).

Cultural determinants. In addition to that which the individual brings to the burial environment, culturally-distinct human behavior is a significant modulator in the decomposition rates of a cadaver (Evans 1963; Holland et al. 1997; Sledzik 1998). Through various ritualistic practices that the living does to the dead, such as mortuary and internment practices, the natural processes of decomposition are affected. In western culture certain post-death practices affect the condition of the corpse. These may include, but are not limited to, autopsy and organ removal, embalming, anatomical preparation, burning and/or disarticulation by criminal, traumatic or natural mechanisms.

Interment practices vary from deliberate exposure to burial where the corpse may be wrapped in plastic, or submerged in water, buried in a sealed casket, wooden box, or wrapped in cloth and placed in dirt or a concrete burial shaft above or below ground. Burial may occur at various depths, or there may be no burial at all with the remains left on the surface to decompose. Containment of the body in clothing, vault, casket, or plastic tarp also contributes to the variation inherent to the decay/preservation dichotomy. Jans et al. (2004) noted that bodies buried intact displayed greater signs of bioerosion at the microscopic level than did those remains that were disarticulated prior to burial.

Environmental determinants. Potentially the most recognized factors controlling the rate of human decomposition are those that are modulated by the environment because of its ability to completely decompose or suspend biological material through freezing (Micozzi 1991), desiccation (Evans 1963; Galloway et al. 1989; Galloway 1997), or adipocere formation by hydrolysis and saponification of adipose (Mant 1987; Forbes et al. 2003; Forbes et al. 2004; Forbes et al. 2005).

Environmental factors that create the varied ecological niches include, but are not limited to, temperature, moisture, seasonality, altitude, latitude, air circulation, burial depth, soil type, vegetation, topography, exposure to direct sunlight, and placement in water. Of these, temperature is significant in that it is a prime mover of all biochemical reactions, including those of decomposition.

There is a direct positive correlation of temperature to biological and chemical reaction rates over the mesophilic interval of 15°C and 35°C. This relationship was defined by Van't Hoff (1884) as the Q_{10} temperature coefficient and is the factor by which a rate changes in a biochemical system with every 10°C increase in temperature (Tibbett et al. 2004; Moorhead and Sinsabaugh 2006). By increasing temperature and physiological reactions, the diffusion of soluble substrates in soil is also accelerated. In application to forensic studies and human cadaver decomposition, Vass (1992) and Megyesi (2005) drew on the basic importance of temperature for driving biological reactions and applied Edwards and colleagues' (1987) concept of accumulated degree days (ADD) to standardize decomposition rates across variable weather regimes.

Additional environmental considerations include soil pH and redox potential. In a terrestrial setting acidic soil dissolves the mineral components of bone (Gordon and Buikstra 1981) and

promotes leaching, allowing additional destruction by microorganisms and the release of volatile compounds (Vass et al. 1992, 2002, 2004, 2008). Soil pH also affects nutrient availability and microbial metabolism. Soil dwelling microorganism activity is highest when pH is near neutral. A high redox potential facilitates oxidation of structural macromolecules such as the triple-helices of collagen fibrils by microorganisms (Child 1995).

Potential decomposer community. The final category of factors that contribute to variation in decomposition rates are the available biological agents that use a cadaver as a resource for acquiring essential nutrients and minerals (Swift et al. 1979; Carter et al. 2007; McGuire and Treseder 2010). Many of the taphonomic agents that consume a cadaver have been identified, and have been studied from the perspective of their specific taphonomic effects. Potential biological consumers of a corpse that have been discussed include, but are not limited to bacteria, fungi, nematodes, diptera, coleoptera, hymenoptera, decapods, murids, suids, canids, felids, ursids, carthids, hyaenids, and hominids.

Understanding these general factors that affect the rate of human decomposition is integral to furthering our understanding of how a human cadaver decomposes through interactions with the surrounding ecological niche. In fact, the four main categories discussed above are similar to those of Jenny's (1941) ecological state factors that regulate soil formation. Jenny (1941) stated that soil formation was a function of climate, topography, potential biota, parent material, and time. In this model, only cultural influence is absent, but could reasonably be included within the framework of potential biota. McGuire and Treseder (2010) point out that potential biota is not just those organisms occupying the niche where the cadaver is placed, but includes taxa that can potentially colonize the area via dispersal, migration, or germination.

Patterns of Human Decomposition

Variation in the rate of decomposition is a universally accepted rule, where the variance in climate across the globe serves as the prime mover of variable decomposition rates (Galloway et al. 1989; Galloway 1997; Sledzik 1998; Mann et al. 1990). That said however, "an organism's chances of becoming fossilized [or recycled] are not randomly distributed in time and space, but follow discernible patterns and measureable probabilities" (Behrensmeyer 1984:558) that are modulated largely by the habitat, the death event, and the organism itself.

Decomposition begins at the moment of death. Perper (1993) defined death as the irreversible cessation of the brain, respiratory and circulatory abilities, causing internal biochemical reactions in response to the depletion of oxygen in tissue. Once the systems of normal living have stopped the internal biological mechanisms that require oxygen for energy production through the central metabolic pathway, which governs the citric acid cycle and oxidative phosphorylation, the multiple internal processes that take place after death ensue.

For convenience, those who study cadaver decomposition superimpose a categorical-ordinal scale based on observable patterns of gross-tissue change in order to better understand and draw interpretations about the complexities inherent to cadaver decomposition (Reed 1958; Payne 1965). Clark and colleagues (1997) provide a summary overview of decomposition stages and modulators, and report that the generally accepted pattern follows a fresh corpse through discoloration and bloating to decay, skeletonization and eventual disarticulation and bone diagenesis. This pattern demonstrates the continuum that is human decomposition, where a complete cadaver becomes totally reincorporated within the landscape or it becomes sequestered within the biogeochemical footprint (e.g., fossilized remains). It follows then that cadaver substrate changes are often associated with a change in analytical / investigatory perspective

(Micozzi 1991). The information in Table 3-1 highlights the generally accepted patterns of human decomposition stages and associated disciplines, indicating the multidisciplinary approach of human decomposition studies. These categorical scales are broadly correlated with time, while it is understood that the rate of transition between stages varies in as much as ecological and environmental conditions vary.

Fresh (Autolysis). Under natural conditions, which are defined here by exclusion of desiccation and freezing, a body will begin to decompose soon after death. The moments immediately following death initiate a complex series of biochemical reactions, affecting the

Table 3-1. Temporal patterns of macroscopic human decomposition and associated investigatory disciplines [a]

Time	Observation	Stage	Discipline (s)
Minutes-Hours	Enzymatic change Cellular respiration Digestion	Fresh Autolysis	Toxicology Pathology
Hours-Day	Mortis triad	Fermentation (s) Bloat	Pathology Entomology
Day-Week	Gross Tissue Decomposition	Putrefaction Active Decay	Pathology Entomology Anthropology
Week-Month	Disarticulation Skeletonization	Advanced Decay	Anthropology
Month-Year	Biostratinomic Diagenesis	Skeletal Remains	Anthropology
Year-Eons	Fossilization Diagenesis	Late-stage Skeletal Decay	Anthropology Geology

[a] Adapted from Reed 1958, Payne 1965, Micozzi 1991, Sledzik 1998

entire microcosm of organic components, and is manifest by cellular destruction by one's own enzymes (Evans 1963; Vass et al. 1992; Perper 1993; Gill-King 1997; Clark et al. 1997; Love and Marks 2003).

The cessation of the circulatory system causes a loss of oxygen transport throughout the body. Without oxygen the central metabolic pathways, including the feedback mechanisms of cellular respiration, fail to produce ATP. The enzyme ATPase further reduces ATP concentration, and as a result starves cells. Because of the need for oxygen, autolysis first occurs in areas that demand high-energy output (i.e., high mitochondrion concentration). Without oxygen, the mitochondria swell, causing the cell and internal cellular organelles to rupture, which is a process similar to cellular apoptosis (Evans 1963). Similarly, the death of a cell initiates the rupture of the lipoprotein membranes of lysosomes that are packed with high concentrations of cellular enzymes (lipases, proteases, DNAses, etc.) that cause a reduction of enteric protein, lipids, carbohydrates, and DNA. Consequently, membrane pumps fail, releasing calcium ions and destroying cell membranes, effectively ending cell to cell adhesion and causing failure of matrix renewal (Lindhal 1993). These biochemical changes cause macroscopic changes known as algor, livor, and rigor mortis, and typically occur within the first 24 hours after death (Pepper 1993; Janaway 1996; Clark et al. 1997; Gill-King 1997; Love 2001; Love and Marks 2003).

Mortis triad. Algor mortis is the modification of body temperature from the 98.6°F to ambient temperature. Traditionally, a cooling rate of 1.5 degrees per hour is accepted, but the correlation is not exactly linear as there tends to be a moment of heat retention immediately after death, followed by a quicker decline, and then a plateau is reached (Clark et al. 1997). Algor mortis may become recognized two hours postmortem.

Intravascular concentration and hemolysis of the blood cells is livor mortis (Spitz and Fisher 1980). As a direct result of gravity, the low-lying body tissues develop a reddish-purple appearance as a subcutaneous pool of degraded blood forms. When a body is discovered supine, lividity appears on the back, buttocks, and calves, and can occur as soon as 20 minutes after death. The pooled blood repositions as pressure is applied to the areas of lividity, and is called blanching. Lividity is considered fixed when blanching of the pooled blood is no longer possible. Fixation can occur approximately eight to 12 hours after death (DiMaio and DiMaio 2001; Payne-James et al. 2003).

Rigor mortis results from an increase in the concentration of free calcium ions that end up in muscle tissue following death. Calcium ions are sticky and bind the inhibitors of the muscle contractile units of actin and myosin, thus giving the muscle a rigid and hard appearance. Rigor initiates by two to six hours postmortem and may persist for one to two days.

Without protection from the intestinal mucosa and normal homeostatic mechanisms, autolysis initiates the breakdown of normal biological structure and function. This permits initial microbe proliferation and transmigration across internal mucosa, allowing microbes to move passively through the body's circulatory and lymphatic systems (Kellerman et al. 1976; Melvin et al. 1984). Enteric heterotrophic microbes metabolize organic macromolecules such as lipids, proteins, amino acids, and nucleic acids selectively using C, N, and P to meet their own metabolic demands (Child 1995). Autolysis initiates putrefaction.

Bloat and Active Decay (Putrefaction). The putrefaction of a corpse is marked by the widespread breakdown of biomolecular components and subsequent destruction and liquefaction of soft tissue by enteric obligate and facultative anaerobic microorganisms, such as members of the genera *Clostridium, Bacteroides, Staphylococcus,* and the Enterobacteriaceae family (Melvin

et al. 1985; Carter et al.2007). Biliary acids form sulfa-hemoglobin complexes that appear as a green discoloration of the skin near the left anterior abdominal wall (Gill-King 1997; Clark et al. 1997). During putrefaction oxygen is depleted from the decomposing corpse, creating a hypoxic environment that promotes anaerobic metabolism and the transmigration from the gastrointestinal tract. The increased levels of anaerobic microbial activity accompany increased levels of carbon dioxide, among other gasses, that cause swelling and bloating (Vass et al. 1992). Two volatile organic compounds produced during this stage are butyric acid and propionic acid, which are formed by anaerobic bacteria (Vass et al. 1992). Gill-King (1997) and Love (2001) report the evolution of CO_2 and the foul-smelling compounds of putrescine and cadaverine from the decarboxylation of the amino acids ornathine and lysine, respectively.

Sulfur-containing amino acids may be reduced by the enzyme cysteine desulfhydrase producing hydrogen sulfide, pyruvic acid, and ammonia. In the presence of iron, hydrogen sulfide forms ferrous sulfide, which appears as a black precipitant in the capillaries near the skin surface of a decomposing corpse. This reduction of sulfide is generally referred to as marbling (Gill-King 1997; Love and Marks 2003).

Microbially-mediated fermentation persists until oxygen replenishes the system. Once oxygen levels increase the substrate microenvironment changes eliciting additional aerobic decay. The rupturing of orifices from putrefactive processes is one example of how oxygen replenishes the system (Gill-King 1997; Micozzi 1991). Replenishing the decomposing corpse with oxygen initiates the transition to late stage decomposition, which involves skeletonization and diagenesis.

Advanced Decay and Skeletal Remains. In the terrestrial setting, skeletal exposure typically originates with the head and face and is often done so with the aid of insect (maggot) activity

provided access. Other early sites of skeletal exposure may include areas evincing traumatic lesions (Mann et al. 1990; Rodriguez 1997). Scavenging accelerates skeletonization and may promote disarticulation and bone loss (Willey and Snyder 1989; Haglund 1997; Klippel and Synstelien 2007). The last portions of soft tissue to remain are the dense connective tissues of joint surfaces and the odor of recent decomposed flesh (Stewart 1979).

Once exposed, the skeleton interacts directly with the environment as it is no longer protected by internal viscera and skin. During late-stage decomposition at advanced or dry–remains stage, microbially-mediated decay persists facilitating the recycling of the organic phase (i.e., Type I collagen), and the few nutrients bound within bone matrix (i.e., calcium, phosphorus) into the environment.

Late-Stage Skeletal Decay (Diagenesis). Microbial effects on bone have been described on remains recovered in forensic, archaeological, and laboratory contexts (Marchiafava 1974; Hackett 1981; Yoshino et al. 1991; Grupe and Garland 1993; Child et al. 1993, Child 1995; Hedges et al. 1995; Bell et al. 1996; Jans et al. 2004). Exposed to both enteric and edaphic microbes, the organic phase of bone (i.e., type I collagen) is consumed, reorganizing bone microstructure. Child et al. (1993) and Child (1995) presented evidence that the non-random destruction of larger amino acids by microbes is simply related to efficiently fulfilling nutritional requirements since there is a larger amount of C readily available in larger amino acids. This selective dietary metabolism effectively reduces the amount of C relative to N, potentially biasing the C/N isotopic ratios. Fungal activity by endophytes further affects preservation as hyphae penetrate bone cortex compromising the structural integrity (Grupe and Piepenbrink 1988).

In addition to biological mechanisms, collagen may also be lost through physicochemical processes (Collins et al. 1995). The loss of the organic phase leads to an unstable inorganic matrix (White and Hannus 1983), causing dissolution and leaching of its key components (e.g., calcium, phosphorus), especially in the presence of naturally acidic soils (Gordon and Buikstra 1981), or those created by the decomposition process (Haslam and Tibbett 2009). In acidic environments bone mineral matrix becomes soluble, but recrystallizes at elevated pH (Berna et al. 2004). The loss of mineral matrix may allow access to the polypeptide chains of collagen and other bone proteins by edaphic microbes. Increased bone porosity (Turner-Walker and Syversen 2002) allows for an increase in inclusions and infiltrates (Grupe and Pipenbrink 1988; Willey and Heilman 1987) further compromising the integrity of bone's original structure.

Due to the micro- and eventual macroscopic destructive activity of microorganisms to osseous tissue the anthropologist should be particularly concerned, given the growing reliance on bone sequestered biomolecules of anthropological and forensic importance. Stable isotopes of carbon, oxygen, nitrogen, and strontium are often used for determining region of origin and diet (Regan 2006; White et al. 2004). Protein extracted from bone is being used in radioimmunoassays for differentiating human from nonhuman bone (Cattaneo et al. 1999; Ubelaker et al. 2004). Since the mid-1990s genetic data have been routinely extracted and analyzed from degraded remains in most forensic biology laboratories (Holland et al. 1993; Fisher et al. 1993; Holland et al. 1995; Coble and Butler 2005). Skeletal elements that have undergone sufficient biochemical and structural modification will prove difficult for age estimation studies based on amino acid profiles (Helfman and Bada 1976; Ogino et al.1985), or histological change (Kerley 1966; Kerley and Ubelaker 1978). All of these biomolecules serve as either an energy source for endogenous and environmental microbes, or are affected directly

by the decomposition process itself (Collins et al. 1995; Grupe and Piepenbrink 1988; Grupe and Garland 1993) that alters the microstructure and composition of bone.

Microbial agents of decomposition

Evans (1963) noted that during decomposition, the bacterial flora transition from the aerobic groups, exemplified by the coliform-staphylococcal-proteus varieties, to the anaerobic, in which the Clostridia predominate. Melvin et al. (1984) and Carter et al. (2007) identified a similar trend, and suggested that the destruction of soft tissue is caused by enteric obligate and facultative anaerobic microorganisms from the genera *Clostridium, Bacteroides, Staphylococcus,* and Enterobacteriaceae family.

With regard to bone tissue, the fungus *Mucor sp*. (Marchiafava et al. 1974) and bacterium *Fusarium sp.* (Hackett 1981) have been isolated from fossilized and archaeological bone, respectively. The cultured organisms were inoculated on fresh bone, producing macroscopic focal destruction (MFD) (Hackett 1981). However, the resulting MFD were not consistent with original observations of microscopic structure of the parent material.

Child (1995) isolated fungi and bacteria from archaeological bone and associated soil, cultured these organisms in a variety of microbiological media, and used collagen as the sole nitrogen source. Viable organisms recovered from the plates were presumptively identified using cultural, morphological and histological staining characteristics. This study reported a number of different organisms, isolated from bone and soil of three different archaeological sites (Figure 3-1).

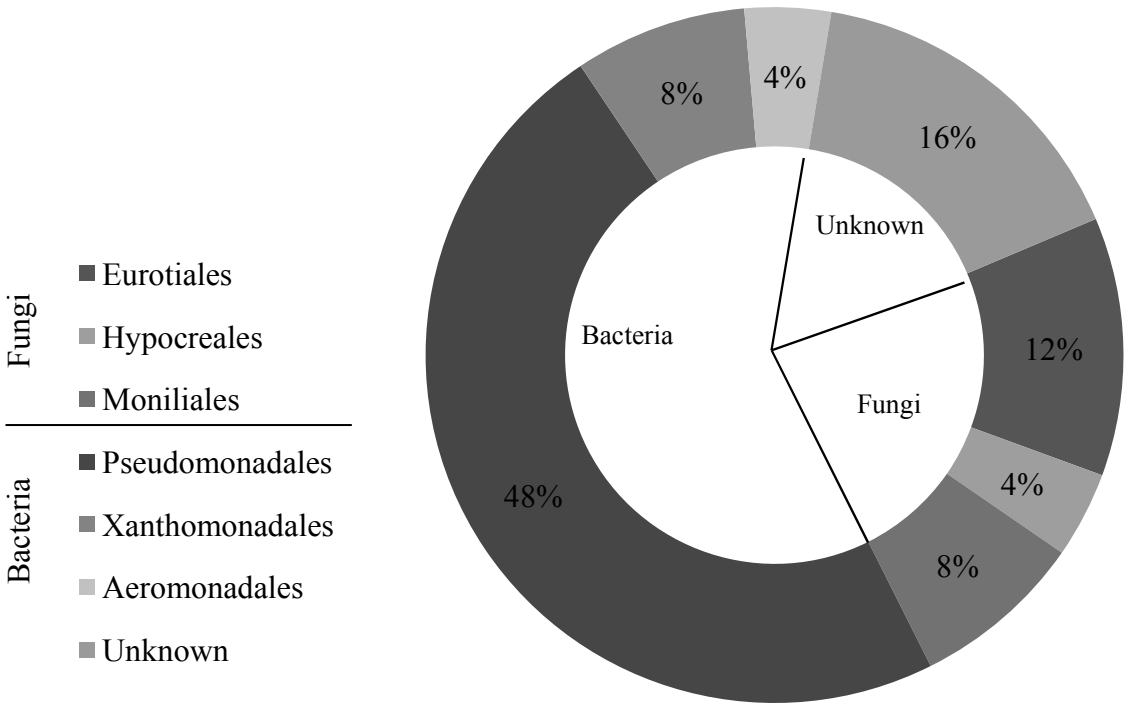

Figure 3-1. Identified fungal and bacterial Orders recovered from archaeological bone and cultured with Bovine tendon growth media (after Child 1995). Organisms were identified morphologically and histochemically.

Decomposition Ecology

At this point in time, the majority of the studies listed above of microbially-mediated decomposition address the biasing effects that microbial decomposers have on the overall preservation of bone structure and biochemistry. While this remains an essential component of decomposition ecology, only recently has microbial community analysis and the effects of microbial activity on human decomposition been systematically evaluated as a viable source of forensic data (Vass et al. 1992, 2002, 2008; Carter and Tibbett 2003; Carter et al. 2007; Benninger et al. 2008; Parkinson 2009; Parkinson et al. 2009; Carter et al. 2010; Dickson 2010).

In order to appreciate the myriad processes and complexities of human decomposition, it is vital to understand the ecology of decomposition. To that end, decomposition ecology lies at the center of the relationships among the potential decomposer populations, the quality of the resource being decomposed, and the cultural and environmental modulators. Therefore, cadaver decomposition ecology and its intrinsic processes determine the preservation / destruction of a corpse, where complex ecosystems of organisms from various trophic levels function as taphonomic agents with deleterious effects on the preservation of a human corpse, bone, and its biochemistry, all the while releasing sequestered nutrients and energy into the surrounding environment.

As stated previously, edaphic fungi and bacteria account for nearly 90% of the mobilization of carbon and nitrogen in an ecosystem. The cycling of carbon and energy associated with cadaver decomposition was explained well by Putman (1978a). Putman's flow diagram demonstrates the movement carbon, and thus energy within an ecosystem (Figure 3-2). Briefly, he explained that decomposition of a corpse occurred in three phases: consumption, leached materials, and residual organic debris that is difficult to decay, such as bone, skin and hair. The

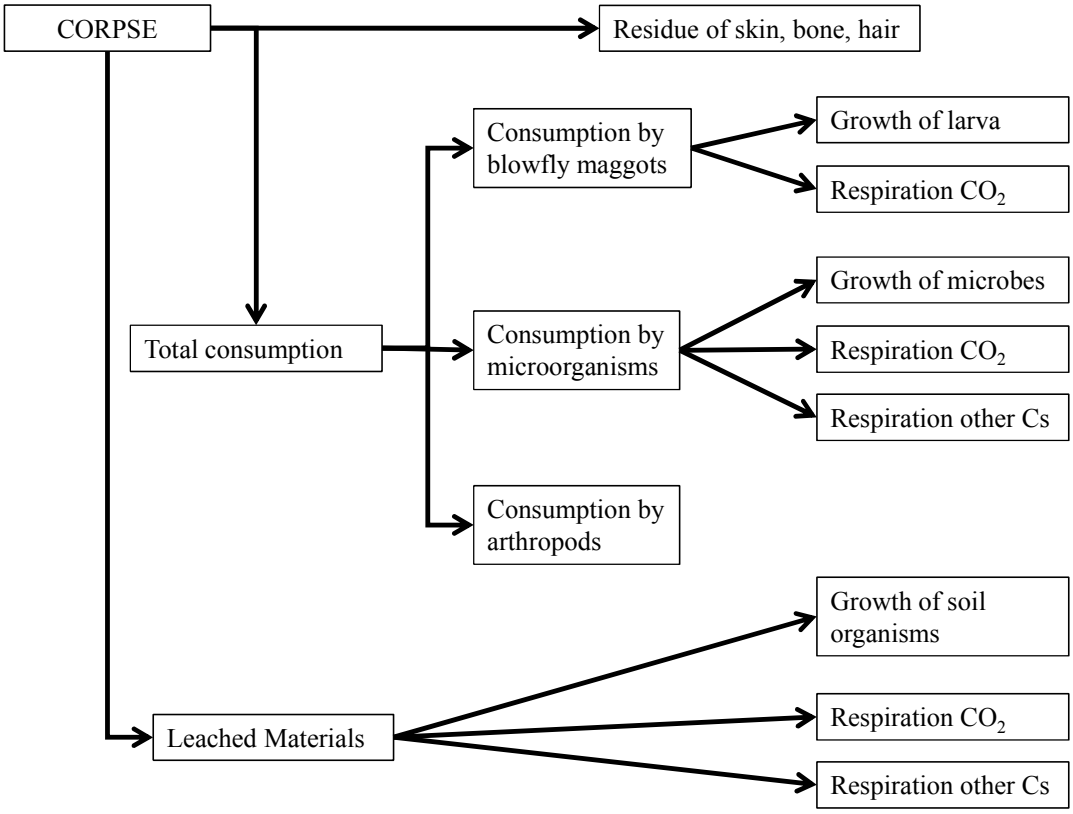

Figure 3-2. Flow-diagram demonstrating the movement of carbon sequestered in a corpse into the environment, primarily through respiration of saprophytic microbes. Redrawn from Putman (1978a).

consumption phase is dominated by primary and secondary consumers that attain nutrients from the corpse, and release carbon through respiration. Similarly, micro- and macro-nutrients are leached from the body by increased moisture availability. This material will also be consumed, primarily by a growing community of aerobic heterotrophic microorganisms provided appropriate physicochemical conditions within the surrounding soil matrix.

Following Putman's model of carbon and energy flow, Carter et al. (2007) explored further the notion of a corpse as a rich source of nutrients and energy. In doing so, Carter and colleagues recognized the under-representation in the literature of the tremendous contribution that carcass decomposition has on the terrestrial landscape, and recommended the concept of a Cadaver Decomposition Island (CDI) (Figure 3-3). A CDI was defined as an island of fertility, where the site of cadaver decomposition is a heterogeneous hub of activity marked by an increase in C, N and water (Carter et al. 2007). Where Carter and colleagues added to Putman's earlier discussion was in their suggestion that decomposition is not an entirely open system, rather it is its own localized ecosystem of increased biological activity, bound in both time and space.

Application of these models to decomposition include Carter and Tibbett's (2003) discussion of taphonomic fungi associated with mammalian decomposition and listed previously identified fungi associated with either early or late stage succession, differentiating them based on nitrogen utilization. Early stage fungi include Ascomycetes, Deuteromycetes, and saprotrophic Basidiomycetes, and late stage fungi include ectomycorrhizal basidiomycetes that may fruit from one to four years after fertilization (Carter and Tibbett 2003). Following this review, Sidrim and colleagues (2010) identified species of the *Aspergillus*, *Penicillium* and *Candida* genera in the bloat and putrefactive stages of human decomposition, while *Aspergillus sp.*, *Penicillium sp*., and

Mucor sp. were the primary residents during the late stage of skeletonization. Organisms were identified by direct examination of morphological and biochemical analyses.

Lorielle (personal communication) applied high-throughput sequencing of DNA extract from 50 year-old bone, identifying 1,038 different sequences with bacteria and fungi representing 45% and 12%, respectively (Figure 3-4). The major bacterial component was identified as species of the bacterial genus *Streptomyces*.

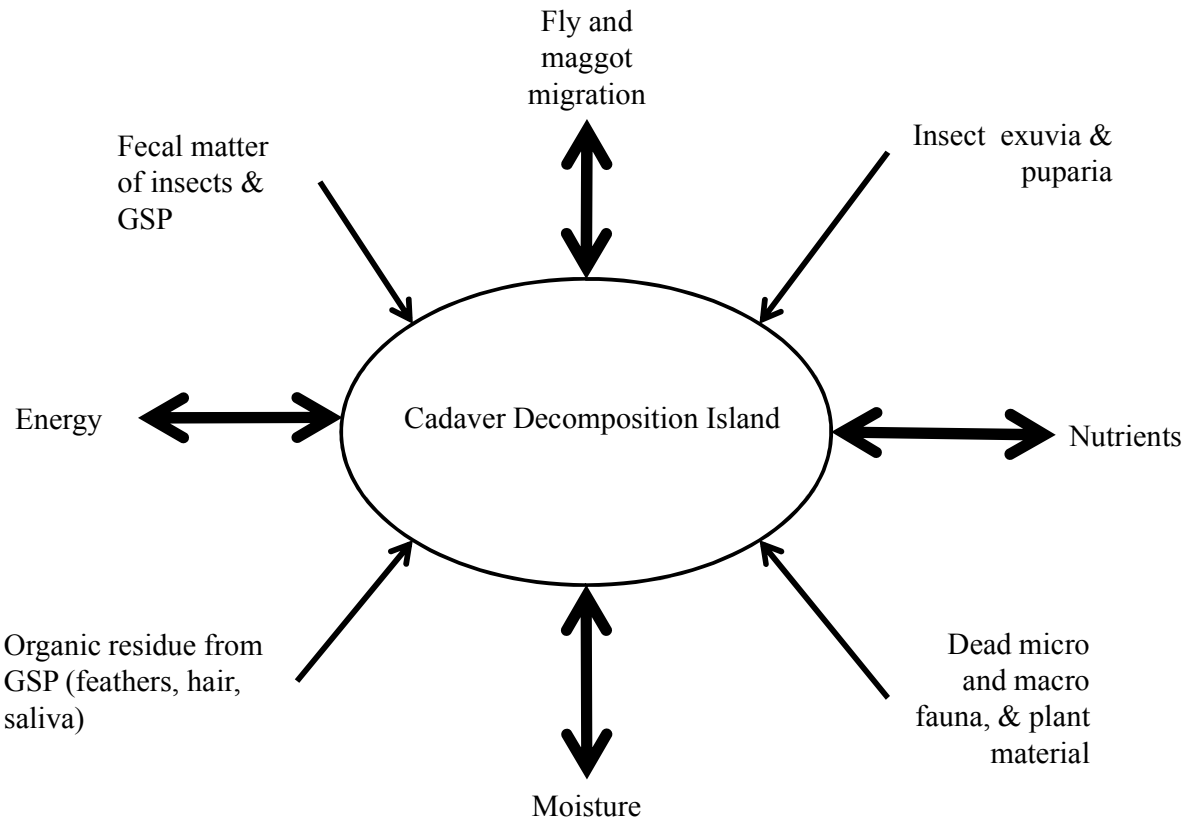

Figure 3-3. Schematic representation of cadaver decomposition as an island of fertility marked by an increase in C, N, and water concentration. Redrawn from Carter et al. (2007).

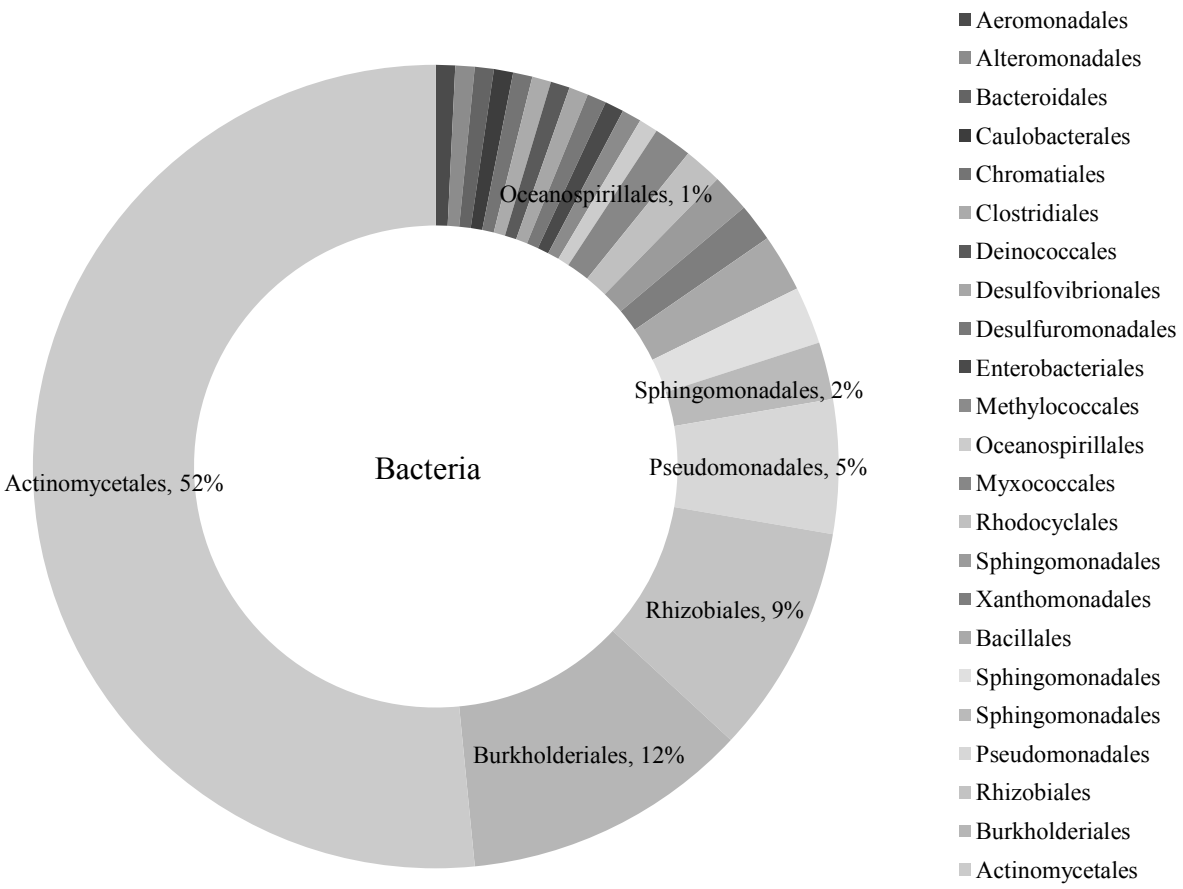

Figure 3-4. Identified bacterial Orders from *in vitro* clonal amplification and sequencing-by-synthesis using Roche 454 Life Sciences technology. The DNA sample was obtained from human bone after exhumation. The exhumation occurred 50 years after death.

Recently, Parkinson (2009) evaluated bacterial communities in soil associated with human and pig (*Sus scrofa*) decomposition. Using an array of molecular techniques, Parkinson identified a vast community of bacterial organisms associated with corporal decomposition. By way of molecular cloning and sequencing of the 16S ribosomal DNA subunit, multiple sequences were obtained and identified using the Ribosomal Database Project (Wang et al. 2007). Twenty-three different bacterial orders were identified from over 500 cloned sequences (Figure 3-5). Through this work Parkinson (2009) was the first to demonstrate by direct identification the complexities of the bacterial community structure associated with human cadaver decomposition. Longitudinal sampling of soil substrate from below six actively decomposing bodies allowed for the assessment of shifting community profiles during decomposition. In doing so, a pattern emerged that supported a changing community structure associated with postmortem interval.

Similarly, Dickson and colleagues (2010) recently identified temporal trends in dominant contributors of the colonizing microbes at pig carcasses suspended in a deep water ecosystem. Early colonizers were identified as members of two genera, the *Arcobacter* and *Flavobacterium*, which are associated with the utilization of amino acids and carbohydrates, respectively. Mid-colonizers were those of the genera *Carnobacterium* and *Aeromonas;* sugar fermenters and reducers of lipids. The latest dominant colonizers were identified as members of the Order Bacteroidales. Identifying changes of dominant microbial abundance demonstrates that microbes may be used as temporal biomarkers of decomposition ecology, while providing limited information regarding the diversity of microorganisms present.

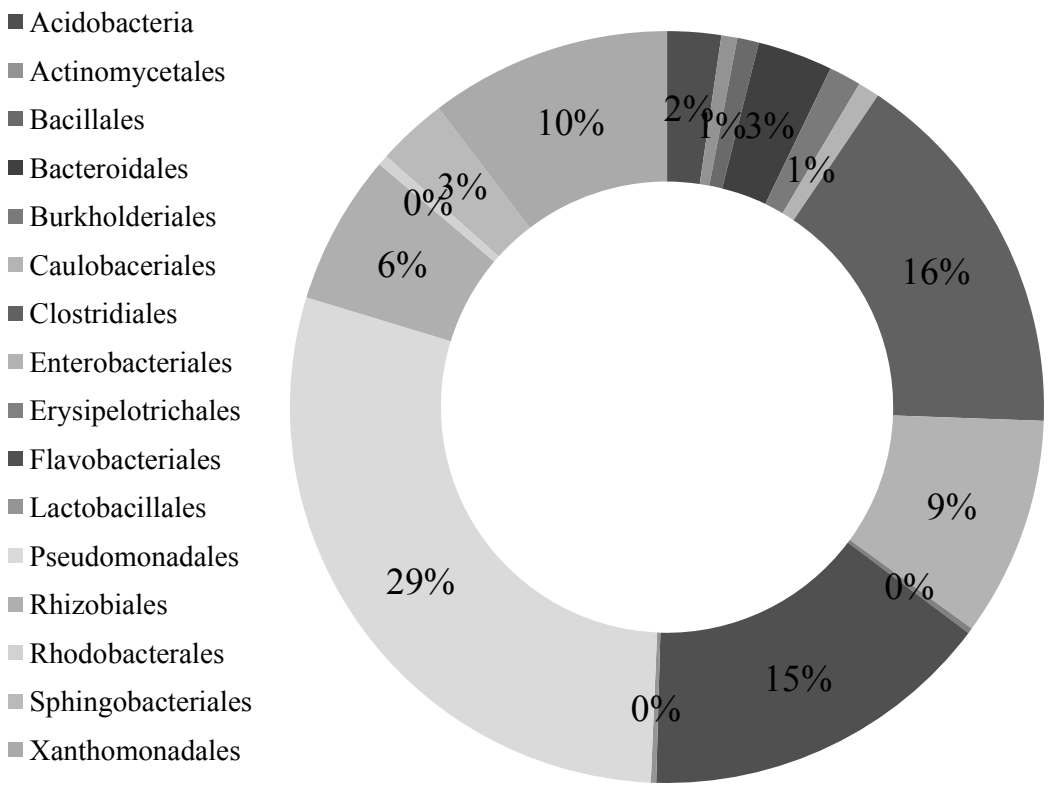

Figure 3-5. Identified bacterial Orders from over 500 clone libraries derived from soil and sand below human and pig corpses (Parkinson 2009). Bacterial organisms were identified by cloning and direct sequencing.

These studies have provided important ecological information related to components of the microbial community (Parkinson 2009; Parkinson et al. 2009), and changes in soil solution (Vass et al. 1992, 2002, 2008; Carter et al. 2007; Benninger et al. 2008) in response to cadaver decomposition. In so doing, the data were derived from observations of isolated decomposition events with little attention being placed on the diversity of soil microbial communities that constitute the indigenous community structure, and how that level of diversity is affected given input from a rich nutrient source. With over thirty years of human decomposition research in a

relatively small 1.28 acre temperate deciduous biome, the University of Tennessee's Anthropological Research Facility presents a most appropriate location to study the effects on the abiotic and biotic structure of the terrestrial landscape. Only by evaluating the ecology of human decomposition can we develop an understanding of the patterns in temporal and spatial variation in the edaphic characteristics and microbial communities of a decomposing human corpse.

CHAPTER 4: THE ANTHROPOLOGY RESEARCH FACILITY

Site Description. The ARF is an outdoor setting that has been used for studies of human decomposition in a natural environment. The facility is situated along the easternmost section of the University of Tennessee Medical Center parking lot in Knoxville, Knox County, Tennessee. An asphalt lot marks the western and southern boundaries, while the east is delineated upslope by a wooden privacy fence. In fact, the entire ARF is delineated by a double row of fencing; one outer chain-link with razor wire and an inner eight foot wooden privacy fence. The Tennessee River forms the northernmost boundary, with the ARF located on the south side of a mostly shale and sandstone cut bank that extends approximately 900 feet above mean sea level. On relevant map sheets the area is referred to as Cherokee Bluff.

The land use history for this specific area is limited to a survey of map sheets archived at the University of Tennessee Map Library, Knoxville (Figures A-1 through A-4). Given the proximity of the ARF to the University Medical Center, the changes in the landscape are associated with the development and history of the university medical center that opened in August 1956 (DeFiore 1996). A review of the available map sheets suggests that sometime between 1942 and 1953 a road was carved from the terrain near the current ARF location. The road connected the town of Vestal, approximately two miles southeast of the current ARF location and Alcoa Pike to the west (Alcoa Highway, US 129). According to DeFiore (1996), the ceremonial ground breaking for the hospital took place in 1953; this road was presumably in place to facilitate construction (Figure A-2).

Twelve years later (Figure A-3) a short, unpaved, dead-end road extended to the east of the newly constructed Vestal-Alcoa Pike road and hospital; a road that may have led to the

University hospital's dump. In 1978, that same small road was no longer depicted (Figure A-4). According to Jantz and Jantz (2008), the 1980 ARF ground breaking was situated on top of the hospital's old dump and incineration site after the location. They report that the incineration site was covered over and its use had ceased several years prior, when burning was banned due to a particularly dry and rainless season.

Climate. The National Climatic Data Center reported annual averages of basic weather data for Knox County (Hartgrove 2006). Reported average daily maximum and minimum temperatures were 20.4°C and 8.9°C, respectively, and annual precipitation was reported as 119.6 cm of rain and 34.3 cm of snow per year. Members of the University of Tennessee Biosystems Engineering and Soil Science Department have recorded weather data from various sites across Tennessee. Among the statewide recording centers, Mr. Wesley Wright has maintained weather data collection from the west side of the main Knoxville campus, which is just north of the ARF across the Tennessee River. The data is accessible online (http://biengr.ag.utk.edu/weather). A review of these data for the five years preceding sampling (2003-2007) was completed. Averages of daily high (21.3°C) and daily low (14.9°C) temperatures, relative humidity (71%) and annual rainfall (94 cm) were recorded and reported here due to the contributions of temperature and moisture to decomposition, and the proximity of the data collection site to the ARF.

Soil Description. A detailed soil description the study area is provided through a joint publication of the USDA and the Natural Resources Conservation Service (NRCS). Results of their collaborative work on regional soil analyses are published in the Soil Survey of Knox County, Tennessee (Hartgrove 2006). Pertinent details of soil description and characteristics for the area encompassing the UT ARF are summarized.

ARF soil is referred as Coghill-Corryton Complex, which is described as very deep, well-drained, clayey soils that formed in residuum derived from interbedded, leached, calcareous sandstone and shale. This type of soil complex is observed in seven percent of the USDA NRCS surveyed areas in Knox County, Tennessee and is typically found along ridgetops, shoulder and side slopes that vary from 5 to 65% with most areas in woodland consisting of mixed hardwoods.

The defined soil units within the ARF are divided into two Coghill-Corryton units: one having slope between 12% and 25% (CcD), and the second having slope greater than 25% and rocky (CcE). The third soil unit is Loyston-Talbott-Rock Outcrop Complex, and is located along the bluff and down slope toward the Tennessee River, forming the northern boundary of the ARF. This area is not included in this study, or any study to date at the ARF.

The CcD Coghill surface sediments are defined by Hartgrove (2006) as partially decomposed hardwood leaf litter and dark reddish brown loam (Munsell 5 YR 3/3) that make up the major component at 70%-85% of the CcD Complex. Twelve to 25% of the same soil complex is composed of Corryton surface soil that is yellowish brown loam (Munsell 10 YR 5/4). The CcE Complex is virtually identical, only differing by increased slope, more rocks, and a greater percent distribution of Coghill and Corryton sediments. The distribution of Coghill and Corryton sediments for the CcE Complex at the surface is more equable than the CcD Complex with 35% to 60% Coghill and 20% to 44% Corryton. The residual percentages of both complexes are composed of minor components.

USDA NRCS (Hartgrove 2006) defines the Coghill Series as formed from interbedded, leached, calcareous sandstone and shale. It is taxonomically classified as fine, mixed, semiactive, thermic Typic Hapludults. The O-horizon (0 cm to 5 cm) is composed of partially

decomposed hardwood litter. The A-horizon (5 cm to 15 cm) is a very friable, strongly acid, dark reddish brown (5YR 3/3) loam with many fine, medium, and coarse roots.

From the same soil unit the Corryton Series are formed from shale with some areas interbedded with seams of limestone or sandstone. This series is taxonomically classified as fine, mixed, semiactive, thermic Typic Hapludults. The A-horizon (0 cm to 15 cm) is a very friable, slightly acid yellowish-brown (10 YR 5/4) loam with very fine roots.

CHAPTER 5: MATERIALS AND METHODS

Soil samples. Soil was collected from the Anthropological Research Facility of the University of Tennessee, Department of Anthropology Forensic Anthropology Center (Figure B-1). A total of 1.28 acres was mapped using previously established geographic-referenced data points and ArcView 9.1. Spatial distribution of human decomposition for the ARF was determined.

Since 2000, the specific location of each corpse at the ARF has been recorded using a Trimble Pak Global Positioning System (GPS). The coordinate data were layered on the map to show the specific location of each corpse (Figure B-2). A five-by-five-meter grid was superimposed. The established units were numbered sequentially beginning with "1", starting in the southwest corner and increasing in value left to right. The frequency of human decomposition per unit was tabulated and the units were stratified by decomposition density. Five strata were established that included units with 0; 1; 2 to 5; 6 to 10; ≥ 11 decomposing corpses per 5-x-5-meter unit (Figure B-3). While the frequency tabulation was an absolute figure for a five year period, the goal of the density plot was to demonstrate the nonrandom placement of bodies on the surface at the ARF. Those areas that are flat and near the road typically have a higher density of human decomposition. Therefore, units were grouped by the amount of decomposition and nominally scaled as none, low, middle, and high.

Soil samples were collected from units following a stratified semi-random sampling strategy. The "semi-random" strategy was chosen since there were so few units of high decomposition density. Therefore, all units that contained six or more bodies were included in the study. Units containing less than five bodies however, were randomized using Microsoft Excel random

number generator and the first ten units from each remaining strata identified by the generated list were selected for inclusion. Forty units were selected; the unit centers were located with the Trimble Pak GPS and marked with a yellow plastic stake (Figure B-4).

Soil samples were collected within a 2-meter radius of the marked unit centroids. The soil was taken from the A Horizon, and was collected from within the first five centimeters; placed on ice and transported to the UT laboratory where the samples were sifted using ASTM-standard soil sieve No. 10 (2 mm mesh). Rocks, macro flora and fauna that did not pass through the sieve were discarded. The sieved samples were stored in a plastic sealable bag and placed in the freezer (-20°C). All soil samples were transported on dry ice to the Armed Forces Institute of Pathology, Washington, DC, where the samples were stored at -20°C until analyses.

Human Bone and Soil Samples. A cross-sectional sampling of fourteen different cadavers from different locations across the ARF was selected for study (Table 5-1). Samples consisted of soil and bone. The top five centimeters of soil was taken from beneath the abdomen, while either the 11th or 12th rib from each corpse was selected. The soil was handled in the same manner as other soil samples. The excised ribs were placed in a plastic bag, annotated with the date and specimen number, and placed on ice for transport to the laboratory where they were stored at -80°C until analysis.

Laboratory Methods of Soil Analysis

Soil Moisture Content. The gravimetric soil water content was determined for the collected soil samples. Gravimetric soil water content is the mass of water in the soil, and is measured as the percent mass loss in oven-dried soil (Voroney 2007). On average, 20.0 g of soil were used for determining soil moisture content. Aliquots of the homogenized soil samples were weighed and the wet mass was recorded. The soil samples were dried in a Fisher Scientific Isotemp

Table 5-1. Biological profile data for human cadavers and description of decomposition.

	Age	Sex	Race	Weight	Autopsy	PMI[1]	Unit	Body Description	Environ
A	67	M	W	114	N	48.0	142	skeletonized, dry	n.d.
B	70	M	W	259	N	47.0	86	skeletonized, dry	n.d.
C	55	M	W	172	N	46.5	87	skeletonized, dry (and collected the morning before sampling)	shaded
D	47	M	W	146	N	24.0	101	partly skeletonized, partly mummified	n.d.
E	59	M	W	n.d.[2]	N	20	82	partly skeletonized, partly mummified, sun bleached on exposed bone, amputee	semi shaded
F	70	M	B	200	N	18.0	87	half skeletonized, half mummified, uncovered	semi shaded
G	47	M	B	250	N	12.0	24	skeletonized, adipocere, semi covered with tarp	shaded
H	71	M	W	190	N	12.0	25	skeletonized, almost no soft tissue, semi covered with tarp	shaded
I	55	M	W	340	N	12.0	97	partially skeletonized, gooey, no maggots (pupal casings), covered with tarp, advanced	shaded
J	26	M	W	115	Y	11.0	166	Skeletonized	shaded
K	50	F	W	185	N	7.0	92	partially skeletonized, gooey, pupal casings, covered with tarp, advanced	exposed
L	53	M	W	n.d.	Y	9.0	117	partially skeletonized, gooey, no maggots, active	shaded
M	88	M	W	175	N	2.0	92	partially skeletonized, gooey, maggots still active, covered with tarp, active	exposed
N	68	M	W	180	N	1.0	93	partially skeletonized, gooey, liquefied, maggots and beetles, covered with tarp , active	exposed
O	43	M	W	225	N	0.5	155	skeletonized, maggots present, advanced	Semi shaded

[1] Postmortem Interval (PMI) recorded in months.

[2] No Data (n.d.)

hybridization incubator (Fisher Scientific, Pittsburgh, PA) at 85°C until there was no more loss of mass per sample tested. Measurements of soil were repeated until the difference between subsequent measures was negligible. A negligible difference was defined as a plus or minus 0.1 g difference between measures. Mass was recorded using a PL1502-S Mettler Toledo balance (Columbus, OH). The results of moisture content are expressed as a percentage of the difference in mass between the wet and dry masses (%MC = [(WM – DM)/DM]*100), where MC is moisture content, WM is wet mass, and DM is dry mass.

Soil pH. Soil acidity and alkalinity was tested using an Accumet® Research AR20 pH meter with a glass body, single junction silver (Ag) / silver chloride (AgCl) electrode (Fisher Scientific, Trenton). The meter was calibrated using auto buffer recognition of USA standardized buffer groups 4, 7, and 10. Prior to measuring any soil, a 25 mL reagent blank of distilled water was tested to verify calibration of the meter and to determine the pH of the distilled water added to the soil. The recorded pH of the distilled water was 7.55 at 25°C.

Three to five gram aliquots of homogenized soil were suspended in 1:5 (w/v) distilled water (pH = 7.55) solution in a 30 mL glass beaker. The soil water solution was stirred vigorously with a glass stirring rod to disperse soil in water. The soil was allowed to settle for 30 minutes, prior to recoding pH. Water soil suspension was maintained at room temperature (25°C). Soil pH was taken by immersing the electrode in the supernatant and then gently swirling the beakers to obtain proper contact between solution and electrodes. The electrode remained submersed until the automatic reading was obtained.

Soil Organic Matter. Soil organic matter (SOM) is the total contribution of plant and animal residues at various stages of decomposition in the soil. Excreta and dead microorganisms also contribute to SOM. For this study, SOM was determined by loss on ignition from 3.0 g aliquots

of homogenized, oven-dried sediment following Heiri et al. (2001). Since organic material turns to ash when baked at high temperatures, the organic content is simply defined as the percent mass loss between pre- and post-bake values (Storer 1984). The method is similar to determining moisture content in soil, but instead of drying soil at 85°C, the samples were placed in ceramic crucibles and baked in a Barnstead Thermoline Type 4800 muffle furnace (Dubuque, IA) at 550°C for four hours. Loss on ignition is a quick and inexpensive way to evaluate total organic content of sediments.

Total Carbon and Nitrogen. The total percent carbon and nitrogen content of the soil was determined by combustion in a pure oxygen environment using a LECO CNS-1000 elemental analyzer (LECO Corporation: St. Joseph, MI). The laboratory analyses were performed by the University of Nebraska-Lincoln Department of Agronomy. Following departmental procedures, a CHN analyzer used a combustion method to convert sample elements to simple gases (CO_2, H_2O, and N_2). The resulting gases were homogenized and extracted under controlled conditions of pressure, temperature, and volume using a chromatographic column. The homogenized gases were separated in a stepwise steady-state manner and quantified as a function of their thermal conductivities. Each measurement was duplicated to evaluate consistency of results.

Lipid-bound Phosphorous. Laboratory analyses to determine microbial biomass by lipid-phosphorus were conducted by the University of Nebraska-Lincoln Department of Agronomy following previously reported extraction and quantification methods described in Drijber et al. (2000) and Benninger et al. (2008). Microbial biomass was estimated by extracting lipid-bound phosphate following a modified Bligh and Dryer lipid extraction, and isolated phospholipid-phosphorus was quantified by colorimetric assay first described by Kates (1986).

Benninger et al. (2008) summarized the extraction method as follows. Two gram slurry of soil and 0.5 mL of deionized water was washed in 2.0 mL of methanol: chloroform (2:1). The supernatant was removed by centrifugation, and the soil slurry was resuspended in 4.0 mL methanol: chloroform: water (2:1:0.8). After centrifugation, the supernatant was combined to the previously removed supernatant. Phase separation of the polar lipid class was achieved by adding equal volumes (2.5 mL) of chloroform and 10 mM ammonium sulfate to the combined lipid extracts. After mixing and spinning, the lower chloroform layer was removed, resuspended in 2.5 mL of HPLC-grade chloroform. The chloroform extracts were combined and dried overnight under N_2. Sulfuric and nitric acids were added at a 5:1 (v/v) ratio to the evaporated extract and placed on a heating block at 130°C until samples became clear, when 2.0 mL of 6M of sodium hydroxide was added. One drop of phenolphthalein was added to the solution followed by drop-wise addition of 6M sodium hydroxide until the solution turned pink, indicating neutral pH. Extracted lipid-bound phosphorus was quantified by adding a colorimetric reagent to the acid-base solution and the absorbency was measured using a Spectronic 20 Genesys spectrophotometer (Spectronic Instruments: Garforth, Leeds, UK) at a wavelength of 880 nm. Known concentrations of phosphorus were serially-diluted and used to create a standard curve by simple log-linear regression. Sample extracts were quantified by comparison to the standard curve generated at each run. All samples were analyzed in duplicate.

Laboratory Methods of DNA Analysis

DNA extraction from soil. Extraction of total DNA from soil was completed using a commercially available extraction kit specifically designed for soils and sediments. Soil is a difficult medium to extract because of the presence and coelution of humic substances (Porteous and Armstrong 1991; Miller et al. 1999). Humic and fulvic acids are aggregates of phenolic,

hydroxyl, and carboxyl groups that form during decomposition in soil and water from highly oxidized aromatic amino acids, sugars, peptides, and aliphatic compounds (Stevenson 1982). Many of the aromatic amino acids are found in proteins of the human body. Linkages are formed among the aromatic structures by hydrogen bonding, and humic substances may chelate with metal ions and clay particles found in many soils.

Humic and fulvic acids are problematic for DNA extraction because the chemical properties are similar to that of double-stranded DNA (Watson and Blackwell 2000). Humic substances compete with DNA for binding to silica-based binding methods, which is a standard method in extraction chemistry for soil (Miller et al. 1999). Given the potential problems of coextracting PCR inhibitors directly from soil, a kit specifically optimized for soil extraction that effectively inhibits binding of humic acids in favor of DNA was chosen.

To that end, the Fast DNA Spin Kit for Soil (MP Biomedicals: Solon, OH) was selected given its success in previous extractions from difficult samples (Layton et al. 2006). Following manufacturers' reference, 400 mg aliquots of homogenized sediment were subject to cell lyses on a laboratory vortex in a 1.0 mL total volume of lysing buffer for 40 seconds. The samples were centrifuged at 14,000 g for 10 minutes to pellet debris. The supernatant was transferred to a new 2.0 mL microcentrifuge tube and 250 µL of protein precipitation solution was added. The samples were mixed by hand and centrifuged for five minutes to precipitate pellet. The supernatant was transferred to a clean 15 mL conical tube, and 1.0 mL of binding matrix was added. The samples were inverted by hand for two minutes and the silica was allowed to settle for three minutes. The silica-binding matrix was transferred to a spin filter, and centrifuged at 14,000 g for one minute and repeated until all binding matrix was added to the filter. The silica pellet was resuspended in a prepared wash, passed through the filter, and the wash was

discarded. The pellet was allowed to air dry, and then resuspended in 100 µL of elution buffer (DNase/pyrogen-free water). After centrifugation at 14,000 g for one minute, the filter was discarded, and the DNA elute was concentrated using a commercially available post-extraction clean-up kit.

Post extraction clean-up of isolated DNA was performed using the MinElute PCR purification column (Qiagen: Germantown, MD), following the manufacturers protocol. The purification procedure removes impurities that co-eluted during the DNA extraction. The column contains a silica membrane that binds DNA in a high-salt buffer and elution occurs in a low-salt buffer or water. When DNA is bound to the membrane, the impurities were removed by washing in a buffer and centrifugation, which effectively pull the impurities through the membrane. All extracted and concentrated samples were stored at 4°C for downstream applications, such as quantification, amplification, denaturing gel gradient electrophoresis, capillary sequencing, and next generation sequencing with the Roche® 454 Life Sciences instrument.

DNA extraction from bone. Soil from below the abdomen and a rib from each corpse were collected and evaluated. DNA extraction from soil was performed as reported above; bone however, followed the demineralization protocol of Loreille et al. (2007), which is a modification of that reported in Edson et al. (2004) for degraded samples. They summarized the extraction protocol as follows. The exterior surfaces of each bone were mechanically abraded with a Dremel® tool (Racine, WI), and the resulting fragments were washed three times in an ultrasonic sonicator using a different solution for each wash: 10% dilution of hypochlorus acid (HClO), sterile distilled water, and 100% ethanol. The fragments were air dried, and pulverized in a sterilized Waring MC2 blender cup (Torrington, CT). Approximately 200 mg of bone powder were demineralized in an extraction buffer (EDTA 0.5 M, 1% lauryl-sarcosinate) and

200 mL of 20 mg/mL Proteinase K, in a rotary shaker overnight at 56 °C (Loreille et al. 2007). The sample was spun to remove debris from solution, and the supernatant was transferred to a Millipore Amicon® Ultra-4 with 30,000 nominal molecular weight cut-off membrane to concentrate DNA. The extracted DNA was purified using the Qiagen MinElute PCR Purification Kit following the manufacture's procedures. The DNA was eluted from the filter in a final volume of 100 µL of sterile water.

Quantification of DNA Extract. Purified DNA extract was quantified using a NanoDrop 2000 Spectrophotometer (Thermo Scientific: Waltham, MA). The NanoDrop is an instrument that measures the quantity of double-stranded DNA in a single aliquot of aqueous extract. Following the Beers-Lambert law of light absorbency, double-stranded DNA concentration is determined based on the absorbency of ultraviolet light at a wavelength of 260 nm (Schy and Plewa 1989). The purity of the DNA extract is determined by the A260/A280 ratio. A high ratio (>2.0) suggests the presence of protein, which absorbs UV-light at 280 nm. A low ratio (<1.5) typically demonstrates coelution of single stranded nucleotides (RNA) that absorbs UV-light at 230 nm. Final concentrations of DNA are reported as ng μL^{-1}, which were determined from 1.0 to 1.5 µL of extract.

Polymerase Chain Reaction (PCR). The polymerase chain reaction (PCR) is an analytical technique of high sensitivity that amplifies a defined section of a targeted molecule (Mullis and Faloona 1987) using specific oligonucleotide primers and a thermostable DNA polymerase enzyme isolated from the gram-negative bacterium *Thermus aquaticus.* PCR thermocycling produces a single end-point product that was visualized by gel electrophoresis using the Lonza FlashGel® System (Rockland, ME). When amplified product was present, it appeared as a band under ultraviolet light. Therefore, the final response of amplification is binary; indicating either

presence or absence of the target molecule, while little is learned about initial target concentration. That stated however, traditional PCR is a robust laboratory method that enables the production of ample target molecules for additional investigation, such as cloning, DGGE, capillary sequencing, and next-generation sequencing.

Amplification. Microbial and human DNA was analyzed using a variety of laboratory platforms. Polymerase Chain Reaction was performed on extracted DNA from all soil and bone samples. PCR product was used for down-stream applications directed at identifying the microbial community structure. For this study, extracted and concentrated DNA was subjected to PCR amplification using previously established primers (Table 5-2) targeting specific DNA regions of bacteria (Lane 1991, Muyzer et al. 1993; Lee et al. 1996; Marchesi et al. 1998), fungi (White et al. 1990; Sandhu et al. 1995), and human mitochondria (Gabriel et al. 2001; Edson et al. 2004). Mixtures of amplified bacterial and fungal taxa were separated by denaturing gradient gel electrophoresis (DGGE) and identified through direct sequencing by capillary electrophoresis of excised bands. Bacterial PCR product was also subjected to a nested emulsion PCR (emPCR) and sequencing using the Roche 454 next-generation sequencer, first described by Margulies and colleagues (2005). The next generation sequencing method was used to establish specific bacterial components of the microbial community.

Bacteria. Specific regions of bacterial DNA that code for a highly-conserved region of the 16S rRNA gene of the small ribosomal subunit were targeted in order to evaluate bacterial diversity at the UT ARF soils. Ribosomal RNA is an essential component of the prokaryotic ribosome; instrumental for protein synthesis of all bacteria. The 16S rRNA gene has stretches of stable sequence interspersed with many regions of variable sequence. The conserved regions are similar for all bacteria, while the interspersed variable regions are useful for separating

Table 5-2. Primer sequences, target regions, and annealing temperatures.				
	Position	**Sequence (5' → 3')**	**T_A [a]**	**Reference**
Bacteria [b]				
16S	F63	CAGGCCTAACACATGCAAGTC	55	Marchesi et al. 1998
	R1387	GGGCGGWGTGTACAAGGC		
	F341	CCTACGGGAGGCAGCAG	55	Muyzer et al. 1993
	R534	ATTACCGCGGCTGCTGG		
	F338	ACTCCTACGGGAGGCAGCAG	53	Lane 1991
	R533	TTACCGCGGCTGCTGGCAC		Lee et al. 1996
Fungi [c]				
28S	F45	ATCAATAAGCGGAGGAAAAG	60	Sandhu et al. 1995
	R843	CTCTGGCTTCACCCTATTC		
18S	F1773 (ITS1)	TCCGTAGGTGAACCTGCGG	55	White et al. 1990
28S	R57 (ITS4)	TCCTCCGCTTATTGATATGC		
Human [d]				
PS1	F16190	CCCCATGCTTACAAGCAAGT	56	Edson et al. 2004
	$R16410_{m19}$	GAGGATGGTGGTCAAGGGAC		
PS2	F15989	CCCAAAGCTAAGATTCTAAT	56	Gabriel et al. 2001
	R16251	GGAGTTGCAGTTGATGT		Edson et al. 2004
MPS1A	F15989	CCCAAAGCTAAGATTCTAAT	50	Gabriel et al. 2001
	R16158	TACTACAGGTGGTCAAGTAT		
MPS1B	F16112	CACCATGAATATTGTACGGT	50	Gabriel et al. 2001
	R16251	GGAGTTGCAGTTGATGT		Edson et al. 2004
MPS2B	F16268	CACTAGGATACCAACAAACC	48	Gabriel et al. 2001
	R16410	GAG GATGGTGGTCAAGGGAC		

[a] Annealing temperature for the listed primer set.
[b] Nucleotide positions of bacterial primers correspond to coordinates of a reference *E. coli* 16S gene.
[c] Nucleotide positions of fungal primers correspond to coordinates of a reference *S. cerevisiae* 28S gene.
[d] Nucleotide positions of human primers correspond to coordinates of the revised Cambridge Reference Sequence (Anderson et al. 1999).

taxonomic units or species. Amplification of all bacteria was completed using previously reported universal primers targeting regions of the 16S rRNA gene (Table 5-2; Figure 5-1).

PCR reactions were carried out in a 50 μL reaction volume. Each reaction tube contained 2.0 μL of each primer (10uM), 5 μL of 10X PCR buffer, 5 μL of 25 mM MgCl, 4 μL of 10 mM dNTPs, 5 μL of non-actylated BSA (2.5 mg mL^{-1}), 1.5μL of Taq Gold polymerase, and 2 μL of DNA template. The final volume was adjusted to 50 μL by addition of uv-treated water. Thermocycling conditions varied slightly depending on annealing temperature of the primer sequence and length of the amplicon. Primers with high GC content required slightly higher annealing temperature, and longer amplicons required longer extension times. Initial laboratory investigation identified Marchesi and colleagues' (1998) universal bacteria primer set 63F/1387R as the most consistent results for UT ARF soil samples. In this case, performance was determined by absence of amplification of target molecules for all negative-control samples, as determined by FlashGel® electrophoresis. For these primers, every reaction began with initial denaturing at 94°C for 10 minutes followed by 36 cycles of 94°C for 60 seconds, 55°C for 60 seconds, and 72°C for 90 seconds. The last cycle was held at 72°C for seven minutes, before the samples were stored at 4°C.

Fungi. Target sequences of fungi were derived from two different, and yet highly-conserved regions of nuclear rRNA genes (Sandhu et al. 1995; White et al. 1990). Like bacteria, the rRNA genes have stretches of stable sequence interspersed with variable regions (Table 5-2; Figure 5-2). The conserved regions are similar for most fungi, whereas the non-coding or internal transcribed spacer regions are variable and useful for separating taxonomic units.

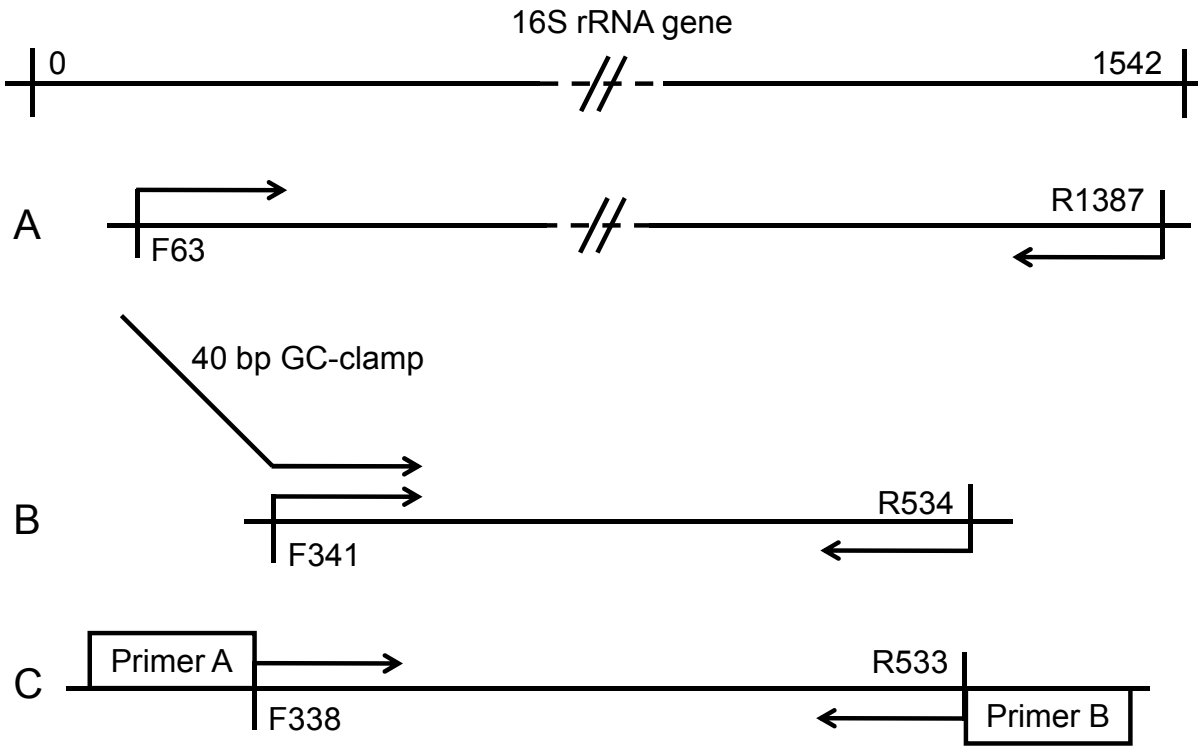

Figure 5-1. Schematic diagram of relative position of each of the three universal bacterial primers sets used. Redrawn from Lane 1991, Muyzer et al. 1993; Lee et al. 1996; Marchesi et al. 1998. Diagram A produces a 1.3 kb amplicon. Diagram B amplifies a smaller section and was used for DGGE, hence the 40 bp GC-clamp. Diagram C illustrates primer configuration used with the Roche® 454 Life Sciences instrument.

The first region targeted corresponds to base pair coordinates 45 to 64 and 825 to 843 of the reference *Saccharomyces cerevisiae* 28S gene, for the forward and reverse primers, respectively (Sandhu et al. 1995). Sandhu and colleagues (1995) reported that their fungal primers amplify a highly variable 799 bp product that is useful for sorting fungal species. The primers were identified by sequencing and aligning variable regions of 28S rRNA genes for all fungi amplified by their laboratory (Shandu et al. 1995). Primers of the second region evaluated are derived from the nuclear internal transcribed spacer (ITS) regions that are located between the small and large subunit RNA genes. The forward primer is positioned near the tail end of the small subunit (18S) and the reverse primer is positioned near the beginning of the large subunit (28S). These primers amplify a region that evolves quickly and varies among species within a genus or even among isolated populations of the same species (White et al. 1990). The repeat units have coding regions for forming a single ribosome; the number of repetitive regions may vary among species.

PCR reactions were carried out in 50 µL reaction volume. Each reaction tube contained 2.0 µL of each 10 uM ITS1 and 10 uM ITS4 primer, 5.0 µL of 10X PCR buffer, 5.0 µL of 25mM $MgCl_2$, 4 µL of 10 mM dNTPs, 5.0 µL of 2.5 mg mL^{-1} non-actylated BSA, 1.5 µL of Taq Gold polymerase, 2.0 µL of DNA template. The final volume was adjusted to 50 µL be adding

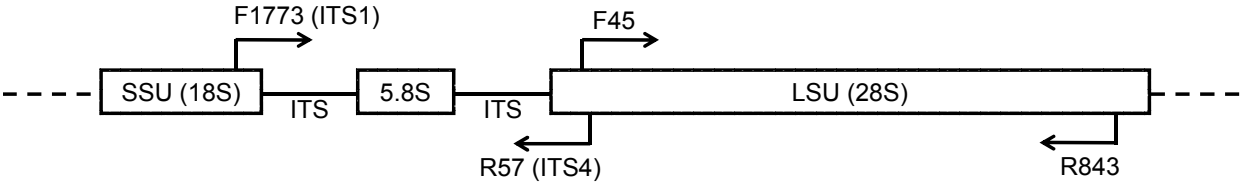

Figure 5-2. Schematic diagram of relative position of each universal fungal primer set used. Redrawn from White et al. (1990) and Sandhu et al. (1995).

UV-treated water. Every fungal amplification reaction using ITS1 and ITS4 began with initial denaturing at 94°C for 10 minutes followed by 30 cycles of 94°C for 45 seconds, 55°C for 45 seconds, and 72°C for 60 seconds (White et al.1990). The last cycle was held at 72°C for seven minutes, before the samples were stored at 4°C.

Human. PCR assays were performed using previously reported (Gabriel et al. 2001; Edson et al. 2004) primers for the first hypervariable region (HV1: 15971-16410 bp) of the human mtDNA control region (Figure 5-3).

Numbering of nucleotide base position followed the revised Cambridge Reference Sequence (Anderson et al. 1999). Five different sets of primers were used for amplification of human mtDNA. Primer Set 1 and 2 (PS1 and PS2) produce two amplicons that cover the entire HV1 region, while the mini-primer sets 1A, 1B, and 2B produce three smaller amplicons, but when aligned during data analysis cover positions the entire HV1 region from positions 15989 to 16410 (Figure 5-4). The small amplicons are useful for analyzing DNA from degraded samples. The mini-primer sets were used on soil samples removed from below an actively decomposing corpse, while the larger PS1 and PS2 were used to amplify DNA from bone.

Thermocycling conditions for primer sets one (PS1) and two (PS2) began with initial denaturating for 10 minutes at 96°C followed by 38 cycles of 20 seconds at 94°C, 20 seconds at 56°C, 30 seconds at 74°C, and followed by a hold at 4°C upon completion (Edson et al. 2004). Reaction volumes and concentrations for each PS reaction tube contained 2.0 µL of each 10 uM primer (e.g., forward and reverse), 5.0 µL of 10X PCR buffer, 5.0 µL of 25 mM $MgCl_2$, 4 µL of 10 mM dNTPs, 5.0 µL of 2.5 mg mL^{-1} non-actylated BSA, 1.0 µL of Taq Gold polymerase, 2.0 µL of DNA template. The final volume was adjusted to 50 µL with UV-treated water.

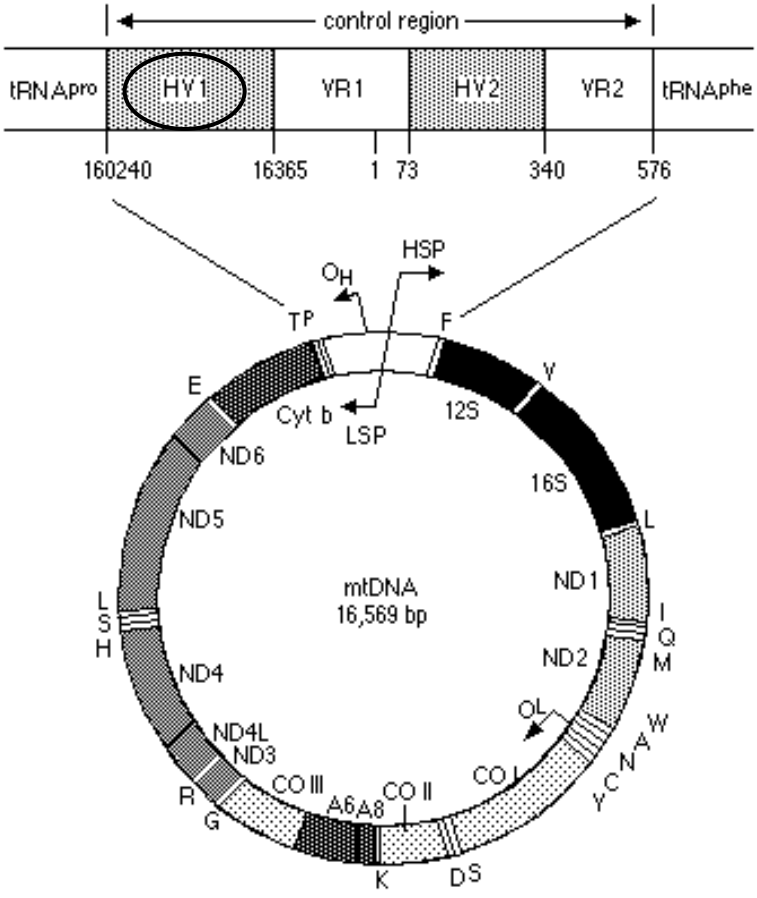

Figure 5-3. Schematic diagram of the mtDNA genome (Holland and Huffine 2000) showing the location of the non-coding Control Region on either side of the origin (O_H), which is nucleotide position 0 following the revised Cambridge Reference Sequence (Anderson et al. 1999). mtDNA sequences for this project were derived from HV1 region (circled).

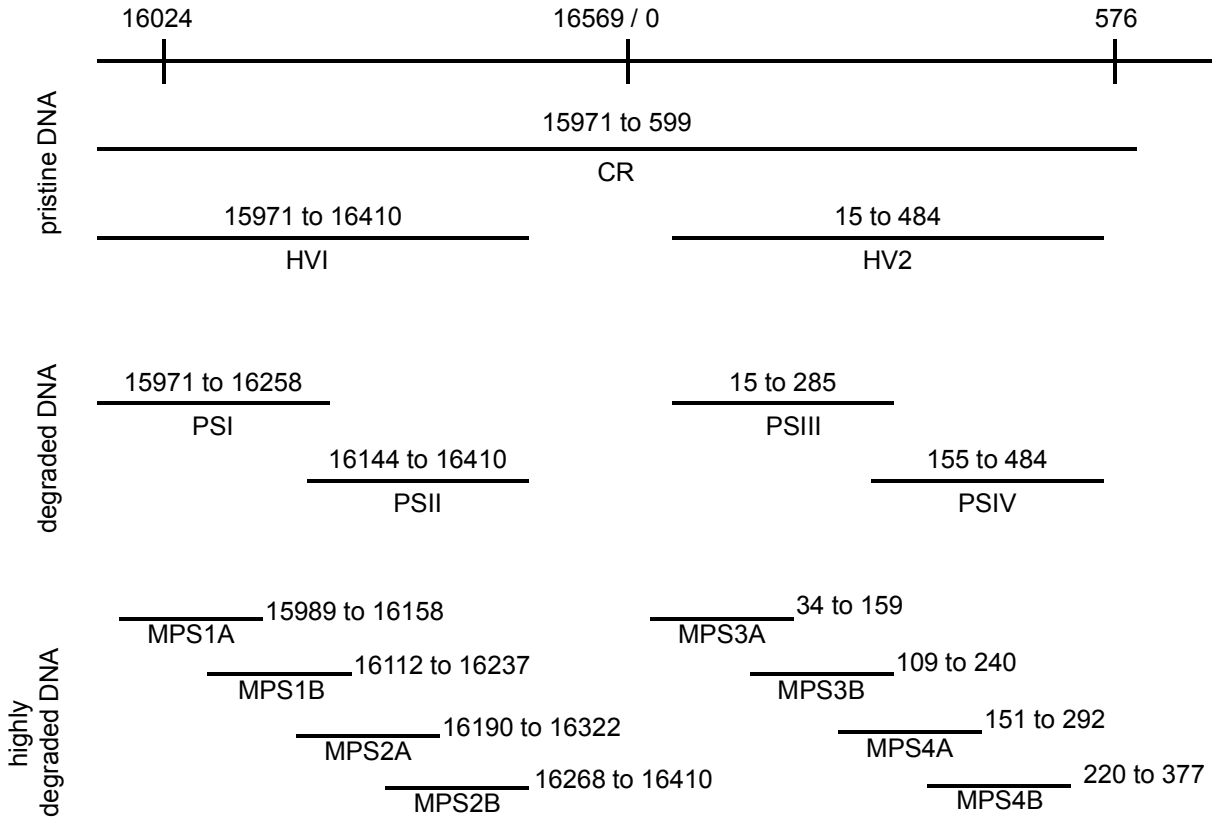

Figure 5-4. Schematic diagram of the mtDNA control region showing amplicon location of the mtDNA primers (redrawn from Holland and Huffine 2000). For this study only PSI, PSII, MPS1A, MPS1B, and MPS2B were used.

Thermocycling conditions of the mini-primer sets followed current AFDIL casework procedures, which are modified from Gabriel et al. (2001) and Edson et al. (2004). Standard procedures are described as follows. Mini-primer sets 1A and 1B were amplified after 7 minutes of enzyme activation at 94°C followed by 45 cycles of 20 seconds at 94°C, 30 seconds at 50°C, 30 seconds at 72°C. The final cycle was held for 7 minutes at 72°C before storing at 4°C. Mini-primer set 2B was amplified with a nearly identical cycling regime, different only in an annealing temperature of 48°C. Reaction volumes and concentrations of each sample for all MPS reactions contained 2.0 µL of each 10 uM primer, 5.0 µL of 10X PCR buffer, 5.0 µL of 25 mM $MgCl_2$, 4 µL of 10 mM dNTPs, 5.0 µL of 2.5 mg mL^{-1} non-actylated BSA, 1.0 µL of Taq Gold polymerase, 2.0 µL of DNA template. The final volume was adjusted to 50 µL with UV-treated water.

Sequencing of Human mtDNA. Each amplification reaction was purified using a master mix of exonuclease I (EXO) and shrimp alkaline phosphatase (SAP; USB Corporation, Cleveland, OH) in a ratio of 2U EXO to 0.1U SAP for each l µL of PCR product 2U (Lorielle et al. 2007). Each reaction was heated to 37.0 °C for 45 min followed by a second hold at 80.0 °C for 20 min. Samples were then stored at 4.0 °C until sequenced.

Purified PCR products were then sequenced with the Big Dye ABI PRISM® Dye Terminator Cycle Sequencing Ready Reaction Kit with AmpliTaq® DNA Polymerase, version 1.1 (Applied Biosystems: Foster City, CA) following the manufacture's protocol and described in Edson et al. (2004). Two sequencing reactions were completed for each sample being sequenced, since one reaction included a single primer (e.g., forward or reverse). Each reaction mixture contained 2.0 µL sequencing primer (10 µM), 1.5 µL of Big Dye Terminator Cycle sequencing kit, 0.5 µL dGTP ABI PRISM® Dye Terminator, 6.0 µL Sequencing Buffer, and 8.0 µL of sterile distilled

water. Final reaction volume was adjusted to 20 µL with 2 µL of purified PCR product. Thermocycling conditions for the sequencing reactions were carried out in 25 cycles of 96°C for 15 seconds, 50°C for 5 seconds, 60°C for 2 minutes, and held at 4°C until analysis.

Sequencing reactions were analyzed on an Applied Biosystems 3100 Genetic Analyzer (Foster City, CA) following purification with AGTC columns (Edge Biosystems: Gaithersburg, MD) and mixing with 10 µL of Hi-Di formamide. Data analysis of mtDNA amplicon sequences were completed using Sequencher™ version 4.8 software developed by Gene Codes Corporation (Ann Arbor, MI). This software was used to align and build a complete mtDNA HVI sequence from contiguous forward and reverse sequences.

Denaturing Gradient Gel Electrophoresis. Extraction of nucleic acids following the above protocol provided DNA of multiple organisms, including that of resident soil microfauna and flora, insects, and even humans. Initial attempts were made to separate different bacterial and fungal taxa using DGGE in conjunction with a combination of the bacterial and fungal primers listed above.

Amplification of 16S and 28S subunits of the rRNA gene using the universal primers listed above produce a mixture of amplicons originating from various bacteria and fungi. Despite the universality of the primers, the internal DNA sequences are variable, making them useful for taxonomic classification. Denaturing gradient gel electrophoresis was used to separate mixtures of amplified PCR product.

The procedure for DGGE requires amplified PCR product to be loaded at the top of an acrymilide gel containing a gradient of denaturing chemicals (urea and formamide) to separate the different taxa. As the DNA travels further from the starting point via electrophoresis, the denaturing chemical increases. Taxon separation was achieved based on the frequency of AT

and GC content. The two complementary pairs of nucleic acids that make up DNA (A: T and G: C) differ in the number of hydrogen bonds between the bases. Adenine and thymine are joined by two H-bonds, where as guanine and cytosine are joined by three H-bonds. The PCR product that has the higher GC content requires a higher concentration of denaturant and therefore travels further down the gel.

Once different taxa are separated on a gel, the bands, theoretically corresponding to a specific taxon, are excised and sequenced. The sequences are then compared to a database of known organisms. In this case, a NCBI BLAST of the obtained sequences was completed to determine Genera and / or species following a 95% similarity index cutoff point.

Extracted DNA from UT ARF soil was submitted to Microbial Insights, Inc (Rockford, TN) for amplification and DGGE. DNA of the bacterial 16S rRNA gene was amplified using primers 341F and 519R (Muyzer et al. 1993) with modifications. The 341-forward primer had an additional 40-nucleotide GC-rich sequence affixed to the 5-prime end of the forward primer. This GC-clamp is an important modification of the 341-forward primer for DGGE because the clamp increases the stability of the transitional molecules as it denatures (Muyzer et al. 1993). Thermocycling conditions consisted of an initial 10 minutes of for denaturing at 94°C, then 34 cycles of 94°C for 30 seconds, 60°C for 45 seconds, and 72°C for 45 seconds, followed by a final five minute extension phase at 72°C. Each PCR reaction contained 1.25 units of Clontech Advantage 2 polymerase (BD Biosciences: San Jose, CA) and 10 pmol of each primer. Final volume was adjusted to 25 µL by addition of nanopure water. Amplification was performed on a Robocycler™ PCR block (Stratgene: La Jolla, CA).

Following Microbial Insights standard laboratory procedures, DGGE analyses were performed using a D-code 16/16 cm gel system, maintaining a constant temperature of 60°C in

0.5x TAE buffer (20 mM Tris-acetate. 0.5 mM EDTA, pH 8.0). Denaturing gradients were formed using 8-10% acrylamide and 30-60% denaturant where 100% denaturant is defines as 7M urea, formamide. Gels were run at 55 volts for 16 hours. Bands within the gel were stained in 0.5x TAE buffer with ethidium bromide (0.5 mg L^{-1}). Dominate bands were excised, eluted in 50 µL of nanopure water and placed at -20°C for one hour to overnight and re-amplified using the same primers and thermocycling conditions listed above. DNA purification of the PCR product was completed following the manufactures directions for the Ultra Clean PCR Clean-up DNA Purification Kit (MoBio Laboratories: Carlsbad, CA). The purified product was sequenced using the 341f primer by capillary sequencing at the University of Tennessee, Knoxville Molecular Biology Resource Facility.

Next-Generation Sequencing. Extracted and purified DNA from both soil and bone was amplified using universal bacterial primers F63 and R1387 of the 16S rRNA gene to produce a 1.3kb PCR product. The amplicon product was submitted to the University of Tennessee Center for Environmental Biotechnology for high-throughput sequencing using Roche® 454 Life Sciences (Branford, CT) instrument, which combined emulsion PCR and pyrosequencing (Ronaghi et al. 1998) in high-density picoliter reactors (Margulies et al. 2005). This relatively new integrated analytical platform has the ability to produce millions of high-quality sequences by emulsion-based clonal amplification (emPCR) instead of traditional laboratory vector-based cloning. Clonal amplification permits targeted-molecule amplification from complex mixtures of amplified product. *In vitro* clonal amplification supplants vector-based clones grown in competent *E. coli* cells by significantly increasing the amount of data produced for analysis (Roesch et al. 2007; Keijser et al. 2008), while reducing laboratory time and total cost associated with amplification, cloning, and sequencing (Margulies et al. 2005).

Amplification Library Preparation. The initial step for clonal amplification required development of an amplicon library of the 16S rRNA genes extracted and amplified from the mixture of bacterial sequences. The 1.3kb PCR product was reamplified using 454-specific primer adapters A and B and a nested primer pair of F338 and R533 (Table 5-3). The fusion primers A and B were affixed to the 5-prime end of each strand. The fusion primers consisted of a 20-mer sequence that included a 4-bp bead-binding tag that facilitated the binding of amplicons to the capture oligonucleotide already annealed to the streptavidin-biotin bead for downstream emPCR and pyrosequencing. The fusion primers also contained a bar-code of an 8-bp sequence. Barcodes were specific to individual soil samples and where combined and analyzed together. The barcoded samples allowed specific samples to be segregated from the mixture during data analysis. A 2-bp internal binding set was attached to the 3-prime end of the barcode that was attached to either the 5-prime end of either F338 or R553 universal bacterial primer (Lane 1991). To complete amplicon library preparation, the double-stranded nested PCR products that contained the special A and B adapters were carried out in a traditional PCR amplification process to generate millions of DNA target amplicons that included the fusion sequences, bookended on the target amplicon sequence.

Emulsion PCR (emPCR). The amplified product containing fusion primers A and B were purified and concentrated following standard molecular laboratory techniques. One to five nanograms of purified double-stranded DNA of the amplicon library was immobilized on a streptavidin-biotin bead that contained a capture oligonucleotide. This process loaded a single template sequence onto a single micron-sized bead. With template attached, the amplification beads were added to a water and oil mixture containing PCR reagents and amplification enzyme. The reagent mixture was emulsified by oscillation creating an oil and water mixture, whereby

Table 5-3. Roche® 454 Life Sciences high-throughput amplification and sequencing primers.				
Name	**Roche Fusion Primers**	**Bar Code & Spacer**		**Forward Primer(16S 338)**
A1338F	GCCTCCCTCGCGCCATCAG	AACCATGC	TC	ACTCCTACGGGAGGCAGCAG
A2338F	GCCTCCCTCGCGCCATCAG	ACACAGAG	TC	ACTCCTACGGGAGGCAGCAG
A3338F	GCCTCCCTCGCGCCATCAG	AACGCGTT	TC	ACTCCTACGGGAGGCAGCAG
A4338F	GCCTCCCTCGCGCCATCAG	ACTCAGTG	TC	ACTCCTACGGGAGGCAGCAG
A5338F	GCCTCCCTCGCGCCATCAG	AGACCACT	TC	ACTCCTACGGGAGGCAGCAG
A6338F	GCCTCCCTCGCGCCATCAG	CGTTCGTT	TC	ACTCCTACGGGAGGCAGCAG
A7338F	GCCTCCCTCGCGCCATCAG	CTGTCTGT	TC	ACTCCTACGGGAGGCAGCAG
A8338F	GCCTCCCTCGCGCCATCAG	CGTAATGC	TC	ACTCCTACGGGAGGCAGCAG
A9338F	GCCTCCCTCGCGCCATCAG	CAGTCTCT	TC	ACTCCTACGGGAGGCAGCAG
A10338F	GCCTCCCTCGCGCCATCAG	CCAATACG	TC	ACTCCTACGGGAGGCAGCAG
				Reverse Primer (16S 533)
B1533R	GCCTTGCCAGCCCGCTCAG	GACAGACA	CA	TTACCGCGGCTGCTGGCAC
B2533R	GCCTTGCCAGCCCGCTCAG	GAAGCAAC	CA	TTACCGCGGCTGCTGGCAC
B3533R	GCCTTGCCAGCCCGCTCAG	GCAACGTT	CA	TTACCGCGGCTGCTGGCAC
B4533R	GCCTTGCCAGCCCGCTCAG	GCGCATAT	CA	TTACCGCGGCTGCTGGCAC
B5533R	GCCTTGCCAGCCCGCTCAG	GCTTCCTA	CA	TTACCGCGGCTGCTGGCAC
B6533R	GCCTTGCCAGCCCGCTCAG	TAATCCGG	CA	TTACCGCGGCTGCTGGCAC
B7533R	GCCTTGCCAGCCCGCTCAG	TAGGAAGC	CA	TTACCGCGGCTGCTGGCAC
B8533R	GCCTTGCCAGCCCGCTCAG	TCAGTCTC	CA	TTACCGCGGCTGCTGGCAC
B9533R	GCCTTGCCAGCCCGCTCAG	TGACACAC	CA	TTACCGCGGCTGCTGGCAC
B10533R	GCCTTGCCAGCCCGCTCAG	TGGTGTTG	CA	TTACCGCGGCTGCTGGCAC

each droplet contained an appropriate amount of PCR reagents and a single capture bead for the amplification of a single DNA molecule following standard thermocycling conditions. At the end of thermocycling the emulsion is broken freeing the beads that are then enriched and purified by mixing magnetic beads that only adhere to the DNA-positive beads. The isolation and capture of the DNA-positive beads were then place in a PitoTiterPlate™ for sequencing-by synthesis.

Pyrosequencing (sequencing by synthesis). After library preparation and emPCR, DNA bound to the capture beads were denatured by washing with NaOH. Now containing single-stranded DNA (ssDNA), the beads were added to a PicoTiterPlate. Through a proprietary process and size restrictions of the wells, only one capture bead was placed in a single well. Each of the 1.6 million wells per plate also contained sequencing enzyme beads and packing beads. The addition of the ssDNA, sequencing enzyme and packing beads contained appropriate reagents for simultaneous sequencing of each bead. The PicoTiterPlate was positioned on the 454 instrument for sequencing, where the wells of the plate were washed sequentially with each of the four dNTPs (TAGC), and always in the same order. If an exposed nucleotide of the ssDNA template was complementary to the specific dNTP wash, then the nucleotide from the wash was annealed for elongation of the dsDNA molecule. Once incorporated a chemiluminescent response was promulgated by the release of a pyrophosphate molecule that was converted to ATP in the presence of adenosine phosphosulfate and sulfurylase. ATP in turn drove the luciferase-mediated oxidation of luciferin creating oxy-luciferin and light. After each wash the emitted light was read by in an internal CCD camera. The intensity of the emitted light was directly proportional to the number of added nucleotides, which was converted into a

recognizable sequence determined by reaching threshold emission and the specific nucleotide wash cycle.

Statistical Analyses

Abiotic Data. All datasets were evaluated for normality and equality of variances. If data sets were normally distributed then standard t-tests and analysis of variance (ANOVA) were used to determine significance, on the other hand non-normally distributed data were evaluated with nonparametric Mann Whitney U tests and analysis of similarity (ANOISM). An alpha of 0.05 was used for all tests of significance regardless of parametric or nonparametric approach.

Nonparametric Mann Whitney U tests were applied to test for significant differences between pairs of the decomposition density bins using the raw data for each of the seven-recorded variables (Moisture content, pH, SOM, C, N, P, and DNA). The raw data for all variables were log-transformed (base 10) and evaluated by Principle Components Analysis (PCA) to determine the distribution of samples in multivariate two-dimensional space. Significant differences based on decomposition bin were assessed for the recorded component scores, and the first and second component scores were plotted against each other. All statistical analyses described above were performed using a combination of SPSS 15.0, Primer v6, and the online RDP.

Biotic Data. Quality-checked sequences covering the V3 region of the 16S rRNA gene derived from the Roche 454 sequence output files were trimmed and aligned using the pyrosequencing pipeline of the Ribosomal Database Project (RDP) (Cole et al. 2009). Trimmed sequences removed the key tags and fusion primers, while the alignment algorithm positioned the sequence files against *E. coli*. After initial processing, the trimmed and aligned sequences were assigned to the most parsimonious bacterial taxonomy following *Bergey's Taxonomic Outline of the Prokaryotes* (Garriety et al. 2004) using RDP-Classifier (Wang et al. 2007). The

RDP-Classifier assigned sequences to a hierarchical structure using a Naïve Bayesian classification algorithm, which assumed independence of all data features (i.e., sequences) and permitted only parent-child relationships (Cheng and Greiner 2001). The classification algorithm was derived from text/word based classification schemes, where oligos of eight base pairs were considered a word. A sequence was assigned to a specific taxon that provided the highest probability score based on the number of "words" occurring in a query (Wang et al. 2007). Each queried sequence was accompanied by a bootstrapped confidence value. Wang and colleagues (2007) described that the confidence in the assignment was based on the number of times a genus was selected from 100 bootstrap trials, and higher-order taxa confidence values were the sum of all genera scores generated for a sequence (Wang et al. 2007). Overall classification at read lengths of 200 bp was determined to be 96.8% and 83.2 % correct classification for bacterial ranks order and genus, respectively. For this study, the RDP default confidence value threshold of an 80% bootstrap cut-off was used for classification of bacterial orders of obtained sequences.

A biologic matrix of bacteria taxonomy by sample was created based on the trimmed and quality checked sequences derived from the Roche® 454 sequencer and RDP-Classifier. A biologic matrix is constructed with sample units arranged in columns against observed taxonomic orders arranged in rows. A general characteristic of a biologic matrix will include frequency counts of observed taxonomic units per sample, and it will include many cells with zero value since there are often many rare taxonomic units among sample units. The biologic matrix was analyzed using Primer v6 (Clarke and Gorley 2006) following methods previously applied by Parkinson (2009) during her analysis of bacterial community structure of terminal

restriction fragment length polymorphisms (TRFLP) and DGGE data from decomposing pigs and humans. Analysis of the raw data was performed using Microsoft Excel.

For this study the frequency distribution of taxonomic orders by samples was used to generate rank-ordered abundance curves and rarefaction curves. Comparison of taxonomic order abundances across decomposition bins within the facility was done using matched rank abundance plots of the frequency data. Matched rank abundance plots provide a quick visual assessment for the level of congruence among the sample sites since one site (None) was chosen as the reference plot for comparison to other bins (Low, Middle, and High).

One problem of plotting the number of identified taxa by the number of identified individuals is that the distribution is sensitive to differences in overall sample size. Therefore, raw frequency distributions were converted to relative abundances, and rarefaction curves were generated in order to eliminate bias introduced due to differences in sample size. A rarefaction curve is an estimate of taxa by any given number of individuals. In other words, at any value along the x-axis (i.e., total number of organisms) there is a corresponding estimated number of species present. This estimate is generated from the entire biotic matrix.

Graphical analyses of abundance were followed by basic univariate biodiversity statistics on the standardized biologic matrix, which included the Pielou's taxon evenness, Margalef's index of taxon richness, and the Shannon index. These diversity measures were calculated using Primer v6 DIVERSE routine. Clarke and Warwick's (2001) description of these measures are repeated here.

Pielou's evenness is a measure that describes the equality of proportions of taxa distributed in a sample. Pielou's measure (J') is defined as $J' = H' / lnS$, where S is the number of species (taxon) observed and H' is the Shannon index (see below).

Margalef's index is a measure of taxon richness, which is the total number of identified unique taxon. This measure is sensitive to sample size, as larger samples sizes will almost always have a greater number of identified taxon than smaller sample sizes. Richness values are also susceptible to populations with high evenness. If taxa are evenly distributed, then the probability of sampling one of any taxon is as likely as sampling any other taxon. On the other hand, if a population has low evenness and is dominated by only a few species, then the probability of recovering the rarer taxon is much less than a sampling of the most abundant taxon. This sensitivity to sample size bias is partially corrected with the Margalef index since taxon richness is roughly normalized for sample size. Margalef's index holds that species richness (SR) = $(S - 1) / lnN$, where S is the number of identified species (taxon) and N is the number of individuals.

The Shannon index provides a rough measure of diversity that is much less biased by sample size than species richness measures, and has been used quite extensively in studies of ecological diversity. The index is defined as $H' = - \sum (P_i) (lnP_i)$, where P_i is the fraction of the ith taxon of the total assemblage. High positive values are suggestive of high diversity.

The standardized biologic matrix was then log-transformed. The standardized and log-transformed data reduced the influence of highly abundant orders, and in turn gave weight to less abundant or rare taxa. After data transformation, a Bray-Curtis (BC) similarity matrix was created following the Primer v6 routine. The BC similarity coefficients were generated on the data using 50 restarts, producing a sample-by-sample matrix, where similarity was determined by a value between 0 and 100. High values indicated more similarity and lower values indicated less similarity between the two samples.

Due to the high frequency of zeros in a biological matrix, nonparametric analyses were used to evaluate the data in relation to the amount of decomposition. Total group and pairwise significance by factor (i.e., decomposition bin) values were assessed by analysis of similarity (ANOISM), a nonparametric multivariate corollary to analysis of variance (ANOVA) on the BC matrix. ANOSIM values produce a correlation coefficient between -1 and 1, where a high value indicated a correlation in abundance between two samples, whereas a low value indicated an inverse relation. Values near 0 suggested little separation of the two samples evaluated.

Multi-Dimensional Scaling (MDS) of the BC matrix was used to create nonparametric ordination plots; a method similar to 2D and 3D principal components analysis (PCA). The MDS plots maximized the sum of pairwise differences between all possible combinations of samples and placed the samples in two or three dimensional space. The closer two samples are to one another on the plot, the more similar they are to one another in relation to samples that are further away.

Hierarchical cluster analysis (CLUSTER) was performed in PRIMER-E v6 on the BC matrix, and was then layered over the MDS data in order to identify significantly different clusters of samples at varying levels of similarity. Complete linkage, also known as furthest neighbor, was selected as the mode of linkage. Significant clusters (structure in the data) were identified by similarity profile permutation tests (SIMPROF), a routine of PRIMER-E v6.

The underlying BC similarity matrix of the biotic data was matched to the environmental data matrix formed by PCA on Euclidean distances between pairs of samples. The matching of the two data matrices occurred by maximizing the rank correlation between the biotic and abiotic similarity matrices, while also evaluating for collinearity issues of abiotic variables.

CHAPTER 6: RESULTS

Abiotic Environmental Data

Evaluation of the raw data (Table C-1) for the eight environmental variables by univariate nonparametric tests identified significant differences for most variables when comparison was made between samples from within the facility to those outside the facility, while differences among the decomposition bins within the facility were limited. Multivariate analysis by principle components analysis identified a specific pattern among the samples taken below the actively decomposing samples.

Soil pH. The pH values for all soil samples in the study have a mean value of 6.46, and standard deviation of 0.77. Highest and lowest values were 7.98 and 4.82, respectively. Pairwise comparisons between bins identified significant differences, while there were no significant differences ($p > 0.05$) among pH values of the designated decomposition density bins inside the facility despite there being an overall higher pH for High in comparison with bins inside the facility. Significant differences were identified ($p \leq 0.05$) between the negative control soil samples outside the facility and soil samples collected from any of the identified decomposition bins (None, Low, Middle, and High) within the facility. Soil pH values between the negative controls and the pooled active-decomposition samples were not significantly different ($p > 0.05$). The spatial distribution of measurement values in relation to decomposition density are provided in Figure D-1 and the probability values and Mann Whitney U test scores are presented in Table E-1.

Soil Moisture Content. For all samples ($n = 70$) the mean percentage of soil moisture content was 11.36% and a standard deviation of 7.51%. Within the facility there were no significant

differences ($p > 0.05$) in the percentage of soil moisture between bins, except for the High versus Low, and Middle decomposition bins. Pooled samples from the Active decomposition sites across the facility were significantly different ($p \leq 0.05$) from the Middle and High decomposition bins, but not bins Low and None. Significant differences ($p \leq 0.05$) were identified between the negative control soil samples outside the facility and all soil samples collected from any of the identified decomposition bins (None, Low, Middle, High, and Active) within the facility. The spatial distribution of measurement values in relation to decomposition density are provided in Figure D-2. Probability values and Mann Whitney U test scores are presented in Table E-2.

Soil Organic Matter. The mean percent organic content determined by loss-on-ignition was determined to be 1.53%, with a standard deviation of 0.70%. There were no significant differences ($p > 0.05$) in the percentage of soil organic matter among the designated decomposition density bins within the facility, including the pooled Active decomposition bin. The only significant differences observed ($p \leq 0.05$) were between the negative control soil samples outside the facility and soil samples collected from any of the identified decomposition bins (None, Low, Middle, High, Active) within the facility. The spatial distribution of measurement values in relation to decomposition density are provided in Figure D-3. Probability values and Mann Whitney U test scores are presented in Table E-3.

Total Carbon Content. The average percent of carbon content per gram of soil for all samples was determined to be 6.96%, with a standard deviation of 3.33%. The results demonstrated no significant differences ($p > 0.05$) in the percentage of total carbon content extracted from soil for any combination of decomposition bin, despite the total variation in percentages for the full dataset. The spatial distribution of measurement values in relation to decomposition density are

provided in Figure D-4. Probability values and Mann Whitney U test scores are presented in Table E-4.

Total Nitrogen Content. The average percent of nitrogen content per gram of soil for all samples was determined to be 0.526%, with a standard deviation of 0.23%. Within the facility there were no significant differences ($p > 0.05$) in the percentage of total nitrogen content extracted from soil when comparisons between bins were made. Significant differences ($p \leq 0.05$) were identified between the negative control soil samples collected outside the facility and all soil samples collected from any of the identified decomposition bins (Low, Middle, High, and Active) within the facility, except for the bin that contained no decomposition. The pooled samples from the active decomposition sites across the facility differed significantly ($p \leq 0.05$) from the Low, Middle and High decomposition bins, and the negative samples taken outside the facility. The spatial distribution of measurement values in relation to decomposition density are provided in Figure D-5. Probability values and Mann Whitney U test scores are presented in Table E-5.

The Carbon : Nitrogen Ratio. The average ratio of carbon to nitrogen for all samples was determined to be 13.3 with a standard deviation of 2.83. There were no significant differences ($p > 0.05$) in the ratios of total carbon to total nitrogen among any of the bins within the facility. Significant differences ($p \leq 0.05$) were identified between the negative control soil samples collected outside the facility and those samples binned as Middle and High, while there were no differences between the Negative controls and the Low and None bins. Interestingly, there were significant differences in this measure of resource quality for the pooled samples of Active decomposition sites ($p \leq 0.05$) and those of no decomposition, which included samples collected

from None and Negative bins. Probability values and Mann Whitney U test scores are presented below in Table E-6.

Lipid-bound Phosphorus. The average lipid-bound phosphorus concentration per gram of soil for all samples was determined to be 6.68, with a standard deviation of 2.56%. There were no significant differences ($p > 0.05$) in the concentration of lipid-bound phosphorus extracted from a gram of soil among the designated decomposition density bins within the facility, including the pooled Active decomposition bin. The only significant differences observed ($p \leq 0.05$) were between the negative control soil samples outside the facility and soil samples collected from any of the identified decomposition bins (None, Low, Middle, High, and Active) within the facility. The spatial distribution of measurement values in relation to decomposition density are provided in Figure D-6. Probability values and Mann Whitney U test scores are presented below in Table E-7.

Extracted DNA. There were no significant differences ($p > 0.05$) in the concentration of total extracted DNA among the designated decomposition density bins within the facility, nor where there differences between any landscape decomposition bin and those samples from outside the facility. Interestingly, the only significant differences observed ($p \leq 0.05$) were between the samples taken from below actively decomposing corpses and all other decomposition bins from both inside and outside the facility. Probability values and Mann Whitney U test scores are presented below in Table E-8.

Multivariate Analysis of Abiotic Environmental Data. The log-transformed abiotic environmetnal data matrix was used for parametric multivatiate analysis of all eight variables, as all variables were normally distributed after transformation. Principle components analysis (PCA) was used to evaluate sample similarity based on Euclidean distances among all pairs of

samples. The two-dimensional ordination plot of 64 samples explained 69% of the observed variation in the eight variables in the analysis, with PC1 contributing 47% and PC2 contributing 22% (Figure 6-1, Left). Separation of control samples from all others based on the first and second principal components was statistically significant at $p < 0.002$ and $p < 0.000$, respectively. In the ordination plot, two clusters of samples were identified (Figure 6-1, Right). The negative control samples that were taken from outside the facility cluster in the lower right of the graph. The second cluster is much larger than the first, and appeared in the upper central half of the graph. The majority of separation among those samples occurred along the PC1 axis. The second cluster is defined mostly by samples taken from below actively decomposing corpses. The remaining samples that were taken from across the facility appear to form a single large grouping located between the negative control samples and those of active decomposition.

The two clusters identified in the first PCA ordination plot (Active and Negative) were reevaluated to the exlcusion of all other samples. The new ordination plot for PC1 and PC2 values explained 72% of the observed variation in the same eight variables. Furthermore, the reanalysis of the Active data, relabeled by months since death, produced an ordination plot with an observable pattern (Figure 6-2). The pattern that emerged was one where the majority of sample separation occurred in the first PC value, whereas the early and late-stage decomposition sites and the negative samples had more similar PC2 values, than did the mid-range decomposition sites. In fact, the separation of PC1 generally follows the PMI data.

Biotic Environmental Data.

Denaturing Gradient Gel Electrophoresis (DGGE). Initial screening of 15 samples by amplification and separation by DGGE produced results for 47% of the identified bands (n = 67).

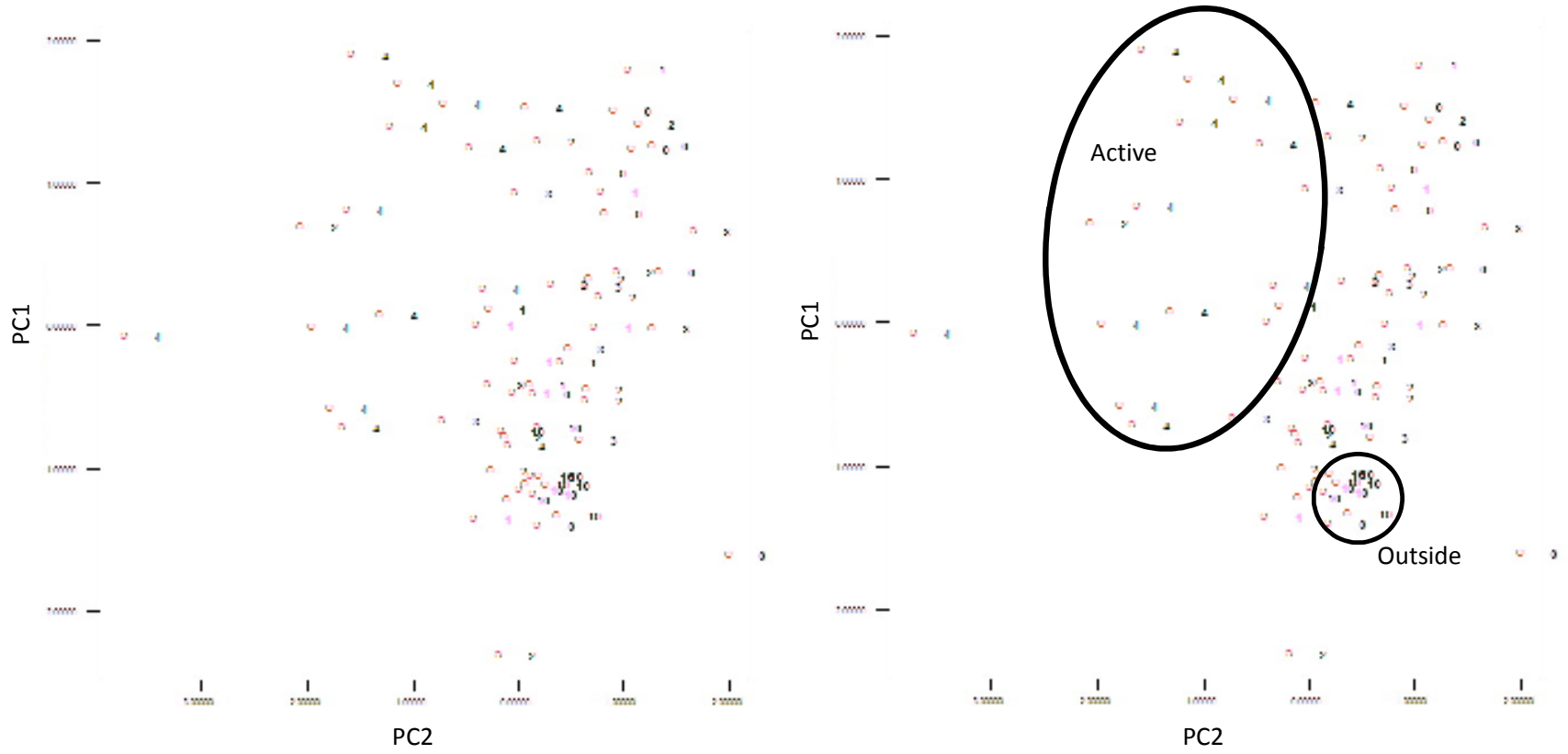

Figure 6-1. Principle Components ordination plots of all samples labeled by decomposition bin. PC1(47%) and PC2 (22%) account for 69% of the observed variation among the eight variables recorded (Left). Two clusters are identified, while the remaining samples tend to clustered among each other with little seperation (Right).

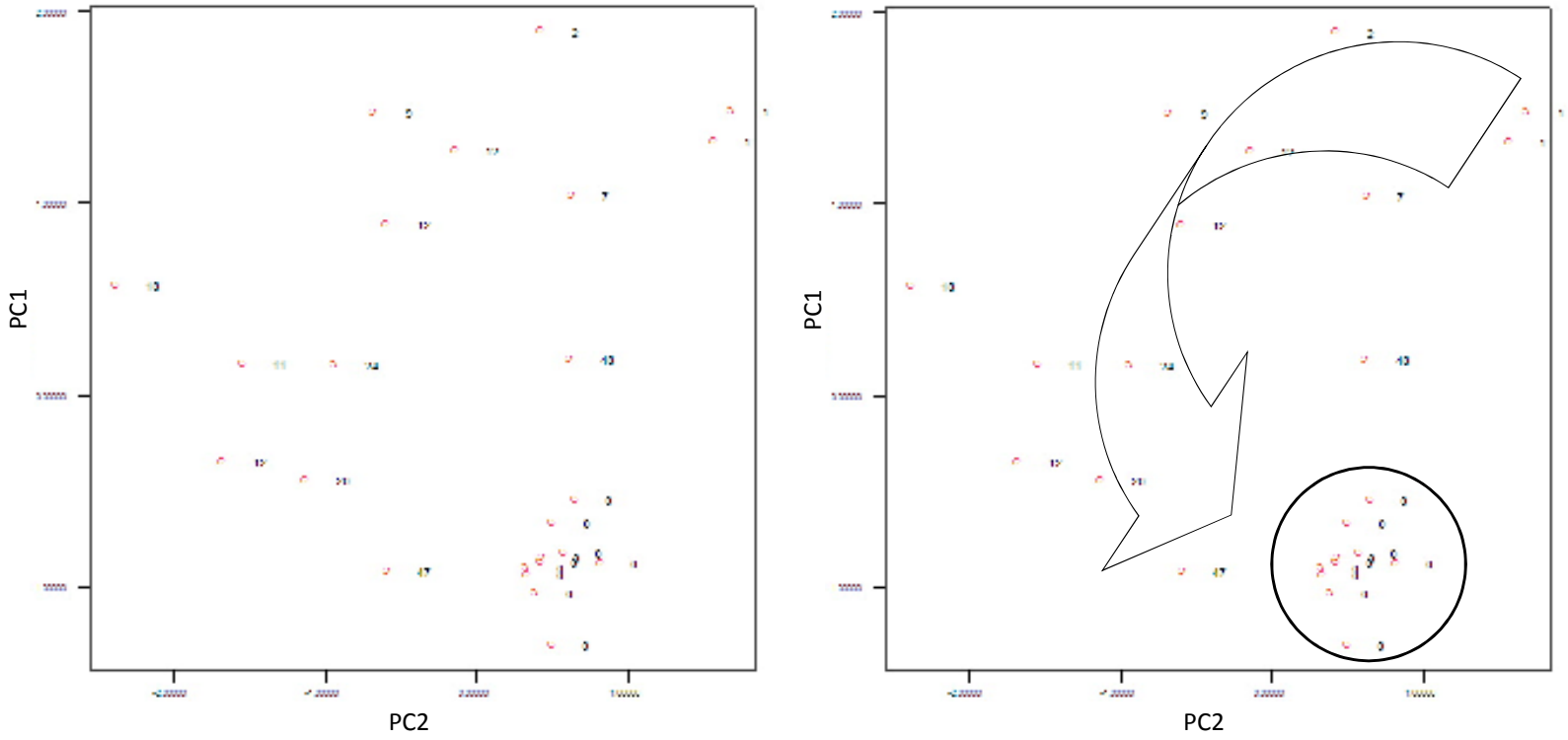

Figures 6-2. Principle Components Analysis of Active and Negative control samples. PC1 and PC2 account for 72% of the observed variation among the eight variables recorded (left). The Active samples are relabeled by months postmortem and vary from two weeks to 48 months. An observable patter emerged by which late-stage decomposition sites approached the negative control samples for the abiotic soil characteristcs evaluated (right).

The first set of samples identified a small set of bacterial and fungal sequences of low diversity and abundance for the number of samples evaluated. Of particular note however, is the importance of sulfur for the metabolism of the identified chemoorganotrophic bacteria. Microbial Insights, Inc reported sequence results from bands excised from Figure 6-3. Identified sequences reported in Table 6-1 include sequential band names, similarity indices, and a description of metabolic activities (Garrity et al. 2007). The higher the similarity index the more reliable the identification. Labeled and excised bands in Figure 6-3 not included in Table 6-1 did not produce a viable match due to sequence mixture. All subsequent DGGE profiles produced gels with many indistinct bands demonstrating a lack of separation, presumably based on the immense diversity of the profiles obtained. Due to the lack of resolution obtained from DGGE, Next Generation Sequencing was attempted in order to provide a clearer picture of overall bacterial diversity.

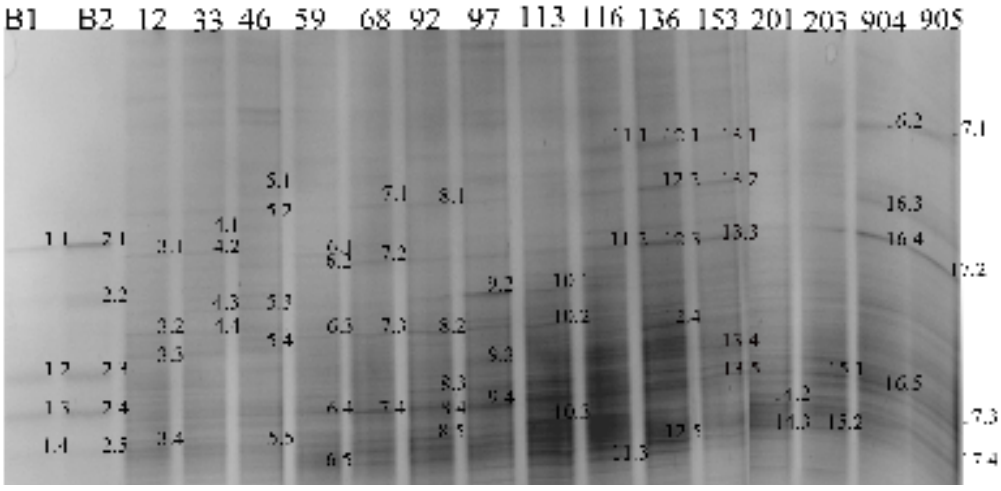

Figure 6-3. DGGE profile of amplified DNA from a portion of the bacterial 16S rDNA gene. All labeled bands were excised, sequenced and classified with the RDP.

Table 6-1. Identified organisms from amplificaion of the 16S and 28S rDNA gene by DGGE.					
Band	**Similar Genus**	**Similarity Index**	**Donors**	**Acceptors**	**Description**
1.1	*Desulfitobacterium spp.*	0.76	H+	Sulfate, sulfite	Anaerobic
1.2	*Thiocapsa spp.*	0.85	H_2, H_2S	Sulfur compounds	Free-living anaerobic phototrophic purple sulfur bacteria, chemoorganotroph, on acetate, phototrophic
2.1	*Desulfitobacterium spp.*	0.74			Anaerobic
2.3	*Thiocapsa spp.*	0.90	H_2, H_2S	Sulfur compounds	Free-living anaerobic phototrophic purple sulfur bacteria, chemoorganotroph, on acetate, phototrophic
2.4	*Thiocapsa spp.*	0.88	H_2, H_2S	Sulfur compounds	Free-living anaerobic phototrophic purple sulfur bacteria, chemoorganotroph, on acetate, phototrophic
2.5	*Desulfobacterium spp.*	0.92	Short chain acids	SO_4-, S_2O_3-	Desulfobacterium autotrophicum ferments pyruvate.
3.3	*Thiocapsa spp.*	0.88	H_2, H_2S	Sulfur compounds	Free-living anaerobic phototrophic purple sulfur bacteria, chemoorganotroph, on acetate, phototrophic
3.4	*Desulfobulbus spp.*	0.93	H2, sulfide, acetate	SO_4-	Desulfobulbus: sulfate-reducing
4.2	*Thiocapsa spp.*	0.86	H_2, H_2S	Sulfur compounds	Free-living anaerobic phototrophic purple sulfur bacteria, chemoorganotroph, on acetate, phototrophic
4.3	uncultured bacterium	1.00			
4.4	*Thiocapsa spp.*	0.84	H_2, H_2S	Sulfur compounds	Free-living anaerobic phototrophic purple sulfur bacteria, chemoorganotroph, on acetate, phototroph
5.1F	*Nectria spp*	0.95			
5.2F	*Penicillium spp.*	0.77			
5.5	*Desulfobacterium spp.*	0.93	Short chain acids	SO_4-, S_2O_3-	Desulfobacterium autotrophicum ferments pyruvate.
6.3F	*Penicillium spp.*	0.94			
7.1F	*Helvella spp.*	0.83			

Table 6-1. Continued.					
Band	**Similar Genus**	**Similarity Index**	**Donors**	**Acceptors**	**Description**
7.4	*Thiocapsa spp.*	0.89	H_2, H_2S	Sulfur compounds	Free-living anaerobic phototrophic purple sulfur bacteria, chemoorganotroph, on acetate, phototrophic
8.1F	uncultured soil fungi	0.79			
8.4	*Thiocapsa spp.*	0.89	H_2, H_2S	Sulfur compounds	Free-living anaerobic phototrophic purple sulfur bacteria, chemoorganotroph, on acetate, phototrophic
9.4	*Thiocapsa spp.*	0.89	H_2, H_2S	Sulfur compounds	Free-living anaerobic phototrophic purple sulfur bacteria, chemoorganotroph, on acetate, phototrophic
10.3F	uncultured soil fungi	0.86			
10.4F	*uncultured Zygomycete*	0.63			
11.1F	*Aspergillus*	0.97			
11.3	*Desulfitobacterium spp.*	0.93			
13.1F	*uncultured soil fungi*	0.88			
14.2F	*Helvella spp.*	0.98			
15.1F	*Thiocapsa spp.*	0.85	H_2, H_2S	Sulfur compounds	Free-living anaerobic phototrophic purple sulfur bacteria, chemoorganotroph, on acetate, phototrophic
16.1F	*Helvella spp.*	0.96			
16.4	*Desulfobacterium spp.*	0.75	Short chain acids	SO_4-, S_2O_3-	Desulfobacterium autotrophicum ferments pyruvate.
16.5	*Thiocapsa spp.*	0.85	H_2, H_2S	Sulfur compounds	Free-living anaerobic phototrophic purple sulfur bacteria, chemoorganotroph, on acetate, phototrophic
17.2	*Desulfobacterium spp.*	0.75	Short chain acids	SO_4-, S_2O_3-	Desulfobacterium autotrophicum ferments pyruvate.
17.3	*Thiocapsa spp.*	0.85	H_2, H_2S	Sulfur compounds	Free-living anaerobic phototrophic purple sulfur bacteria, chemoorganotroph, on acetate, phototrophic

Next Generation Sequencing. High-throughput sequencing produced 3.65 MB of raw sequence data for the amplified 16S rDNA gene. After trimming and aligning the raw sequences, a total of 6,410 bacteria where identified, which represented 101 taxonomic orders. These data were derived from 40 soil samples taken inside the facility (Tables F-1 through F-4).

Rank abundance plots and relative rank abundance charts of all taxa by samples demonstrated overall similarity among the frequency distribuion of identified bacterial orders by decomposition bins (None, Low, Middle, and High). Across the four rank abundance plots, decomposition bins show high similarity among identified taxa, when None was set as the reference and compared to Low, Middle, and High decomposition bins (Figures 6-4 and 6-5). The percent similarities among identified taxa based on the relation to None were 76%, 82%, and 66% for the Low, Middle, and High bins, respectively. The highest similarity percentage is also the bin with the greatest number of identified organisms (n = 2,235). When sample size was controlled by rarefaction curve analysis, similar results were obtained for the four decomposition bins (data not shown).

The relative organism abundance of bacterial orders based on the raw counts was charted with the bacterial taxa that contributed to 75% or greater of the total population for each decomposition bin (Figures G-1 through G-4). The rank ordered bacterial taxa that contributed at least 75% of the total population per bin are listed in Table 6-2. Briefly, all samples regardless of decomposition bin appeared to be dominated by common soil dwelling organisms of Actinomycetales and Rhizobiales. There is overall congruence among the four sample bins. However, there is an observable pattern in the abundance of certain bacterial rank orders as some taxon (i.e., *Burkholderiales* and *Flavovbacterales*), increased in rank with increasing human

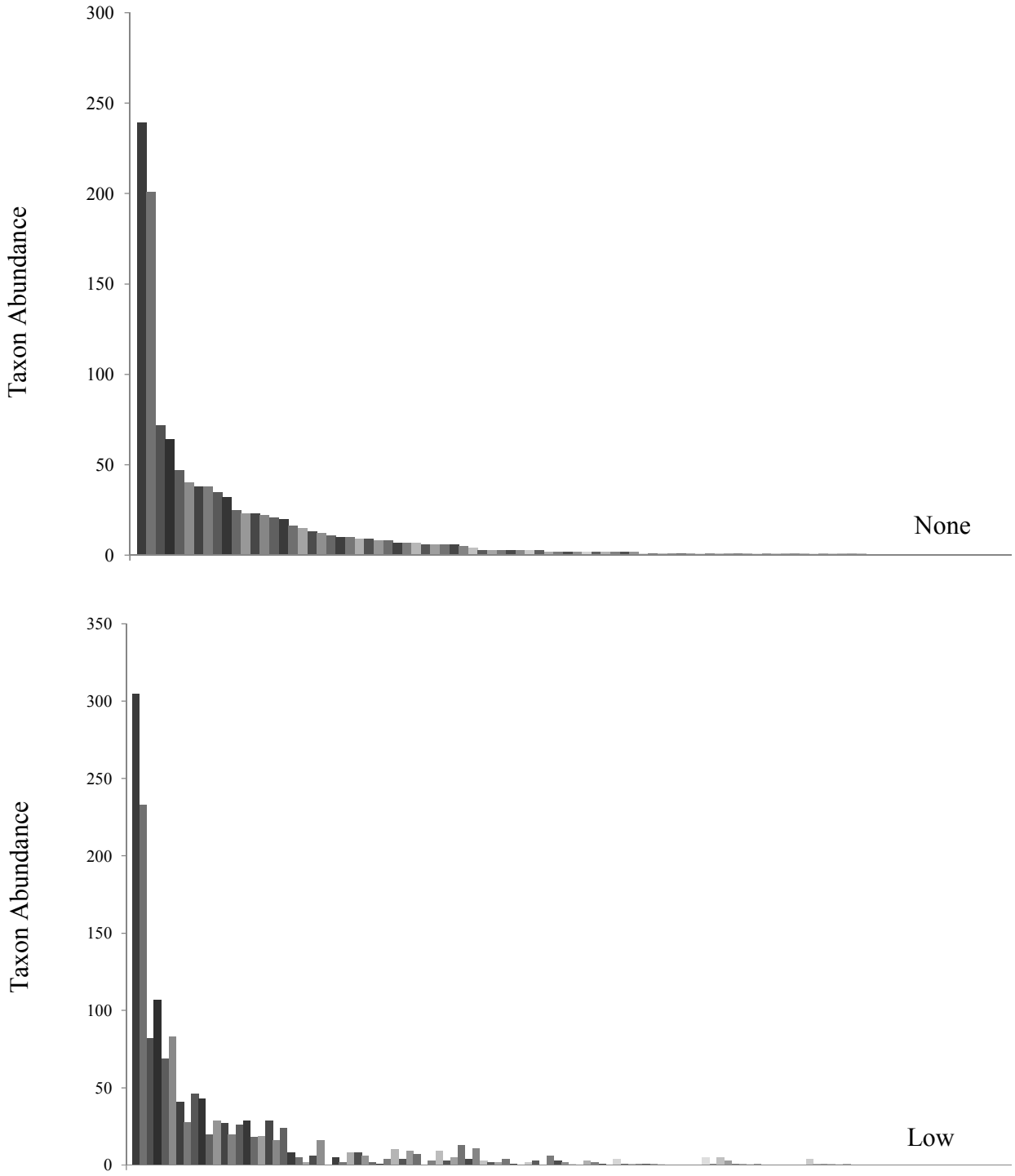

Figure 6-4. Abundance charts for decomposition bins None(top) and Low (bottom) inside the facility. Bin None is set as the reference sample.

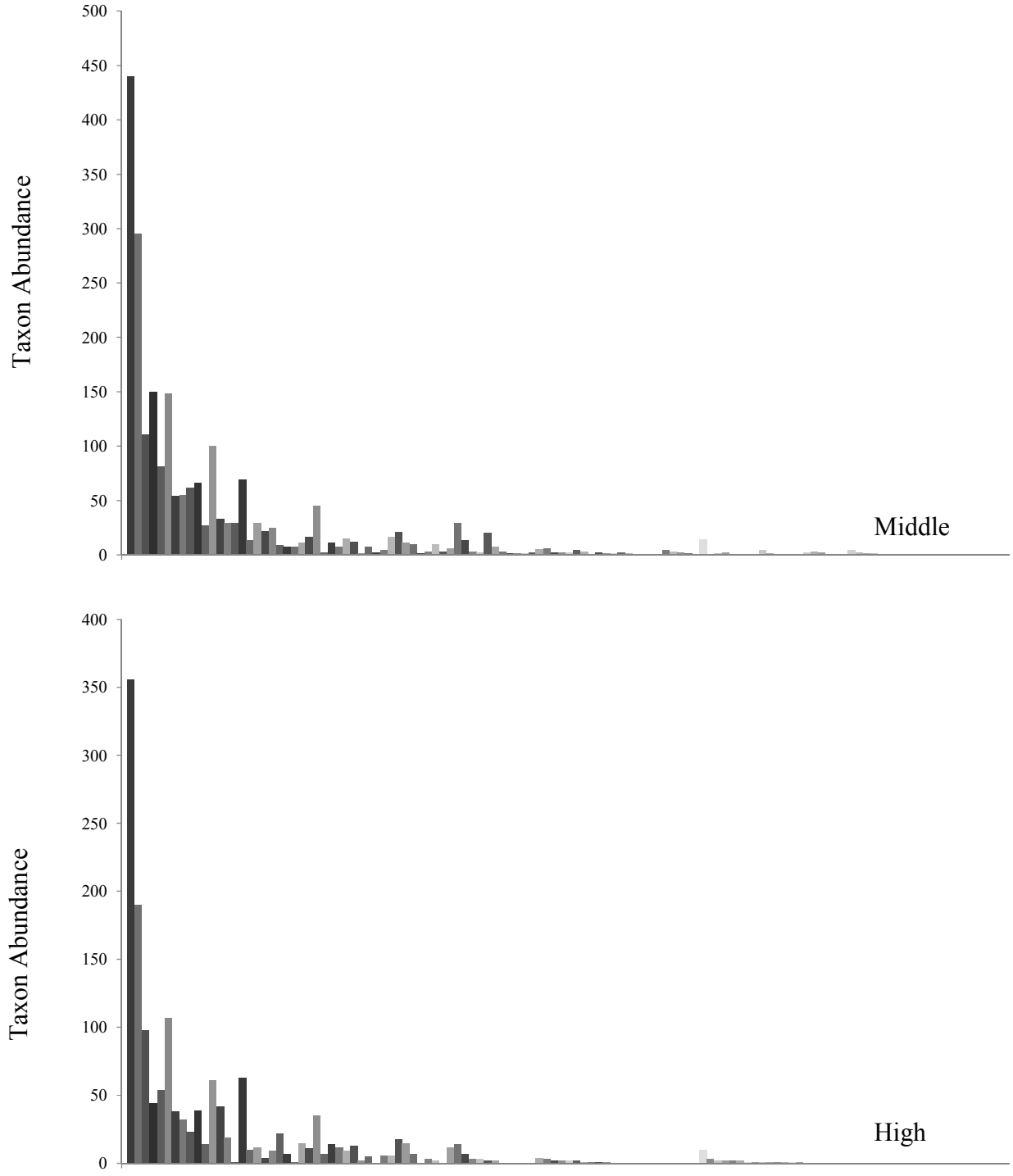

Figure 6-5. Abundance chart for decomposition bins Middle (top) and High (low) inside the facility. Bin None is set as the reference sample.

decomposition activity. These taxa may prove significant as markers of human decomposition, and are bolded below in Table 6-2.

Univariate biodiversity statistics of the fully-standarized biologic matrix produced statistical measures of taxonomic richness, evenness, and diversity for each sample site that confirmed the visual assessment of the rank abundance plots. The average number of taxon and individual organisms represented was 32 and 168, respectively. Margalef's index of species richness, which is normalized for sample size, varied from 4.07 to 9.89, with a mean of 6.21 and standard

Table 6-2. Rank order of relative abundance for each of the decomposition bins within the Anthropology Research Facility.

None	**Low**	**Middle**	**High**
Actinomycetales	Actinomycetales	Actinomycetales	Actinomycetales
Rhizobiales	Rhizobiales	Rhizobiales	Rhizobiales
Sphingomonadales	Gp6	Gp6	Sphingobacteriales
Gp6	Sphingobacteriales	Sphingobacteriales	Sphingomonadales
Myxococcales	Sphingomonadales	Sphingomonadales	**Burkholderiales**
Sphingobacteriales	Myxococcales	Xanthomonadales	Xanthomonadales
Nitriliruptorales	Caulobacterales	Myxococcales	Myxococcales
Acidimicrobiales	Solirubrobacterales	**Burkholderiales**	Gp6
Caulobacterales	Acidimicrobiales	Solirubrobacterales	**Flavobacteriales**
Solirubrobacterales	Xanthomonadales	Caulobacterales	Solirubrobacterales
Alphaproteobacteria	**Burkholderiales**	Nitriliruptorales	Acidimicrobiales
Flavobacteriales	Nitriliruptorales	Thermoleophilales	Thermoleophilales
Xanthomonadales	Gemmatimonadales	Acidimicrobiales	Nitriliruptorales
Rhodospirillales	**Flavobacteriales**	**Flavobacteriales**	

deviation of 1.34. Similarly, Pielou's measure of evenness was determined to have a mean score and standard deviation of 0.82 and 0.05, respectively. The high evenness scores suggested a relatively even distribution of community profiles between samples. Likewise, the Shannon diversity index was equably distributed across all samples with a mean and standard deviation of 2.80 and 0.26, respectively.

An Analysis of Variance (ANOVA) for each univariate measure of diversity (i.e., Margalef's index of species richness, Pielou's evenness index, and the Shannon diversity index) demonstrated overall agreement in community profile when the sample units were factored by decomposion bin. Each measure failed to exclude the null hypothsis, indicating overall biologic similarity among all decomposition bins inside the facility.

Nonparametric mulivariate analyses of the Bray-Curtis similarity matrix by multi-dimensional scaling (MDS) identified clusters of samples within and among decomposition bins in two-dimensional space. Within each decomposition bin, groupings of sample units with the greatest similarity appeared closer together. For bins None, Low, and Middle each map included no less than four clusters of samples at 60% similarity (Figures 6-6 through 6-8). Sample units within the High bin were characterized by only two clusters at the same level of similarity (Figure 6-9). When all samples were combined and plotted by decomposition bin the MDS plot generated separation among of the samples (Figure 6-10). An Analysis of Similarity (ANOSIM) among the four clusters identified significant differences in community composition between samples of None versus High and Low versus High, while all other pairwise comparisons failed to exclude the null hypothesis (Table 6-3).

Library comparison of the DNA sequences using the RDP Library Comparison routine identified significant differences for a hand full of taxa between the None and High

decomposition bins. The High bin was characterized by elevated levels of Actinomycetales ($p = 0.0002$) and the two suborders Corynobacterineae ($p = 0.0003$) and Micrococcineae ($p < 0.0000$), Burkholderiales ($p = 0.0017$) and its family Comamonadaceae ($p < 0.0000$), and Bacteroidetes ($p < 0.0000$) with order Spingobacteriales ($p = 0.0017$), while having a reduced concentration of Acidobacteria ($p = 0.0128$).

Reevaluation of samples within the bins of None and High by MDS (Figure 6-11) were layered with taxon that demonstrated differences on the rank-order abundance plots and those that were determined to be significantly different based on the RDP library comparison routine. When these taxa were layered over the MDS plot, simple trends were observable. Acidomicrbiales dominated the areas with no decomposition (Figure 6-12), where as Burkholderials, Spingobacteriales were more prevalent in the areas under constant human decomposition (Figure 6-13). As for the order Desulfarculales, they were most prevalent in the bins of high decomposition and virtually nonexistent in the areas with no reported history of human decomposition (Figure 6-14).

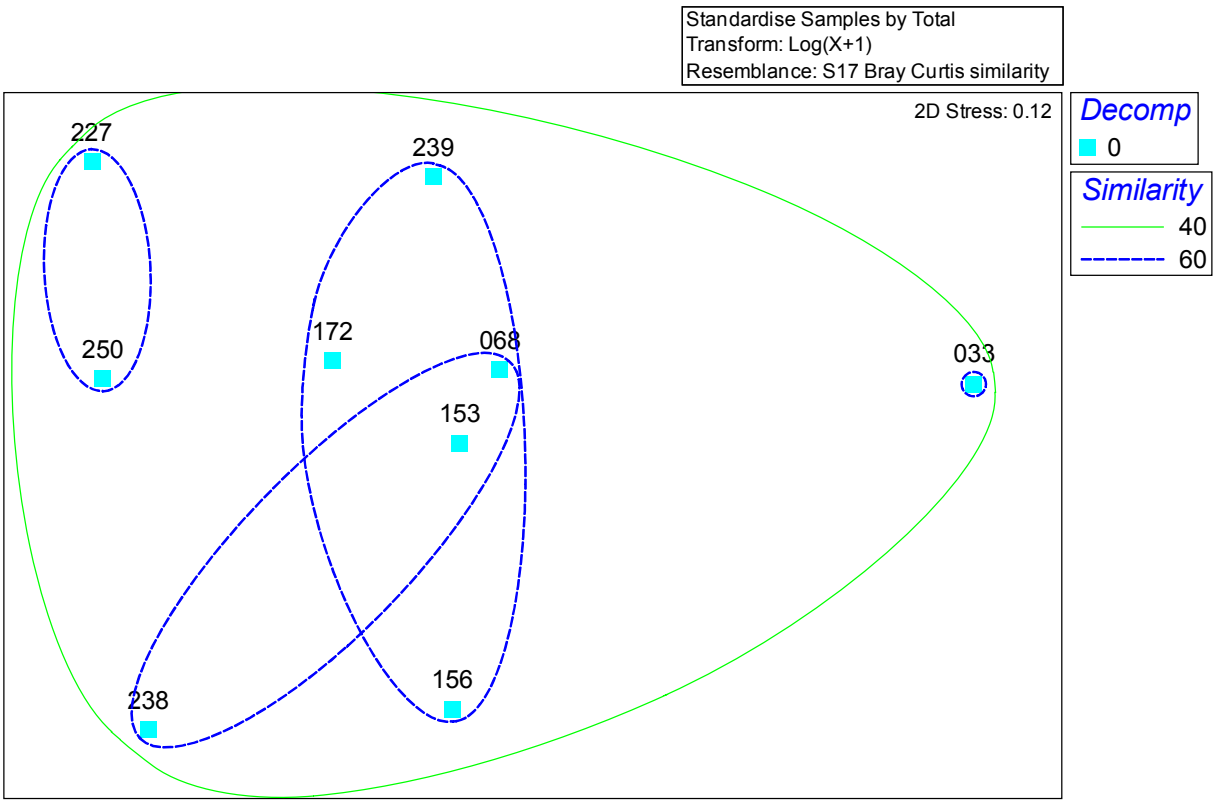

Figure 6-6. Multidimensional scale ordination of Bray-Curtis similarity matrix for decomposition bin None (0).

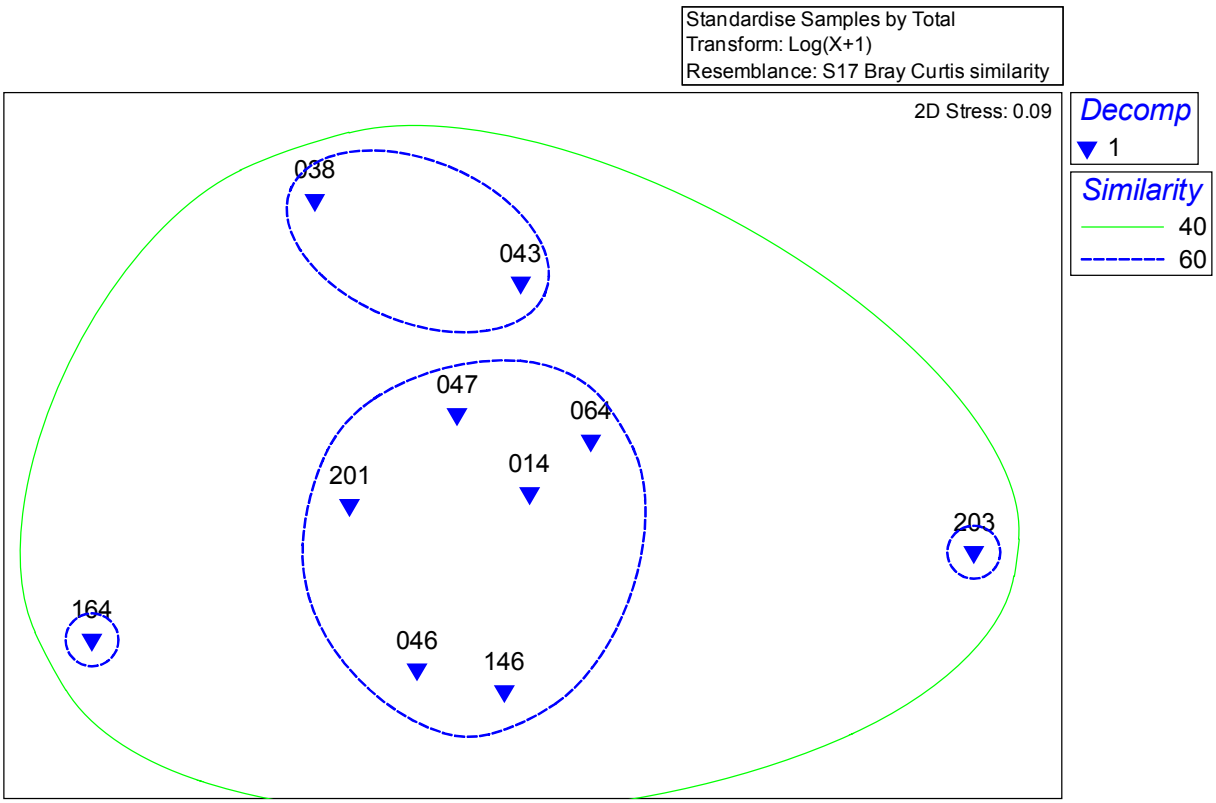

Figure 6-7. Multidimensional scale ordination of Bray-Curtis similarity matrix for decomposition bin Low (1).

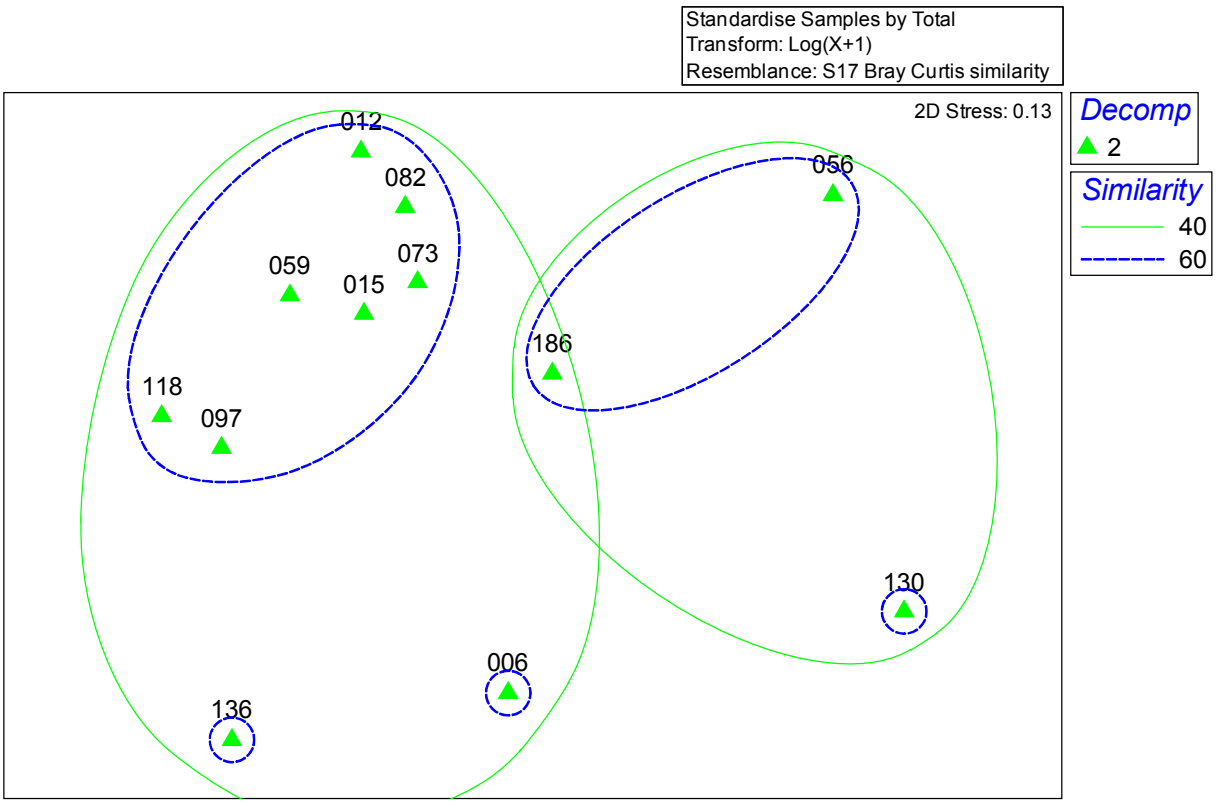

Figure 6-8. Multidimensional scale ordination of Bray-Curtis similarity matrix for decomposition bin Middle (2).

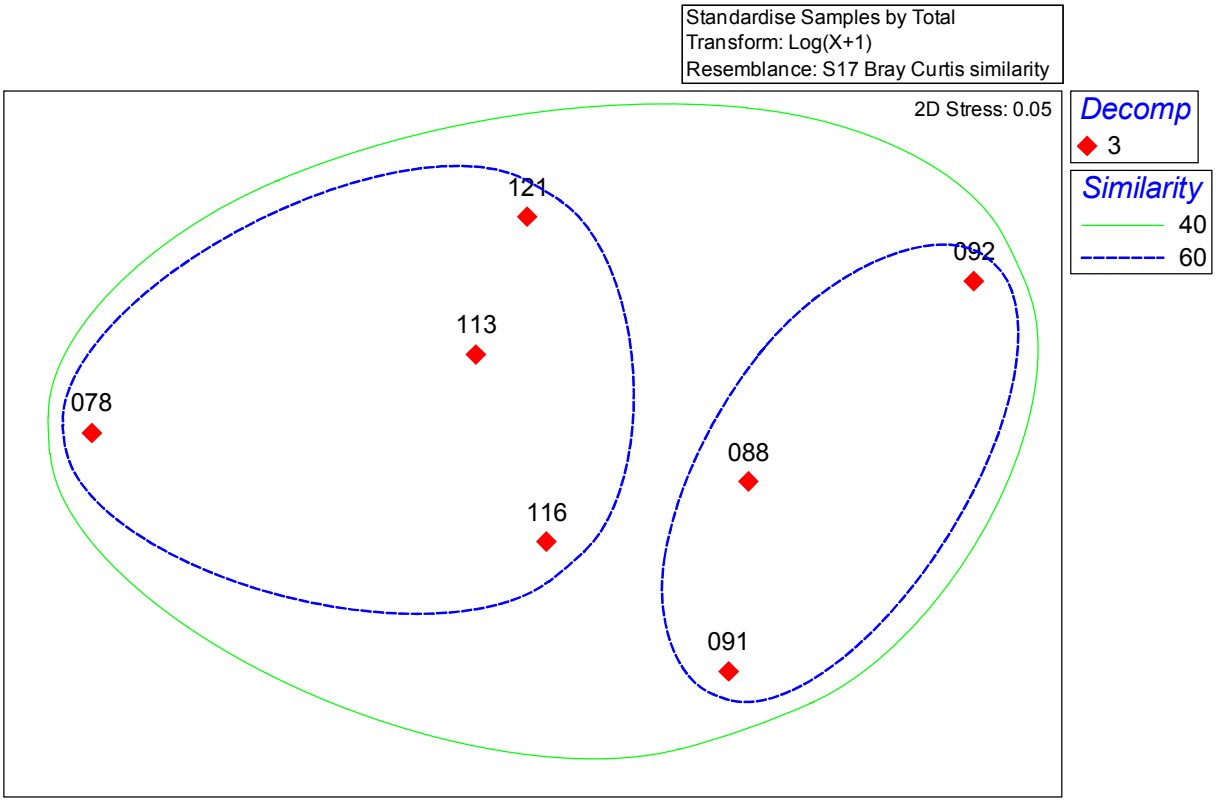

Figure 6-9. Multidimensional scale ordination of Bray-Curtis similarity matrix for decomposition bin High (3).

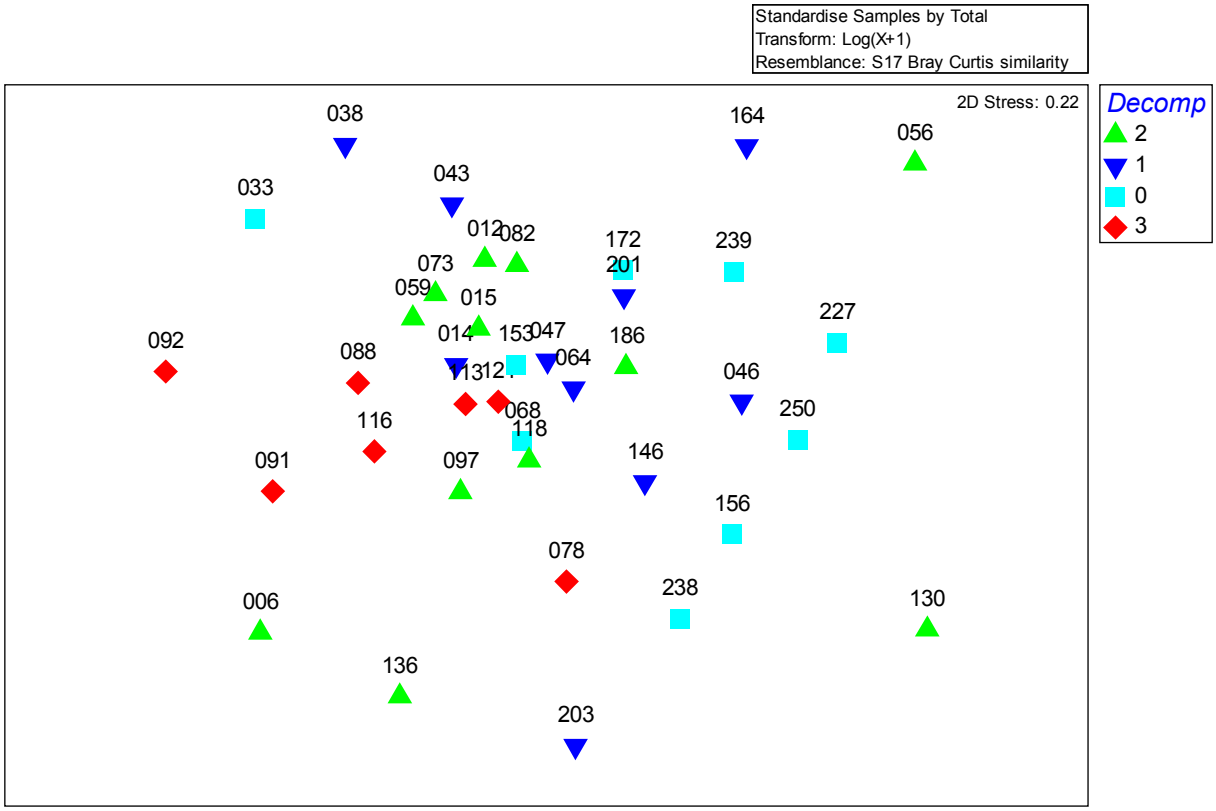

Figure 6-10. Multidimensional scale ordination of Bray-Curtis similarity matrix for all decomposition bins inside the facility.

Table 6-3. Analysis of Similarities (ANOSIM) One-Way Analysis.					
Global Test					
Sample statistic (Global R): 0.04					
Significance level of sample statistic: 0.186					
Number of permutations: 999 (Random sample from a large number)					
Number of permuted statistics greater than or equal to Global R: 185					
Pairwise Tests					
Group	**R-statistic**	**Sig. Level (α=.05)**	**Possible Permutations**	**Actual Permutations**	**No. ≥ Obs.**
0, 1	0.047	0.210	92378	999	209
0, 2	0.039	0.231	293930	999	230
0, 3	**0.36**	**0.001**	**11440**	**999**	**0**
1, 2	-0.09	0.983	646646	999	982
1, 3	**0.159**	**0.048**	**19448**	**999**	**47**
2, 3	-0.061	0.722	50388	999	721

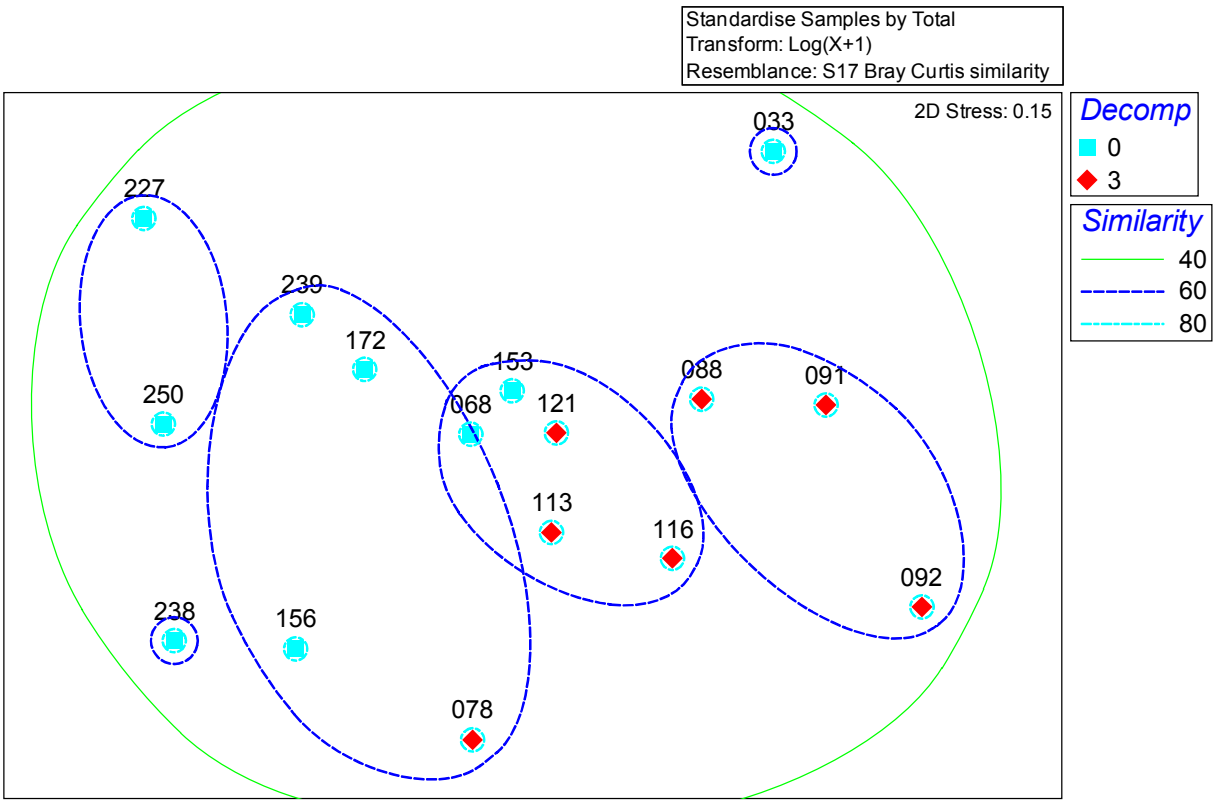

Figure 6-11. Multidimensional scale ordination of Bray-Curtis similarity matrix for decomposition bins None and High showing separation.

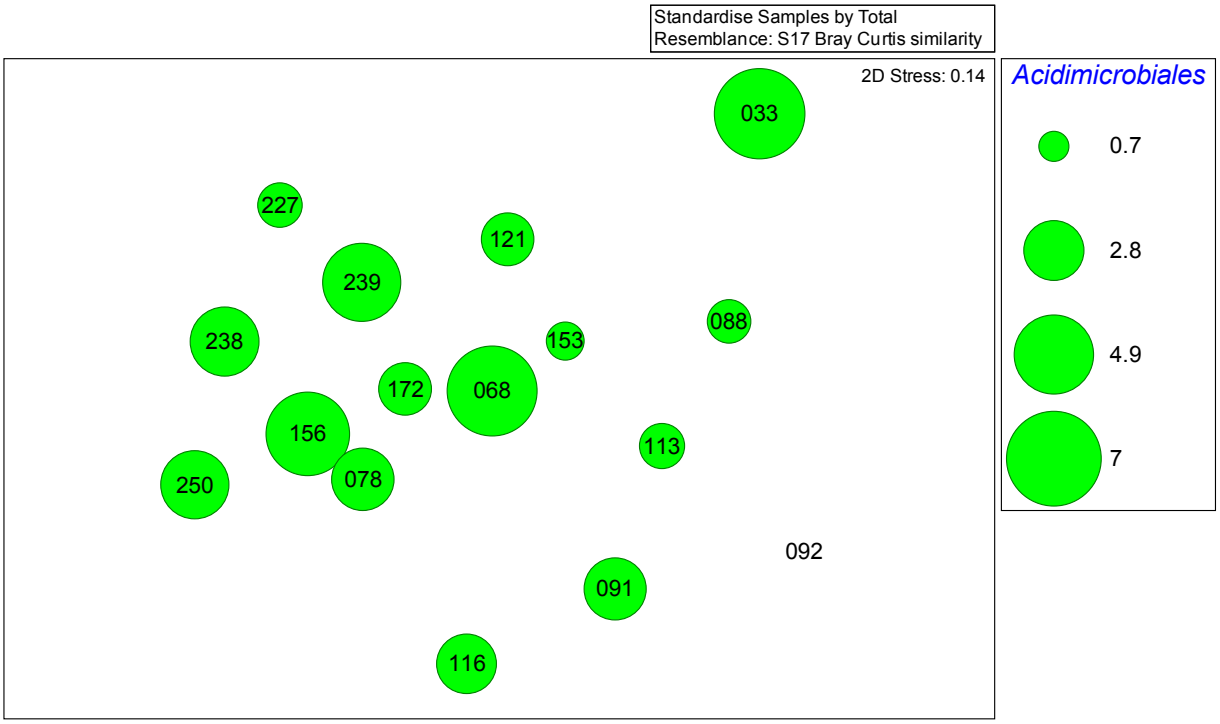

Figure 6-12. Multidimensional scale ordination of Bray-Curtis similarity matrix for decomposition bins None and High with abundance data for Acidimicrobiales layered per sample site.

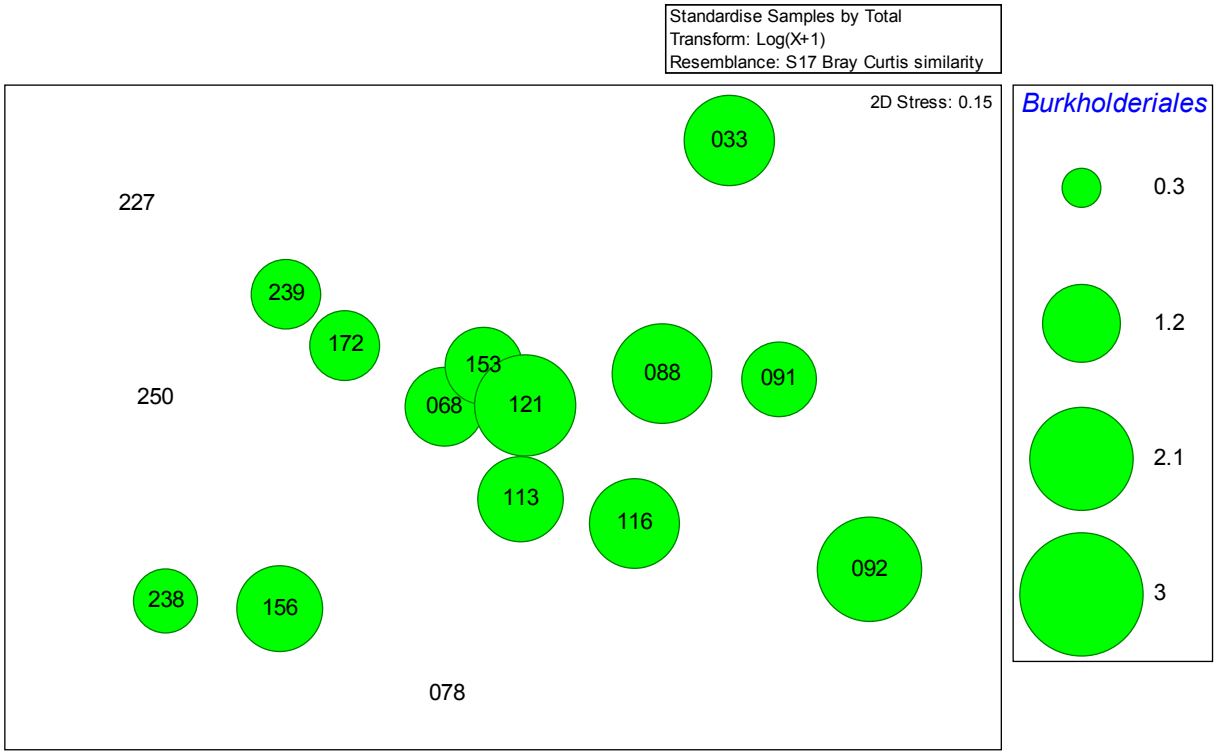

Figure 6-13. Multidimensional scale ordination of Bray-Curtis similarity matrix for decomposition bins None and High with abundance data Burkholderiales layered per sample site.

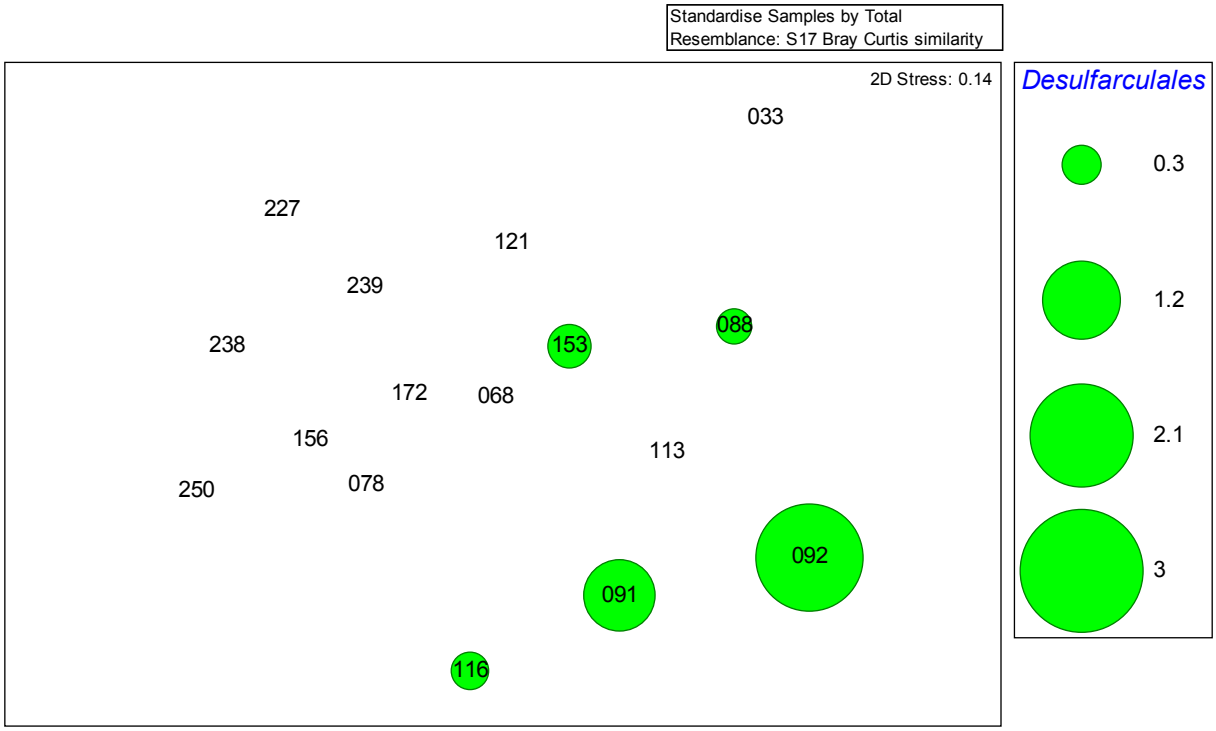

Figure 6-14. Multidimensional scale ordination of Bray-Curtis similarity matrix for decomposition bins None and High with abundance data for Desulfarculales layered per sample site.

CHAPTER 7: DISCUSSION

Paleontologists, archaeologists and anthropologists alike have adapted the theoretical framework provided by Efremov's taphonomy in order to differentiate observable patterns in preservation, destruction, assemblage formation, and natural from non-natural effects on the corpse and bone. In order to study effectively the patterns and trends of human decomposition given its complexity, a taphonomic framework is necessary. Taphonomy contributes the broader ecological prospective that permits understanding of myriad postmortem processes.

This research project evaluated the composition of the abiotic and biotic soil environmental parameters associated with human decomposition from a site where studies of human decomposition in the terrestrial landscape have occurred for the past 30 years. With the increased awareness of carcass enrichment of soil (Vass et al. 1992, 2002, and 2008) and its relationship to microbiology and ecosystem function (Putman 1978a; Putman 1978b; Towne 2000; Hopkins et al. 2000; Dent et al. 2004; Carter et al. 2007; Benninger et al. 2008; Carter et al. 2010) this research set out to establish a baseline survey of abiotic edaphic features and background levels of the indigenous microbial community at the University of Tennessee Anthropology Research Facility. In doing so, the data that were generated for the individual samples were stratified based on the density distribution of cadaver decomposition in order to test for differences among the different areas within the facility as well as an area of similar ecology outside the facility with no history of human decomposition.

In the earlier works of Putman (1978a, 1978b), Swift et al. (1979), and Vass et al. (1992, 2002, 2008) detailed discussions and data were presented on the increased heterogeneity and biological activity associated with cadaver decomposition and nutrient cycling. These

discussions lead Carter et al. (2007) to suggest that decomposition of a corpse is a highly-specialized event that radically changes the landscape over a finite spatial and temporal dimension; hence his Cadaver Decomposition Island (CDI). Building on Vass's earlier work, Carter's concept was followed and further supported by Benninger et al. (2008) who identified decay curves of C, N, and lipid-bound phosphorus associated with PMI. Similarly Haslam and Tibbett (2009) reported a trend for increased soil pH soon after death, which would then revert to basal soil levels or even below normal pH three to four weeks postmortem. Most recently Carter et al. (2010) conclude that moisture content of gravesoils can modify the rate of cadaver decomposition by accelerating or decelerating the rise and fall of microbial biomass, pH, and ninhydrin-reactive nitrogen.

Recording the landscape patterns in abiotic edaphic parameters of pH, moisture content, organic matter, carbon, nitrogen, and generalized biomass data for lipid-bound phosphorus and total extractable DNA consistently identified statistical differences between the 40 samples taken within the facility to those taken outside the facility. The only consistently significant differences in abiotic data within the facility occurred between the 40 landscape samples, arranged by decomposition bin, and those soil samples taken below actively decomposing corpses. The PMI for the actively decomposing remains varied from two weeks to four years. Interestingly, there were virtually no differences among the binned landscape samples of None, Low, Middle, and High decomposition within the facility.

Soil pH values outside the facility are on average lower than those from within the facility, which is most likely due to increased ammonification of soils within the facility, than outside. Microbially-mediated conversion of organically-bound N from an abundant source of decomposing human protein to inorganic ammonia (NH_3^+) and ammonium (NH_4^+) binds free H^+

ions, removing their contribution to acidic conditions. Coupled with the ammonification, many other base-forming cations ($Ca^{2+,}$ Mg^{2+}, K^{+}, and Na^{+}) are readily available from the decomposing corpse that are preferentially bound to clay and organic matter particles in negatively-charged soils instead of the acid-forming cations of H^{+}, Al^{3+}, Fe^{2+} (McCauley et al. 2009).

On average, the soil outside the facility was drier than those within the facility. The higher moisture content of the soil within the facility, could be explained by treatment (i.e., decomposition events), but when moisture values within the facility were layered using ArcGIS, the simplest explanation of the observable pattern is one where moisture content was most often associated with topography, shade, and land use, rather than frequency of decomposition events.

As with soil moisture content, the soils outside the facility were on average lower in organic matter content than the soils within the facility. Soil organic matter (SOM) is formed as combination of plant and animal residues, cells and tissues of the indigenous microbial population in various stages of decomposition (Brady and Weil 1999); therefore, SOM is the net difference between what is formed and what has decomposed. It seems appropriate then, that the organic content of the soil within the facility is greater than outside given the processes of human decomposition that deposit vast amounts of protein and cellular debris into the soil. What is interesting to note however, is the similarity in organic matter content associated with the differences in frequency distribution of decomposition events. By simply plotting the values in real space, the high organic matter content within the facility appears to correlate with high moisture content.

Given the higher organic content within the facility than outside, it follows that the total carbon and total nitrogen content would be greater within the facility than outside. While there are no significant differences in carbon content, there are slightly higher values for the samples

taken inside versus those taken outside. In addition there is greater variability in carbon content inside than outside. One explanation for the lack of significant differences in carbon content is that the areas within the facility support a greater microbial biomass than the areas outside, and much of the available carbon is readily incorporated into living biomass and returned to the atmosphere though microbial respiration. The nitrogen content on the other hand shows a downward trend when evaluated against the amount of human decomposition, and a similar effect is observed with the ratio of carbon to nitrogen. This ratio is typically applied as an indication of resource quality. The observable trend is one that supports saturation of the facility soil with a high-resource quality when compared to the samples from outside the facility.

A significant ($p < 0.05$) increase in soil-extractable phosphorous was observed for the samples inside the facility compared to those outside. Benninger et al. (2008) also detected a significant ($p < 0.01$) increase in phosphorus concentrations beneath decomposing *Sus scrofa* over a 100 day cycle compared to control sites. Towne (2000) reported similar observations in phosphorus concentration, and suggested that the elevated levels remained three years postmortem. Citing Dent et al. (2004), Benninger and colleagues (2008) explained that phosphorus stores in the body are found in a number of components such as proteins, sugar phosphates, and phospholipids. Lipid-bound phosphorus also accumulates in the body due to diet. Therefore, a decomposing corpse will release a large amount of P to the surrounding grave soil (Benninger et al. 2008). It is important to note that while lipid-P is generally used as a measure of microbial biomass (Drijber et al. 2000), the measurement of lipid-P in studies of cadaver decomposition cannot differentiate between phosphorous derived from the microbial communities or from those of the carcass itself (Benninger et al. 2008). In spite of this, the data

suggest a strong significant ($p < 0.01$) increase in Lipid-P in soil of the facility; thereby indicating an influx of human derived material with an associated increase of microbial activity.

The other measure of biomass evaluated was the concentration of extracted DNA from soil. Like lipid-P, it is impossible to discriminate the origin of the recovered DNA at this level of analysis, given the microcosm of biological activity, as well as the contribution of the decomposing corpse and other dead soil dwelling organisms. There were no significant differences ($p > 0.1$) in the total concentration of recovered DNA by decomposition bin or in comparison to the samples outside the facility. The lack of differences is believed to be an artifact of DNA extraction bias from soil itself, rather than any meaningful biological reality. With over 10^9 organisms per gram of soil (Paul 2007) plus a pool of another 10^{14} bacteria found in humans (Wilson 2008) there is an inordinate amount of DNA present – not to mention the numerous grazers, scavengers, and predators that may also contribute to the pool of extractable DNA. Similarly, Leckie et al. (2004) found no correlation between DNA extracted and biomass as measured by phospholipid fatty acid or chloroform fumigation extraction. Feinstein et al. (2009) confirmed this by indicating that the lack of correlation is due to different degrees of incomplete cell lysis in single DNA extractions.

Multivariate PCA of all combined abiotic edaphic data for each of the decomposition bins produced a two dimensional ordination plot that separated all facility samples from control samples. The separation based on the first and second principal components were statistically significant at $p < 0.002$ and $p < 0.000$, respectively. This plot also demonstrated an overall failure to exclude the null hypotheses for virtually every Mann Whitney U test performed on the decomposition bins (None, Low, Middle, and High) inside the facility, as these samples clustered together on the PCA plot.

In order to understand better the indigenous microbial community composition of the facility, each soil sample addressed above was also analyzed for bacterial community analysis by amplification of the 16S rDNA gene. This gene is present in all prokaryotes, and is present with varying degree. In other words, some bacteria have more copies of this gene than others. This reality potentially skews abundance data based on DNA analysis from amplified regions, given the greater probability of sequencing organisms with more 16S rDNA genes, than others with fewer copies of this gene (Chandler et al. 1997). Other constraints of bacterial amplification for community analyses involve preferential denaturation of organisms with low GC content and unequal annealing efficiencies (Reysenbach et al. 1992). Nonetheless, this region is highly conserved in specific stretches, while variable in others; thereby enabling differentiation of taxonomic units based on DNA sequence. Analysis of the 16S rRNA genes is the choice *de facto* for studies of microbial ecology and taxonomy.

Analyses of the biotic data matrix developed from sites across the facility suggested a lack of significant difference for most pairwise comparisons of the decomposition bins. There were however, differences between None and High bins. That said, the lack of difference was generally consistent with the abiotic data. This concordance between data sets should not be to terribly surprising since it is well understood that the edaphic physicochemical, environmental conditions and available resources are the selecting force of the microbial community (Moorhead and Sinsabaugh 2006).

The dissimilarity between bins None and High were explained through a comparison of the DNA sequences of the two libraries. This comparison identified significant differences in certain taxa. In relation to bin None, the High bin was characterized by elevated levels of Actinomycetales (Suborders: Corynobacterineae and Micrococcineae), Burkholderiales (Family:

Comamonadaceae), Bacteroidetes, and Spingobacteriales, while having a reduced concentration of Acidimicrobiales. All contain genera ubiquitously distributed in soil.

Acidimicrobiales was more dominant for the samples with no previously identified human decomposition, than the sample units where decomposition was constant. They are common soil-dwelling organisms, whose relative abundance increases as pH decreases (Jones et al. 2009). This effect can be seen on the corresponding MDS plot. This observation is concordant with the slight increase in pH of samples from areas of constant human decomposition, presumably from the ammonification of the soils that have undergone constant human decomposition.

Of the taxa that were reported in higher concentrations between these two bins, the Burkholderiales are reported by Garrity et al. (2005) as phenotypically, metabolically, and ecologically diverse, and include strictly aerobic and facultative anaerobic gram-negative chemoogranotrophs, obligate and facultative chemolithotrophs, and nitrogen-fixing organisms. A wide variety of organic substances can be used as sources of carbon and energy for growth, which are characterized by the presence of hydroxy fatty acids of 14, 16, and 18 carbon atoms.

Actinomycetales and the suborder Corynobacterianeae are mostly acid-fast bacteria with high GC content that are widely distributed in soil. They have been characterized as aerobic, with most species being facultative anaerobic chemoogranotrophs (Jones and Collins 1986). However, this group includes the genus *Mycobacterium*, which was the identified genus contributing to the difference. Members of the genus *Mycobacterium* are almost entirely aerobic organisms of soil that use ammonia or amino acids as nitrogen sources and glycerol as a carbon source, while some require supplements of hemin, mycobactins and other iron transport compounds (Wayne and Kubica 1986). The other significantly different Actinomycetales is the Micrococcineae suborder. The Micrococcineae is described by Schleifer (1986:1001) as aerobic or facultatively

anaerobic. They are chemoorganotrophs, metabolizing via respiration and/or fermentative processes. Carbon and energy sources are obtained from carbohydrates and/or amino acids. The majority of this suborder was characterized nearly entirely by the family Microbacteriaceae, which are gram-positive soil dwelling chemoorganotrophs.

The phylum Bacteroidetes and one of its taxonomic orders Spingobacteriales were also statistically different between the High and None samples. Bacteroidetes is a diverse phylum whose members are widely distributed in soils, sea water and the human gut. They generally metabolize sugars directly from the environment or release them from long-chain-polysaccharides, such as cellulose and chitin. Sphingobacteriales are aerobic decomposers of long-chain-polysaccharides and incorporate sphingolipids into their cell walls. The Sphingobacteriales contains the family Chitinophagaceae, which composed 62 % of all Bacteroidetes identified in the High bin. Chitinophagaceae has been described by Larkin (1986) as gram-negative aerobic chemoorganotrophs that hydrolyze chitin and not cellulose (Sangkhobol and Skerman 1981). Given the strong chitin-consuming abilities of certain Sphingobacteriales, their greater abundance with areas that have experienced high levels of decomposition is understandable, as these bacteria would be aptly supported by massive colonies of insect puparia and exuvia.

While not statistically different, it is interesting to note the greater presence of sulfate-reducing bacteria in areas of high decomposition. Sulfur is an essential element of amino acids, vitamins, and hormones. During decomposition, sulfur compounds are integral in the formation of early macroscopic change of gross tissue, such as green discoloration of the lower abdomen and the formation of iron sulfide (Love and Marks 2003, Dent et al. 2004). Vass et al. (2004) identified sulfur-containing compounds liberated from shallow burial rather early in the

decomposition process. The early release of sulfur compounds results from metabolic activity of the sulfa-centric / sulfate-reducing bacteria.

Next-generation 454 sequencing identified members of the Desularculales taxonomic order. Garrity et al. (2005) describe Desulfarculales as gram-negative, strictly anaerobic chemoorganotrophs that use higher fatty-acids as electron donors and carbon sources. All organic substances are completely oxidized to CO_2, which separates Desulfarculales from other sulfate-reducing bacteria. Sulfate and other oxidized sulfur compounds serve as terminal electron acceptors and are reduced to H_2S (Garrity et al. 2005). Furthermore, DGGE analysis identified many bands as anaerobic chemoorganotrophic bacteria of *Thiocapsa sp.* and *Desulfobacterium sp*. They are characterized as free-living phototrophic purple sulfur bacteria and anaerobic fermenters of pyruvate, respectively. The purple sulfur bacteria use H_2S as their reducing agent and produce elemental sulfur through oxidation of H_2S.

The taxonomic units that were identified as significantly different between bins of None and High, and that appeared in greater abundance in the areas associated with constant human decomposition are all chemoorganotrophs, meaning they use organic compounds as their source of carbon and energy. The source of carbon varies however, as some acquire it through the reduction of sugars, amino acids, and chitin. The abundance of sugars and proteins deposited in the burial environment from a corpse would be suitable to support large populations of chemoorganotrophic microbes, while other bacteria are supported by the presence of higher tophic levels, such as insects.

Given these results, the potential for refining PMI estimates based on abiotic and biotic datasets is great. When analyzed against recorded time since death, the abiotic soil data presented a generalized trend where after four years the soil conditions began to mimic those of

the negative control samples (see Figure 6-3). Not only did these samples separate nicely with time, but the data are also consistent with generalized decomposition patterns of volatile organic compounds (Vass et al. 1992, 2002, 2008), soil C, N and biomass (Benninger et al. 2008), bacteria (Parkinson 2009), soil pH (Haslam and Tibbett 2009), and water (Carter et al. 2010) where the measured variable deviates from background and returns to basal levels. As these parameters change through a local impulse of carcass derived material, the microbial community will change. The study presented here indicates a change in soil microbe community structure as a result of decomposition (see Figure 6-11). Parkinson (2009) was the first to demonstrate this through a longitudinal analysis of bacterial tRFLP of soil. Her study identified the same ephemeral deviation and return to control levels, suggesting shifts in the composition of the bacterial communities were associated with macroscopic stages of decomposition and the communities were characterized by the presence of human-derived organism.

By evaluating the effects of decomposition across the ARF landscape, few human-specific organisms were identified in any great number. This was mostly due to the fact that human gut-anaerobic bacteria will not survive outside the body on the soil surface in an oxygen-rich environment. The presence of human-gut anaerobes would likely be a marker of early stage decomposition. Since no early-stage organisms were found in great abundance, the differences in bacterial communities between the areas of high and no human decomposition may prove useful for understanding communities of late-stage decomposition as those differences were based on common soil bacteria.

CHAPTER 8. CONCLUSIONS

This project evaluated the landscape patterns of abiotic and biotic edaphic characteristics at the University of Tennessee Anthropology Research Facility, an effective 1.28 acre plot of land that has been used for studying human decomposition for the past 30 years. The goal of this project was threefold: to determine soil characteristics of areas within the facility that have no recorded history of human decomposition for comparison to those areas with an increasing concentration of human decomposition and to areas outside the facility. It was hypothesized that the increased levels of decomposition would change the background physicochemical nature of the soil, which would then cause a shift in the underlying soil bacterial community.

The abiotic data consisted of soil pH, percent soil organic matter, moisture, carbon, nitrogen, lipid-bound-phosphorus, and DNA content for soil samples collected across the UT ARF landscape in order to determine the abiotic matrix. A biological matrix of bacterial taxonomy was generated for the 40 samples inside the facility. Taxonomic identification was based on amplification of the 16S rDNA gene using universal bacterial primers. The identified taxonomy was evaluated for differences among the decomposition bins and identified taxa.

Results of the abiotic soil properties demonstrated few differences among the predefined bins of decomposition density, suggesting homogeneity of recoded soil parameters inside the facility. However, significant differences were observed between samples inside the facility to the negative control samples taken outside the facility, indicating that while landscape samples inside the facility may be similar to themselves they are dissimilar to those taken approximately one kilometer to the south in a similar temperate forest biome. Similarly, samples taken below actively decomposing corpses were different from all other samples in abiotic properties,

suggesting an ephemeral pulse in the recorded soil characteristics associated with human decomposition.

When all abiotic data were taken together, a multivariate analysis for the negative control samples and those obtained from below actively decomposing corpses that varied from two weeks to four years postmortem demonstrated a temporal shift away from negative control samples. The greatest deviation occurred at 18 to 24 months. After which time, the samples became more similar to control samples. The observed temporal effect was best defined by an overall decrease in the concentration of C, N, SOM, and Lipid-P biomass. For this study, the sample with the shortest PMI was two weeks and the corpse was already in a post-bloat / active stage of decomposition. The samples obtained from late stage decomposition were collected below bodies that were fully skeletonized. Given the data, these results support an initial pulse of nutrients into the soil, and between two weeks and four years postmortem there is a decline in the concentration of the recorded soil parameters. The soil samples began to mimic negative control samples by four years postmortem.

The biotic data that were generated for the samples within the facility remained concordant with the abiotic data, but demonstrated significant differences between the areas of high decomposition to those with no history of decomposition. The bins of high decomposition were marked by a different bacterial community in response to soil saturation from carcass enrichment. The areas with high levels of human decomposition were characterized by greater abundance of chemoorganotrophic and sulfate-reducing bacteria, and a reduction in Acidobacteria from those areas of no recorded human decomposition. The bins with high levels of N input that results from protein reduction by microorganisms are those of high decomposition. In effect, the increased soil pH resulting from human decomposition removes

the filter that permits Acidobacteria to thrive at the expense of less acid-tolerant organisms. Such a change indicated a shift in the indigenous community of soil-dwelling bacteria in response to carcass enrichment and ammonification of the soil.

The abiotic data suggested a lack of differentiation within the facility, and yet all samples were quite dissimilar from those taken outside the facility. The biotic data confirmed the similarity inside the facility, but also identified one significant difference between the bins of High and No human decomposition. Taken in sum, results of analyses of both the abiotic and biotic datasets support the CDI concept (Carter et al. 2007) of carcass enrichment of the soil following decomposition, given the consistent differences among the samples and variables within the facility to those taken outside the facility. These observations suggest a homogenization of the facility landscape. The cause of this may be a combination of the constant decay of human remains, myriad land-use histories, and / or the culmination of 30 years of research and education activity. These findings suggest that after 30 years of use the facility has become an island in its entirety.

In summary, the addition of a rich nutrient source, such as a human, to the landscape results in an increase in the carrying capacity of the niche at multiple trophic levels until the substrate cache of energy-bound biomolecules and nutrients are depleted. Thirty years of decomposition research at the ARF has forced a shift in the underlying bacterial community in response to the enrichment of the soil with increased nitrogen and carbon-containing compounds. The baseline data presented in this work provides a control dataset for further exploration regarding the biogeochemical relationships among microbial organisms, soil characteristics, and cadaver decomposition. Within this relationship there exists a potential for developing new models relating to postmortem interval estimation and clandestine grave location.

LIST OF REFERENCES

Aturaliya S, Lukasewycz A (1999) Experimental forensic and bioanthropological aspects of soft tissue taphonomy: 1. Factors influencing postmortem tissue desiccation rate. Journal of Forensic Sciences 44:893–896.

Bass WM (1984) Time interval since death: a difficult decision. In Rathbun TA and Buikstra JE (eds), *Human Identification: Case Studies in Forensic Anthropology.* CC Thomas: Springfield.

Bass WM (1997) Outdoor decomposition rates in Tennessee. In Haglund WD and Sorg MH (eds), *Forensic Taphonomy: The Postmortem Fate of Human Remains*. CRC Press: Boca Raton.

Behrensmeyer AK (1984) Taphonomy and the fossil record. *American Scientist* 72:558-566.

Bell LS, Skinner MF, and Jones, SJ (1996) The speed of post mortem change to the human skeleton and its taphonomic significance. *Forensic Science International* 82:129–140.

Benninger LA, Carter DO, and Forbes S (2008) The biochemical alteration of soil beneath a decomposing corpse. *Forensic Science International* 180:70-75.

Berna F, Matthews A, and Weiner (2004) Solubilities of bone mineral from archaeological sites: the recrystallization window. *Journal of Archaeological Sciences* 31:867–882.

Blumenschine RJ (1995) Percussion marks, tooth marks and the experimental determinations of the timing of hominid and carnivore access to long bones at FLK *Zinjanthropus*, Olduvai Gorge, Tanzania. *Journal of Human Evolution* 29:21-51.

Bonnichsen R and Sorg MH (1989) *Bone Modification*. University of Maine, Center for the Study of the First Americans, Orono.

Brady NC and Weil RR (1999) *The Nature and Properties of Soils*. Prentice Hall: Upper Saddle River.

Brain CK (1981) Hunters or the Hunted?: An Introduction to African Cave Taphonomy. University of Chicago Press: Chicago.

Burges A (1967) The decomposition of organic matter in the soil. In: Burges A and Raw F (eds) *Soil Biology*, Academic Press: New York.

Campobasso CP, Vella GD, and Introna F (2001) Factors affecting decomposition and diptera colonization. *Forensic Science International* 120:18-27.

Carter DO and Tibbett M (2003) Taphonomic mycota: fungi with forensic potential. *Journal of Forensic Sciences* 48:168-171.

Carter DO, Yellowlees D, Tibbett M (2007) Cadaver decomposition in terrestrial ecosystems. *Naturwissenschaften* 94:12-24.

Carter DO, Yellowlees D, Tibbett M (2010) Moisture can be the dominant environmental parameter governing cadaver decomposition in soil. *Forensic Science International* 200:60-66.

Castellano MA, Villanueva EC and von Frenckel R (1984) Estimating the date of bone remains: a multivariate study. *Journal of Forensic Sciences* 29:527-534.

Cattaneo C, Dimartino S, Scali S, Craig OE, Grandi M, Sokol RJ (1999) Determining the human origin of fragments of burnt bone: a comparative study of histological, immunological and DNA techniques. *Forensic Science International* 102:181–91.

Chandler DP, Fredrickson JK, and Brockman FJ (1997) Effect of PCR template concentration on the composition and distribution of total community 16S rDNA clone libraries. *Molecular Ecology* 6:475-482.

Cheng J and Greiner R (2001) Learning Bayesian Belief Network Classifiers: Algorithms and System, p 141-151. In Stroulia E and Matwin S (eds) *Advances in Artificial Intelligence, 14th Biennial Conference of the Canadian Society for Computational Studies of Intelligence, AI 2001* Ottawa, Canada, June 2001 Proceedings. Springer-Verlag: Berlin.

Child AM, Gillard RD, and Pollard AM (1993) Microbially-induced promotion of amino acid racemization in bone: isolation of the organisms and detection of their enzymes. *Journal of Archaeological Science* 20:159-168.

Child AM (1995) Towards an understanding of the microbial decomposition of archaeological bone in the burial environment. *Journal of Archaeological Science* 22:165-174.

Clark MA, Worrell MB, and Pless JE (1997) Postmortem Changes in Soft Tissues. In Haglund WD and Sorg MH (eds), *Forensic Taphonomy: The Postmortem Fate of Human Remains*. CRC Press: Boca Raton.

Clarke KR and Gorley RN (2006) *PRIMER v6: Users Manual/Tutorial*. PRIMER-E: Plymouth.

Clarke KR and Warwick RM (2001) *Change in Marine Communities: An Approach to Statistical Analysis and Interpretation, 2nd edition*. Primer-E: Plymouth.

Coble MD and Butler JM (2005) Characterization of new miniSTR loci to aid analysis of degraded DNA. *Journal of Forensic Sciences* 50: 43-53.

Cole JR, Wang Q, Cardenas E, Fish J, Chai B, Farris RJ, Kulam-Syed-Mohideen AS, McGarrell DM, Marsh T, Garrity GM, and Tiedje JM (2009) The Ribosomal Database Project: improved alignments and new tools for rRNA analysis. *Nucleic Acids Research* 37 (Database issue).

Coleman DC, Crossley Jr. DA, and Hendrix PF (2004) *Fundamentals of soil ecology*, 2nd edition. Elsevier Academic Press: Burlington.

Collins MJ, Riley MS, Child A and Turner-Walker G (1995) A basic mathematical simulation of the chemical degradation of ancient collagen, *Journal of Archaeological Science* 22:175-183.

Dart RA (1957) The Osteodontokeratic Culture of Australopithecus Prometheus. *Transvaal Museum Memoir*, *No 10*. Pretoria.

DeFiore JC (1996) *Miracle in the Valley: A History of the University of Tennessee Medical Center at Knoxville, 1944 – 1995*, University of Tennessee Press: Knoxville.

Dent BB, Forbes SL, and Stuart BH (2004) Review of human decomposition processes in soil. *Environmental Geology* 45: 576-585.

DiMaio VJM and DiMaio DJ (2001) *Forensic Pathology*. CRC Press: Boca Raton.

Dickson GC, Kieser J, Mass EW and Poulter RTM (2010) Marine bacteria: forensic indicators of submersion interval. AAFS Published Abstract, 62nd Annual Meeting of the American Academy of Forensic Sciences.

Dominguez-Rodrigo M and Barba R (2006) New estimates of tooth mark and percussion mark frequencies at the FLK Zinj site: the carnivore-hominid-carnivore hypothesis falsified. *Journal of Human Evolution* 50:170-194.

Drijber RA, Doran JW, Parkhurst AM, and Lyon DJ (2000) Changes in soil microbial structure with tillage under long-term wheat-fallow management. *Soil Biology and Biochemistry* 32:1419-1430.

Edson SM, Ross JP, Coble MD, Parson TJ, Barritt SM (2004) Naming the dead - confronting the realities of rapid identification of degraded skeletal remains. *Forensic Science Review* 16:63-88.

Edwards R, Chaney B, and Bergman M (1987) *Pest & Crop Newsletter,* pp. 5-6. No. 2.

Efremov IA (1940) Taphonomy: new branch of paleontology. *Pan American Geologist* 74:81-93.

Evans WED (1963) *The Chemistry of Death*. Charles C. Thomas: Springfield.

Feinstein LM, Jun-Sul W, and Blackwood CB (2009) Assessment of bias associated with incomplete extraction of microbial DNA from soil. *Applied Environmental Microbiology* 75:5428-5433.

Fisher DL, Holland MM, Mitchell L, Sledzik PS, Wilcox AW, Wadhams M, Weedn VW (1993) Extraction, evaluation, and amplification of DNA from decalcified and un-decalcified United States Civil War bone. Journal of Forensic Sciences 38:60-68.

Forbes SL, Keegan J, Stuart BH, and Dent BD (2003) A gas chromatography-mass spectrometry method for the detection of adipocere in grave soils. *European Journal of Science and Technology* 105: 761-768.

Forbes SL, Stuart BH, Dadour IR, Dent BB (2004) A preliminary investigation of the stages of adipocere formation. *Journal of Forensic Sciences* 49:566–574.

Forbes SL, Dent BB, Stuart DH (2005) The effect of soil type on adipocere formation. *Forensic Science International* 154: 35–43.

Gabriel MN, Huffine EF, Ryan JH, Holland MM, Parsons TJ (2001) Improved mtDNA sequence analysis of forensic remains using a "mini-primer" set amplification strategy. *Journal of Forensic Science* 46:247-253.

Galloway A (1997) The process of decomposition: a model from the Arizona-Sonoran desert. In Haglund WD and Sorg MH (eds), *Forensic Taphonomy: The Postmortem Fate of Human Remains*. CRC Press: Boca Raton.

Galloway A, Birkby WH, Jones AM, Henry TH, Parks BO (1989) Decay rates of human remains in an arid environment. *Journal of Forensic Sciences* 34:607-616.

Garrity GM, Bell JA, Lilburn TG (2004) Taxonomic outline of the procaryotes. *Bergey's Manual of Systematic Bacteriology*. Springer-Verlag: New York.

Garrity GM (2005) *Bergey's Manual of Systematic Bacteriology, 2nd edition, Volume 2*. Springer-Verlag: New York.

Gifford DP (1981) Taphonomy and paleoecology: a critical review of archaeology's sister disciplines. In Schiffer MB (ed): *Advances in Archaeological Method and Theory*, *Volume 4*. Academic Press: New York.

Gill-King H (1997) Chemical and ultrastructural aspects of decomposition. In Haglund WD and Sorg MH (eds), *Forensic Taphonomy: The Postmortem Fate of Human Remains*. CRC Press: Boca Raton.

Gordon CC and Buikstra JE (1981) Soil pH, bone preservation, and sampling bias at mortuary sites. American Antiquity 46:566-571.

Grupe G and Piepenbrink H (1988) Trace element contaminations in excavated bones by microorganisms. In *Trace Elements in Environmental History*, edited by G Grupe and B Herrmann, pp. 103-112, Springer-Verlag, Berlin.

Grupe G and Garland AN (1993) *Histology of Ancient Human Bone: Methods and Diagnosis*. Springer-Verlag: Berlin.

Hackett CL (1981) Microscopical focal destruction (tunnels) in exhumed human bones. *Medicine, Science and the Law* 21:243-265.

Haglund WD and Sorg MH (1997) *Forensic Taphonomy: The Postmortem Fate of Human Remains*. CRC Press: Boca Raton.

Haglund WD (1997a) Dogs and Coyotes: Postmortem Involvement with Human Remains. In Haglund WD and Sorg MH (eds), *Forensic Taphonomy: The Postmortem Fate of Human Remains*. CRC Press: Boca Raton.

Haglund WD (1997b) Rodents and Human Remains. In Haglund WD and Sorg MH (eds), *Forensic Taphonomy: The Postmortem Fate of Human Remains*. CRC Press: Boca Raton.

Hartgrove NT (2006) *Soil Survey of Knox County, Tennessee. USDA: Natural Resources Conservation Services, National Cooperative Soil Survey*.

Haslam TCF and Tibbett M (2009) Soils of contrasting pH affect the decomposition of buried mammalian (*Ovis aries*) skeletal muscle tissue. *Journal of Forensic Sciences* 54:900-904.

Hedges REM, Millard AR, Pike AWG (1995) Measurements and relationships of diagenetic alteration of bone from three archaeological sites. *Journal of Archeological Science* 22:201-209.

Heiri O, Lotter AF, and Lemcke G (2001) Loss on ignition as a method for estimating organic and carbonate content in sediments: reproducibility and comparability of results. *Journal of Paleolimnology* 25:101-110.

Helfman PM and Bada JL (1976) Aspartic acid racemization in dentine as a measure of ageing. *Nature* 262: 279-281.

Holland MM, Fisher DL, Mitchell LG, Rodriquez WC, Canik JJ, Merril CR and Weedn V (1993) Mitochondrial DNA sequence analysis of human skeletal remains: identification of remains from the Vietnam War. *Journal Forensic Sciences* 38:542-553.

Holland MM, Fisher DL, Roby RK, Ruderman J, Bryson C, Weedn VW (1995) Mitochondrial DNA sequence analysis of human remains. *Crime Lab Digest* 22:3-8.

Holland MM and Huffine EF (2000) Molecular Analysis of the Human Mitochondrial DNA Control Region for Forensic Identity Testing. *Current Protocols in Human Genetics* Supplement 26 August, Unit 14.7.

Holland TD, Anderson BE, and Mann RW (1997) Human variables in the postmortem alteration of human bone: examples from U.S. war casualties. In Haglund WD and Sorg MH (eds), *Forensic Taphonomy: The Postmortem Fate of Human Remains*. CRC Press: Boca Raton.

Hopkins DW, Wiltshire PEJ, Turner DB (2000) Microbial characteristics of soils from graves: an investigation at the interface of soil microbiology and forensic science. *Applied Soil Ecology* 14:283–288.

Jans MME, Nielsen-Marsh CM, Smith CI, Collins MJ, and Kars H (2004) Characterisation of microbial attack on archaeological bone. *Journal of Archaeological Science* 31:87-95.

Jantz LM and Jantz R (2008) The Anthropology Research Facility: the outdoor laboratory of the Forensic Anthropology Center, University of Tennessee. In: Warren MW, Walsh-Haney HA, Freas LE (eds), *The Forensic Anthropology Laboratory*. CRC Press: Boca Raton.

Jenny H (1941) *Factors of Soil Formation: A System of Quantitative Pedology*. McGraw-Hill: New York.

Jones D and Collins MD (1986) Irregular, nonsporing gram-positive rods. In Sneath PHA, Mair NS, Sharpe ME, and Holt JG (eds) *Bergey's Manual of Systematic Bacteriology, Volume 2*. William & Wilkins: Baltimore.

Jones RT, Robeson MS, Lauber CL, Hamady M, Knight R, and Fierer N (2009) A comprehensive survey of soil acidobacterial diversity using pyrosequencing and clone library analyses. *The ISME Journal* 3:442-453.

Kates M (1986) Techniques in lipidology: isolation, analysis, and identification of lipids. In: Burdon RH and Van Kippenberg PH (eds), *Laboratory techniques in Biochemistry and Molecular Biology, Volume 3, Part 2:123-127*. Elsevier: New York.

Keijser BJF, Zaura E, Huse SM, van der Vossen JMBM, Schuren FHJ, Montijn RC, ten Cate JM, and Crielaard W (2008) Pyrosequencing analysis of the oral microflora of healthy adults. *Journal of Dental Research* 87:1016-1020.

Kerley ER (1966) The microscopic determination of age in human bone. *American Journal of Physical Anthropology* 23:149-164.

Kerley ER and Ubelaker DH (1978) Revisions in the microscopic method of estimating age at death in human cortical bone. *American Journal of Physical Anthropology* 49:545–546.

Klippel WE and Synstelien JA (2007) Rodents as taphonomic agents: bone gnawing by brown rats and gray squirrels, *Journal of Forensic Sciences* 52:765-773.

Lane D (1991) 16s/23s rRNA sequencing, pp 115-175. In Stackebrandt E and Goodfellow M (eds), *Nucleic Acid Techniques in Bacterial Systematics*. John Wiley & Sons: West Sussex.

Larkin JM (1986) Nonphotosynthetic, nonfruiting gliding bacteria. In Staley JT, Bryant MP, Pfennig N, and Holt JG (eds) *Bergey's Manual of Systematic Bacteriology, Volume 3.* William & Wilkins: Baltimore.

Layton A, Mckay L, Williams D, Garrett V, Gentry R, and Sayler G (2006) Development of *Bacteroides* 16S rRNA gene TaqMan-based real-time PCR assays for estimation of total, human, and bovine fecal pollution in water. *Applied and Environmental Microbiology* 72:4214-4224.

Leckie SE, Prescott CE, Grayston SJ, Neufeld JD, and Mohn WW (2004) Comparison of chloroform fumigation-extraction, phospholipid fatty acid, and DNA methods to determine microbial biomass in forest humus. *Soil Biology and Biochemistry* 36**:**529-532.

Lee DH, Zo YG, and Kim SJ (1996) Non-radioactive method to study genetic profiles of natural bacterial communities by PCR-single-strand-conformation polymorphism. *Applied Environmental Microbiology* 62:3112-3120.

Loreille OM, Diegoli TM, Irwin JA, Coble MD, and Parsons TJ (2007) High efficiency DNA extraction from bone by total demineralization. *Forensic Science International: Genetics* 1:191-195.

Love JC and Marks M (2003) Taphonomy and time: estimating the postmortem interval. In Steadman DW (ed), *Hard Evidence: Case Studies in Forensic Anthropology*. Prentice Hall: Upper Saddle River.

Mann RW, Bass WM, and Meadows L (1990) Time since death and decomposition of the human body: variables and observations in case and experimental field studies, *Journal of Forensic Sciences* 35:103-111.

Mant AK (1987) Knowledge acquired from post-War exhumations. In Boddington A, Garland AN, and Janaway C (eds), *Death, Decay and Reconstruction: Approaches to Archaeology and Forensic Science*, Manchester: University Press, 65-78.

Marchiafava V, Bonucci E, and Ascenzi A (1974) Fungal osteoclasia: a model of dead bone resorption. *Calcified Tissue Research* 14:195–210.

Marchesi JR, Sato T , Weightman AJ, Martin TA, Fry JC, Hiom SJ, and Wade W (1998) Design and evaluation of useful bacterium-specific PCR primers that amplify genes coding for bacterial 16S rRNA. *Applied Environmental Microbiology* 64:795-799.

Martin RD (1993) Primate origins: plugging the gaps. *Nature* 363:223-234.

Margulies M, Egholm M, Altman WE, Attiya S, Bader JS, Bemben LA, Berka J, Braverman MS, Chen YJ, Chen Z, Dewell SB, Winter A, Drake J, Du L, Fierro JM, Forte R, Gomes XV, Godwin BC, He W, Helgesen S, Ho CH, Hutchison SK, Irzyk GP, Jando SC, Alenquer MLI, Jarvie TP, Jirage KB, Kim JB, Knight JR, Lanza JR, Leamon JH, Lee WL, Lefkowitz SM, Lei M, Li J, Lohman KL, Lu H, Makhijani VB, McDade KE, McKenna MP, Myers EW, Nickerson E, Nobile JR, Plant R, Puc BP, Reifler M, Ronan MT, Roth GT, Sarkis GJ, Simons JF, Simpson JW, Srinivasan M, Tartaro KR, Tomasz A, Vogt KA, Volkmer GA, Wang SH, Wang Y, Weiner MP, Willoughby DA, Yu P, Begley RF, Rothberg JM (2005) Genome sequencing in microfabricated high-density picolitre reactors. *Nature* 437:376-380.

McCauley A, Jones C, and Jacobson J (2009) Nutrient Management Module No. 8: Soil pH and Organic Matter. *Nutrient Management 4449-8*. Montana State University Extension: Bozemen.

McGuire KL and Treseder KK (2010) Microbial communities and their relevance for ecosystem models: Decomposition as a case study. *Soil Biology and Biochemistry* 42:529-535.

Megyesi MS, Nawrocki SP, and Haskell NH (2005) Using accumulated degree-days to estimate the postmortem interval from decomposed human remains. *Journal of Forensic Sciences* 50:618-626.

Melvin JR Jr, Cronholm LS, Simson LR, and lsaacs AM (1984) Bacterial transmigration as an indicator of time of death. *Journal of Forensic Sciences* 29:412-417.

Micozzi MS (1991) *Postmortem Change in Human and Animal Remains*. Charles C. Thomas: Springfield.

Miller DN, Bryant JE, Madsen EL, and Ghiorse WC (1999) Evaluation and optimization of DNA extraction and purification procedures for soil and sediment samples. *Applied and Environmental Microbiology* 65: 4715-4724.

Moorhead DL and Sinsabaugh RL (2006) A theoretical model of litter decay and microbial interaction. *Ecological Monographs* 76: 151–174.

Mullis KB and Faloona FA (1987) Specific synthesis on DNA in vitro via a polymerase-catalyzed chain reaction. *Methods in Enzymology* 155:335-350.

Muyzer G, De Waal EC, Uitierlinden AG (1993) Profiling of complex microbial populations by denaturing gradient gel electrophoresis analysis of polymerase chain reaction-amplified genes coding for 16S rRNA. *Applied Environmental Microbiology* 59:695-700.

Ogino T, Ogino H, and Nagy B (1985) Application of aspartic acid racemization to forensic odontology: post mortem designation of age at death. *Forensic Science International* 29:259-267.

Olson JS (1963) Energy storage and the balance of producers and decomposers in ecological systems. *Ecology* 44: 322-331.

Parkinson RA (2009) *Bacterial Communities Associated with Human Decomposition*. Dissertation, Victoria University of Wellington.

Parkinson RA, Dias KR, Horswell J, Greenwood P, Banning N, Tibbett M and Vass AA (2009) Microbial community analysis of human decomposition in soil. In Ritz K, Dawson LA, Miller D (eds), *Criminal and Environmental Soil Forensics*. Springer: New York.

Parsons TJ and Weedn VW (1997) Preservation and recovery of DNA in postmortem specimens and trace samples. In WD Haglund and MH Sorg (eds): *Forensic Taphonomy: the Postmortem Fate of Human Remains*, pp.459-468. CRC Press: Boca Raton.

Paul EA (2007) *Soil Microbiology, Ecology, and Biochemistry, 3rd edition*. Academic Press: Amsterdam.

Payne JA (1965) A summer carrion study of the baby pig *Sus scrofa* Linnaeus. *Ecology* 46:592-602.

Payne-James J, Busuttil A, and Smock W (2003) *Forensic Medicine: Clinical and Pathological Aspects.* Greenwich Medical Media Limited: San Francisco.

Perper J (1993) Time of death and changes after death. In W Spitz (ed): *Medicolegal Investigation of Death: Guidelines for the Application of Pathology to Crime Investigation*. Charles C Thomas: Springfield.

Perry WL III, Bass WM, Riggsby WS, and Sirotkin K (1988) The autodegradation of deoxyribonucleic acid (DNA) in human rib bone and its relationship to the time interval since death. *Journal of Forensic Sciences* 33:144-153.

Putman RJ (1978a) Patterns of carbon dioxide evolution from decaying carrion. Decomposition of small mammal carrion in temperate systems 1. *Oikos* 31:47-57.

Prostgate J (2000) *Microbes and Man, 4th edition*. Cambridge University Press: Cambridge.

Porteous LA and Armstrong JL (1991) Recovery of bulk DNA from soil by a rapid, small-scale extraction method. *Current Microbiology* 22:345-348.

Putman RJ (1978b) Flow of energy and organic matter from a carcass during decomposition. Decomposition of small mammal carrion in temperate systems 2. *Oikos* 31:58-68.

Putman RJ (1983) Carrion and dung: the decomposition of animal wastes. *The Institute of Biology's Studies in Biology no. 165*. Edward Arnold Ltd: London.

Regan LA (2006) *Isotopic determination of region of origin in modern peoples applications for identification of US war dead from the Vietnam conflict*. University of Florida: Gainsville.

Reed HB (1958) A study of dog carcass communities in Tennessee, with special reference to the insects. *American Midland Naturalist* 59:213-245.

Reysenbach A, Giver L, Wickham G, and Pace N (1992) Differential amplification of rRNA genes by polymerase chain reaction. *Applied and Environmental Microbiology* 58:3417-3418.

Ricklefs RE (1997) *The Economy of Nature*, Fourth edition. WH Freeman and Company: New York.

Rodriguez WC and Bass WM (1983) Insect Activity and its Relationship to Decay Rates of Human Cadavers in East Tennessee. *Journal of Forensic Sciences* 28:423-432.

Rodriguez WC and Bass WM (1985) Decomposition of buried bodies and methods that may aid in their location. *Journal of Forensic Sciences* 30:836-852.

Rodriguez WC (1997) Decomposition of Buried and Submerged Bodies. In WD Haglund and MH Sorg (eds.): *Forensic Taphonomy: the Postmortem Fate of Human Remains*, pp.459-468. CRC Press: Boca Raton.

Roesch LFW, Fulthorpe RR, Riva A, Casella G, Hadwin AKM, Kent AD, Daroub SH, Camargo FAO, Farmerie WG, and Triplett EW (2007) Pyrosequencing enumerates and contrasts soil microbial diversity. *International Society for Microbial Ecology* 1:283-290.

Ronaghi M, Uhlen M and Nyren, P (1998) A sequencing method based on real-time pyrophosphate. *Science* 281:363–365.

Sandhu GS, Kline BC, Stockman L, and Roberts GD (1995) Molecular Probes for Diagnosis of Fungal Infections. *Journal of Clinical Microbiology* 33:2913-2919.

Sangkhobol V and Skerman VBD (1981) Chitinophaga, a new genus of chitinolytic myxobacteria. *International Journal of Systematic Bacteriology* 31:385-293.

Schleifer KH (1986) Gram-positive cocci. In Sneath PHA, Mair NS, Sharpe ME, and Holt JG (eds) *Bergey's Manual of Systematic Bacteriology, Volume 2*. William & Wilkins: Baltimore.

Schy WE and Plewa MJ (1989) Use of the diaminobenzoic acid fluorescence assay in conjunction with UV absorbance as a means of quantifying and ascertaining the purity of a DNA preparation. *Analytical Biochemistry* 180:314-318.

Sledzik PS (1998) Forensic taphonomy: postmortem decomposition and decay. In: Reichs KJ (ed) *Forensic osteology: Advances in the Identification of Human Remains*, second edition. Charles C. Thomas: Springfield.

Sidrim JJC, Moreira Filho RE, Cordeiro RA, Rocha MFG, Caetano EP, Monteiro AJ and Brilhante RSN (2010) Fungal microbiota dynamics as a postmortem investigation tool: focus on Aspergillus, Penicillium and Candida species. *Journal of Applied Microbiology* 108:1751–1756.

Spitz WU and Fisher RS (1980) *Medicolegal Investigation of Death: Guidelines for the Application of Pathology to Crime Investigation*, 2nd edition. Charles C Thomas: Springfield.

Stevenson FJ (1982) *Humus Chemistry*. Wiley-Interscience: New York.

Storer DA (1984) A simple high sample volume ashing procedure for determining soil organic matter. *Communications in Soil Science and Plant Analysis* 15:759-772.

Swift MJ, Heal OW, Anderson JM (1979) *Decomposition in terrestrial ecosystems*. Blackwell Scientific: Oxford.

Tibbett M, Carter DO, Haslam T, Major R, Haslam R (2004) A laboratory incubation method for determining the rate of microbiological degradation of skeletal muscle tissue in soil. *Journal of Forensic Sciences* 49:560-565.

Towne EG (2000) Prairie vegetation and soil nutrient responses to ungulate carcasses. *Oecologica* 122:232–239.

Turner-Walker and Syversen (2002) Quantifying histological changes in archaeological changes in archaeological bones using BSE SEM image analysis. *Archaeometry* 44: 461–468.

Ubelaker DH and Adams BJ (1995) Differentiation of perimortem and postmortem trauma using taphonomic indicators, *Journal of Forensic Sciences* 40:509-12.

Ubelaker DH (1997) Taphonomic applications in forensic anthropology. In Haglund WD and Sorg MH (eds): *Forensic Taphonomy: The Postmortem Fate of Human Remains*. CRC Press: Boca Raton.

Ubelaker DH, Lowenstein JM, Hood DG (2004) Use of solid-phase double-antibody radioimmunoassay to identify species from small skeletal fragments. *Journal of Forensic Sciences* 49:924-929.

Van't Hoff, JH (1884) *Etudes de dynamique chemique*. Frederik Muller & Co: Amsterdam.

Vass AA, Bass WM, Wolt JD, Foss JE, Ammons JT (1992) Time since death determinations of human cadavers using soil solution. *Journal of Forensic Sciences* 37:1236–53.

Vass AA, Barshick S-A, Sega G, Caton J, Skeen JT, Love JC, Synstelien JA (2002) Decomposition chemistry of human remains: a new methodology for determining the postmortem interval. *Journal of Forensic Sciences* 47:542-553.

Vass AA, Smith RR, Thompson CV, Burnett MN, Wolf DA, Synstelien JA, Gulgerian N, and Eckenrode BA (2004) Decompositional Odor Analysis Database. *Journal of Forensic Sciences* 49:760-769.

Vass AA, Smith RR, Thompson CV, Burnett MN, Dulgerian N, Eckenrode BA (2008) Odor Analysis of Decomposing Buried Human Remains. *Journal of Forensic Sciences* 53:384-391.

Voroney RP (2007) The soil habitat. In Paul EA (ed) *Soil Microbiology, Ecology, and Biochemistry, 3rd edition*. Academic Press: Amsterdam.

Wang Q, Garrity GM, Tiedje JM, and Cole JR (2007) Naïve Bayesian Classifier for Rapid Assignment of rRNA Sequences into the New Bacterial Taxonomy. *Applied Environmental Microbiology* 73:5261-7.

Watson RJ and Blackwell B (2000) Purification and characterization of a common soil component which inhibits the polymerase chain reaction. *Canadian Journal of Microbiology* 46:633-642.

Wayne LG and Kubica GP (1986) The Mycobacteria. In Sneath PHA, Mair NS, Sharpe ME, and Holt JG (eds) *Bergey's Manual of Systematic Bacteriology, Volume 2*. William & Wilkins: Baltimore.

White CD, Longstaffe FJ, and Law KR (2004). Exploring the effects of environment, physiology and diet on oxygen isotope ratios in ancient Nubian bones and teeth. *Journal of Archaeological Science* 31:233-250.

White EM and LA Hannus (1983) Chemical Weathering of Bone in Archaeological Soils. *American Antiquity* 48:316-322.

White TJ, Bruns T, Lee S, Taylor J (1990) Amplification and direct sequencing of fungal ribosomal RNA genes for phylogenetics. In Innis MA, Gelfand DH, Sninsky JJ, and White TJ (eds) *PCR Protocols: A Guide to Methods and Applications.* Academic Press: San Diego.

Willey P and Heilman A (1987) Estimating time since death using plant roots and stems. *Journal of Forensic Sciences* 32:1264-1270.

Willey P and Snyder LM (1989) Canid modification of human remains: implications for time-since death estimation. *Journal of Forensic Sciences* 34:894-901.

Wilson M (2008) *Bacteriology of Humans: An Ecological Perspective*. Blackwell Publishing: Malden.

Yoshino M, Kimijima T, Miyasaka S, Sato H, and Seta S (1991) Microscopical study on time since death in skeletal remains. *Forensic Science International* 49:143–158.

APPENDICIES

APPENDIX A:

Historical U.S. Geological Survey map sheets showing the location of the University of Tennessee Anthropology Research facility.

Figure A-1. Knoxville 7.5 minute series 147-NW, 1942.

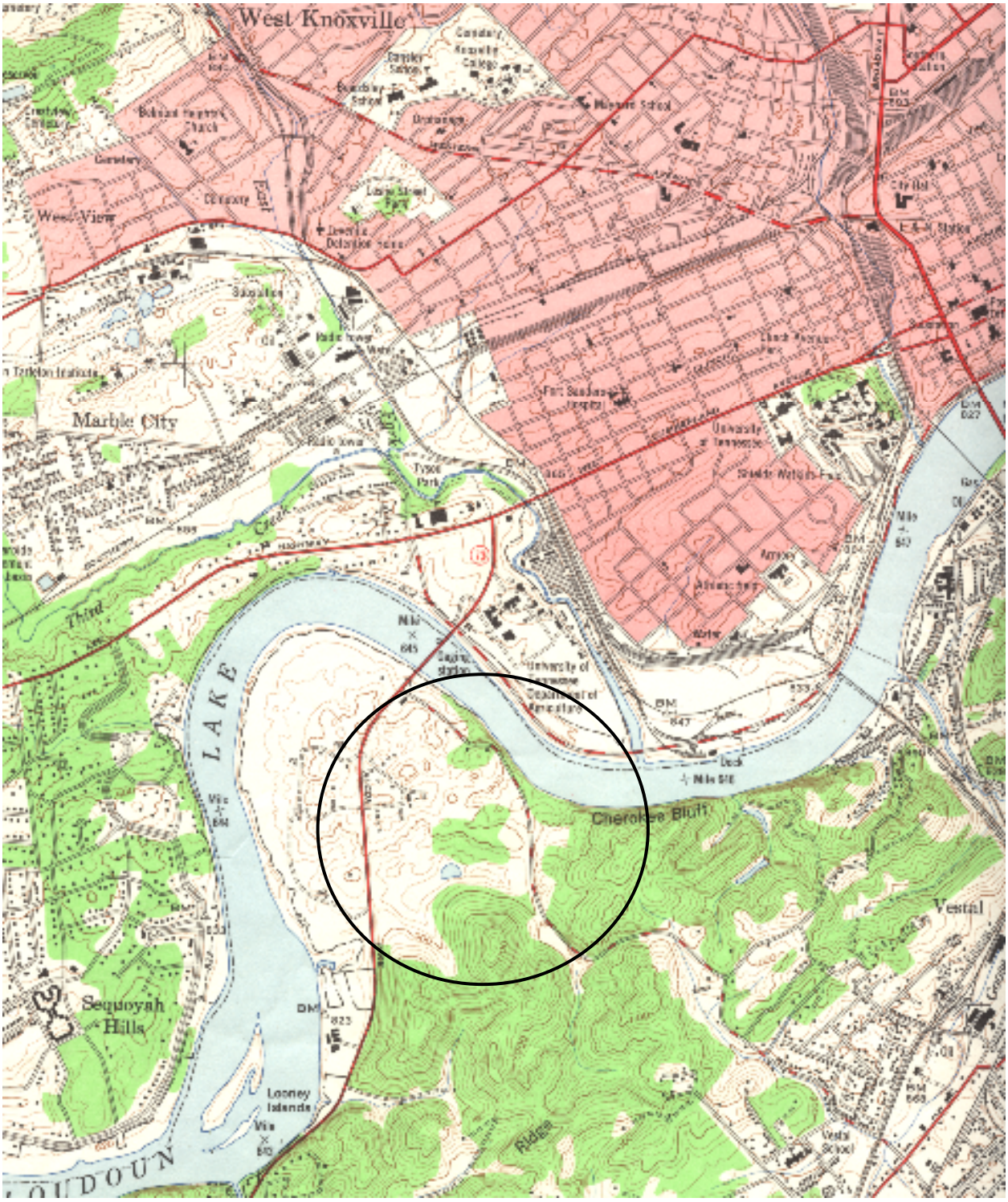

Figure A-2. Knoxville 7.5 minute series 147-NW, 1953.

Figure A-3. Knoxville 147-NW, 1965. The small unpaved road is marked with an arrow.

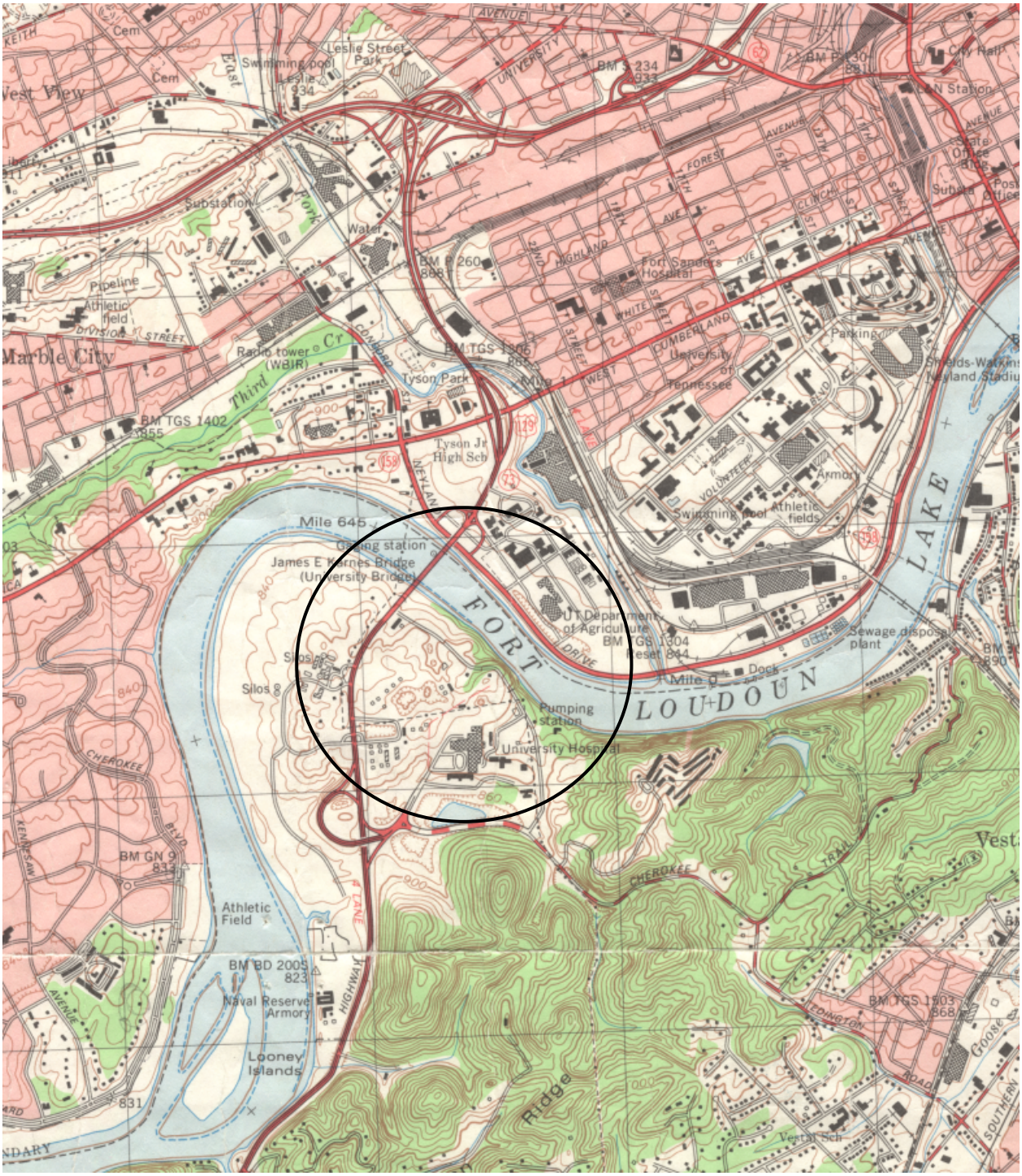

Figure A-4. Knoxville 7.5 minute series 147-NW, 1978.

APPENDIX B:

ArcGIS maps of the University of Tennessee Anthropology Research Facility showing the distribution of cadaver decomposition across the facility.

Figure B-1. Aerial photograph of ARF with outline of facility marked in black.

Figure B-2. Map of ARF with body location determined by GPS waypoint demonstrating nonrandom placement of bodies over a four year period (2001-2005).

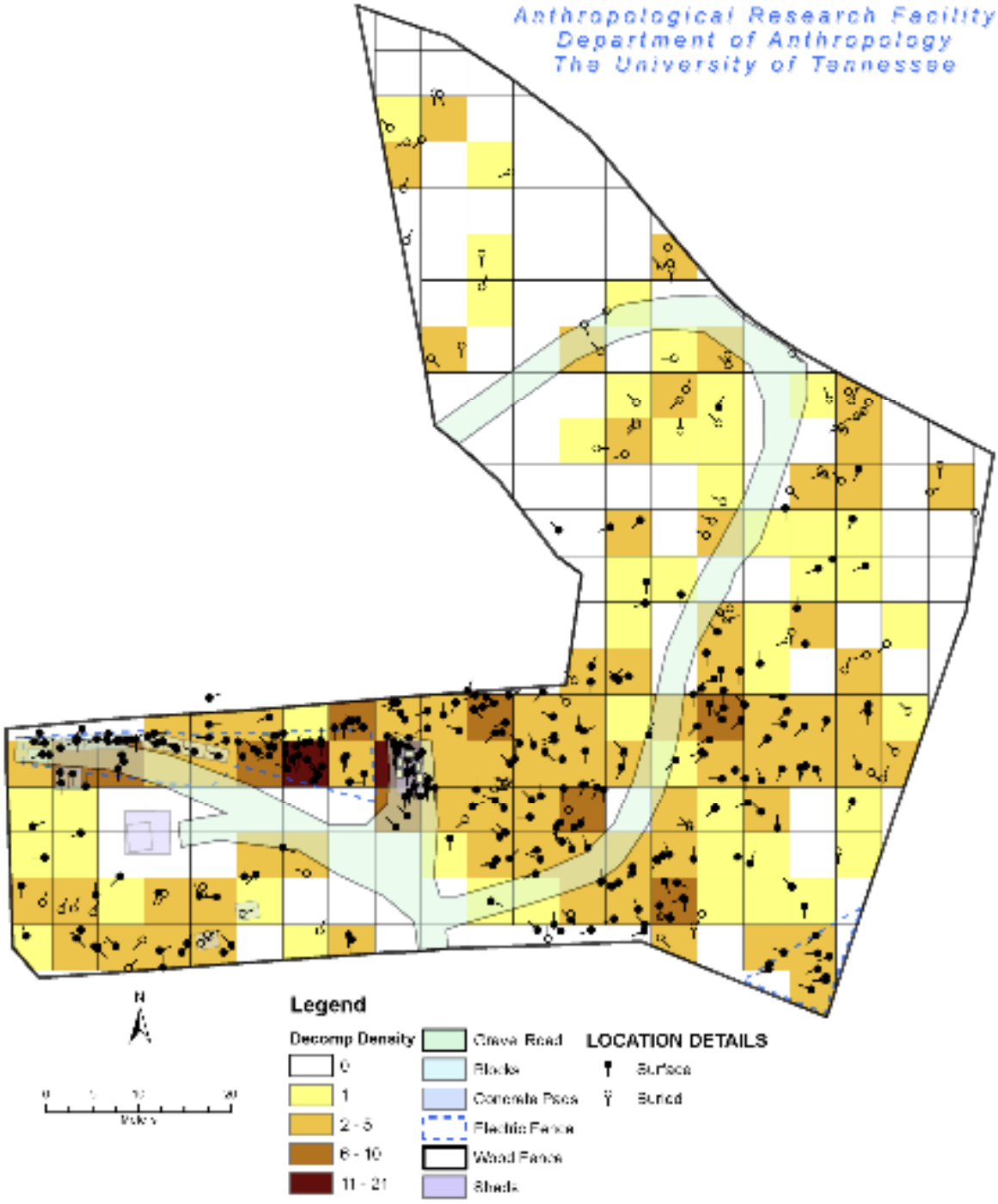

Figure B-3. Decomposition density demonstrating nonrandom placement of corpses over a four year period (2001-2005). Dark-colored units indicate areas of frequent body decomposition.

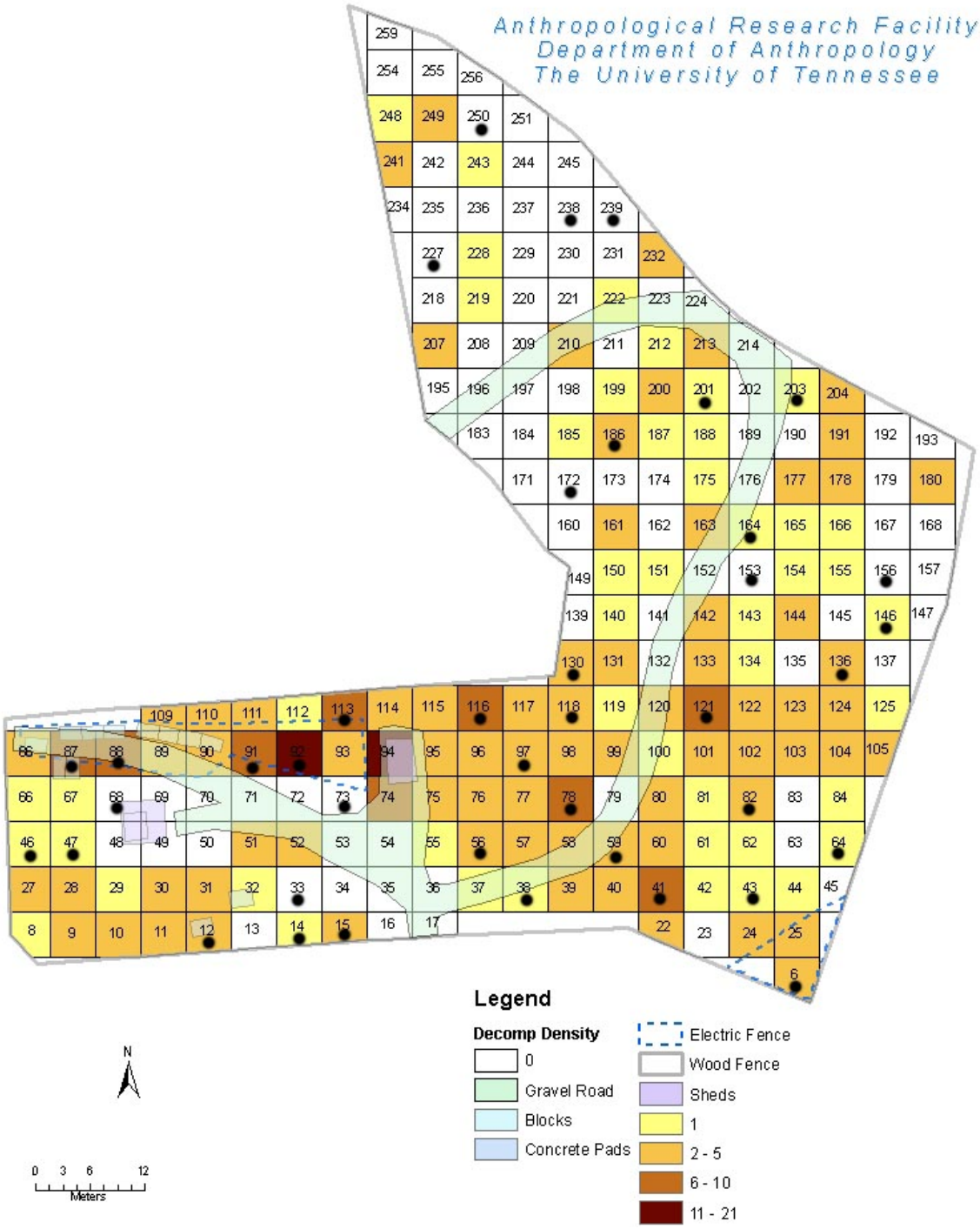

Figure B-4. Decomposition density at ARF demonstrating areas of continual use relative to those areas of infrequent use. Black dots indicate selected units for analysis.

Appendix C:

Abiotic Environmental Data Series

H_2O, percent moisture content of soil
LOI, percent organic content by loss on ignition
pH, soil acidity / alkalinity
C, percent of total carbon g^{-1} soil
N, percent of nitrogen g^{-1} soil
C:N, ratio of carbon to nitrogen
Phos., Lipid-bound phosphorus $\mu g\ \mu L^{-1}$
DNA, total extract ng μl^{-1}

Table C-1. Abiotic Environmental Data Series.										
Sample No.	**Decomposition Bin**		**H_2O**	**LOI**	**pH**	**C**	**N**	**C:N**	**Phos.**	**DNA**
006	Middle	2	16.48	4.37	4.89	5.13	0.58	8.78	5.33	68.62
012	Middle	2	10.29	1.11	7.47	3.53	0.30	11.57	3.59	64.16
014	Low	1	7.77	1.31	6.99	4.68	0.39	11.96	6.02	45.40
015	Middle	2	7.50	1.46	7.21	7.75	0.59	13.23	8.17	32.06
033	None	0	4.55	0.88	7.98	3.91	0.28	13.83	3.43	4.79
038	Low	1	13.98	0.68	7.14	3.17	0.29	10.95	3.64	46.03
041	High	3	7.45	1.13	5.71	4.85	0.40	12.10	3.92	42.64
043	Low	1	10.90	1.12	6.35	5.07	0.39	13.13	7.26	57.04
046	Low	1	10.29	1.44	6.20	5.85	0.39	15.06	8.47	18.13
047	Low	1	11.36	1.76	5.67	5.11	0.40	12.74	8.37	32.42
056	Middle	2	8.57	2.48	7.04	15.17	0.97	15.70	9.25	28.35
059	Middle	2	12.99	1.27	6.25	5.14	0.40	13.01	5.51	10.22
064	Low	1	17.57	1.80	6.54	10.52	0.59	17.99	8.98	40.51
068	None	0	8.99	1.28	6.46	4.15	0.35	11.94	7.03	24.03
073	Middle	2	5.78	1.59	7.09	8.93	0.57	15.67	7.40	35.12
078	High	3	7.74	1.64	7.34	7.72	0.58	13.20	6.59	34.30
082	Middle	2	11.48	1.42	6.36	7.95	0.54	14.66	6.63	16.33
087	High	3	12.93	2.66	7.44	7.32	0.54	13.58	11.14	23.75
088	High	3	4.37	1.43	7.88	11.28	0.53	21.16	10.27	63.11
091	High	3	5.41	1.51	7.66	6.71	0.54	12.53	7.46	14.17
092	High	3	9.82	1.48	6.82	10.94	1.01	10.88	8.65	51.37
097	Middle	2	13.51	1.32	6.62	7.13	0.50	14.21	7.99	39.09
113	High	3	7.39	1.22	7.37	3.51	0.30	11.64	6.62	21.69
116	High	3	9.74	1.34	6.22	4.90	0.42	11.54	4.93	30.98
118	Middle	2	21.68	2.23	6.76	10.77	0.70	15.41	9.58	78.60
121	High	3	7.98	1.50	6.51	6.64	0.54	12.37	4.92	16.04
130	Middle	2	7.78	0.89	7.06	4.15	0.35	11.99	5.51	53.21
136	Middle	2	6.43	2.12	6.68	4.79	0.35	13.62	3.99	18.83
146	Low	1	15.69	1.68	6.07	4.95	0.37	13.38	6.62	55.59
153	None	0	17.24	2.25	6.43	12.99	0.69	18.81	8.95	28.67
156	None	0	23.57	2.32	6.74	13.81	0.96	14.45	10.09	20.25
164	Low	1	27.41	3.15	6.77	13.78	0.83	16.56	12.12	28.57
172	None	0	13.04	1.70	7.29	7.14	0.54	13.22	9.44	11.05
186	Middle	2	12.57	0.79	7.07	1.97	0.18	11.18	1.86	23.99
201	Low	1	13.33	1.41	7.44	5.22	0.40	12.97	5.40	41.11
203	Low	1	14.01	1.41	6.97	3.84	0.33	11.63	6.08	58.58

Table C-1. Continued.										
Sample No.	**Decomposition Bin**		**H_2O**	**LOI**	**pH**	**C**	**N**	**C:N**	**Phos.**	**DNA**
227	None	0	2.70	0.96	6.72	3.15	0.29	11.03	4.73	21.55
238	None	0	19.08	2.06	7.04	9.46	0.57	16.50	7.23	100.10
239	None	0	21.85	2.90	7.28	12.07	0.76	15.81	7.79	21.44
250	None	0	22.22	1.84	7.03	10.57	0.70	15.08	9.40	89.29
901	Outside	9	7.00	1.58	7.33	4.99	0.40	12.32	8.08	20.58
902	Outside	9	9.88	1.54	7.28	6.50	0.48	13.55	7.75	31.86
903	Outside	9	4.89	1.31	6.87	4.01	0.36	11.06	6.05	35.75
904	Outside	9	7.05	0.80	6.92	3.21	0.30	10.73	5.34	17.84
905	Outside	9	6.06	1.50	6.46	5.61	0.47	12.01	8.18	29.46
906	Outside	10	1.63	1.07	6.01	5.56	0.38	14.59	4.74	64.61
907	Outside	10	0.80	0.70	6.02	5.21	0.35	14.97	4.35	31.08
908	Outside	10	1.68	0.92	5.81	5.16	0.35	14.92	4.24	33.66
909	Outside	10	1.91	1.16	5.90	5.86	0.38	15.46	4.53	*
910	Outside	10	1.50	0.92	6.13	4.69	0.32	14.47	4.14	*
911	Outside	10	1.20	0.73	5.86	5.32	0.36	14.61	4.85	*
912	Outside	10	1.07	0.73	5.67	5.65	0.34	16.79	4.74	*
913	Outside	10	1.41	0.89	5.60	4.38	0.30	14.63	4.52	*
914	Outside	10	1.41	0.91	5.90	5.16	0.33	15.48	4.51	*
915	Outside	10	1.18	0.73	5.76	5.23	0.36	14.69	4.61	*
A	Active	4	8.41	1.13	6.01	8.43	0.54	15.47	6.40	88.67
C	Active	4	14.20	0.93	7.46	4.30	0.35	12.35	3.80	57.66
D	Active	4	13.44	1.01	6.23	5.95	0.63	9.40	6.40	84.46
E	Active	4	9.11	1.25	5.08	4.36	0.44	9.90	3.10	47.40
F	Active	4	17.92	1.08	4.82	4.09	0.67	6.08	5.00	207.26
G	Active	4	17.79	2.65	5.48	12.47	1.20	10.36	5.90	58.99
H	Active	4	15.01	0.93	5.70	4.02	0.49	8.25	4.50	57.34
I	Active	4	19.21	1.50	5.59	7.19	0.73	9.84	9.10	107.70
J	Active	4	32.36	1.02	5.39	5.34	0.62	8.62	5.00	60.63
K	Active	4	15.88	1.69	5.97	10.88	0.78	13.89	10.80	88.30
L	Active	4	35.76	1.93	6.38	10.13	1.19	8.51	14.10	70.43
M	Active	4	13.65	2.62	5.32	12.78	1.12	11.39	12.20	178.23
N	Active	4	16.61	2.34	5.11	12.09	0.60	20.02	11.03	203.88
O	Active	4	22.46	3.07	4.98	15.76	0.80	19.80	2.52	14.16

APPENDIX D:

Contour maps showing the distribution of abiotic environmental data plotted in reference to decomposition density.

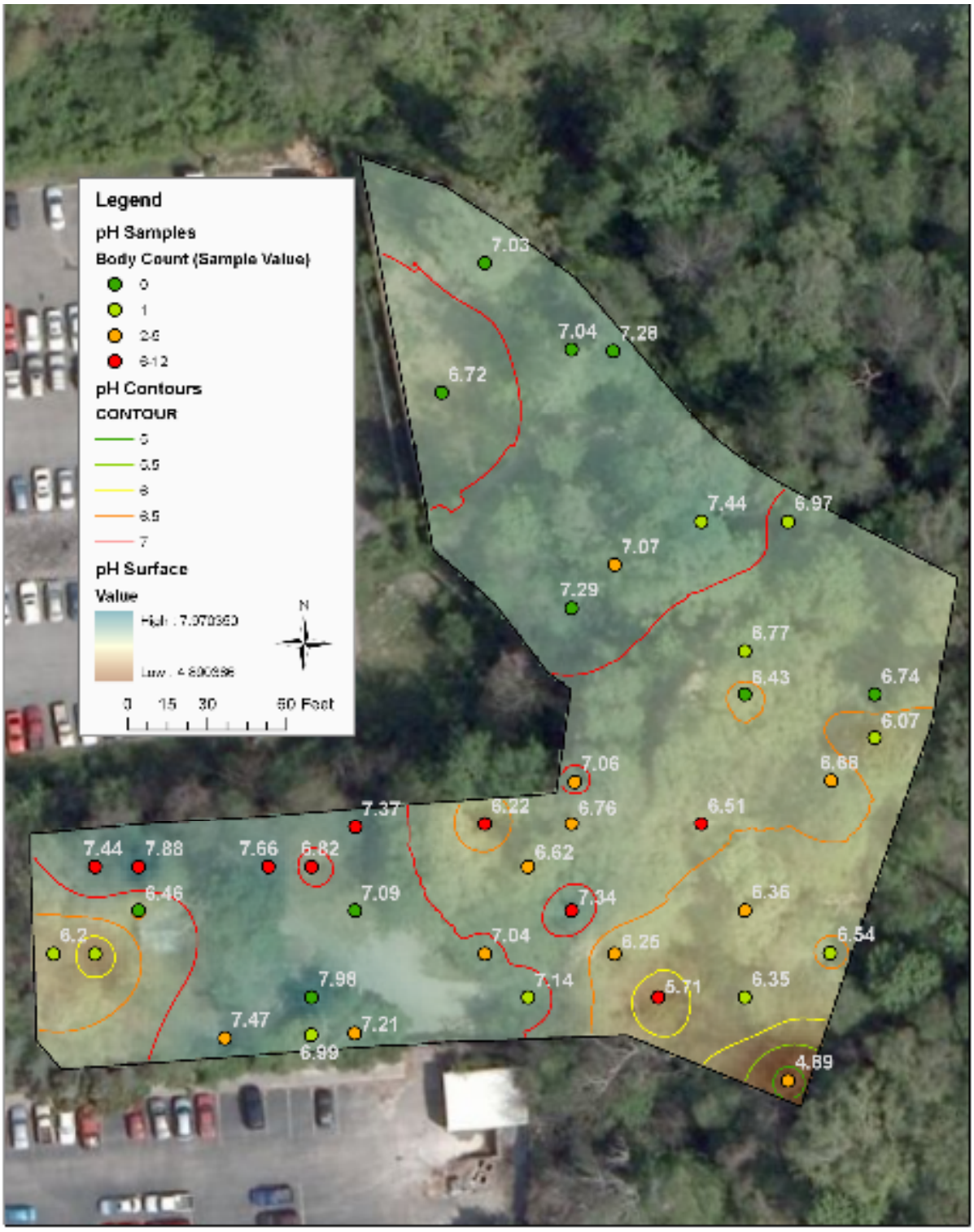

Figure D-1. Distribution of soil pH values across UT ARF.

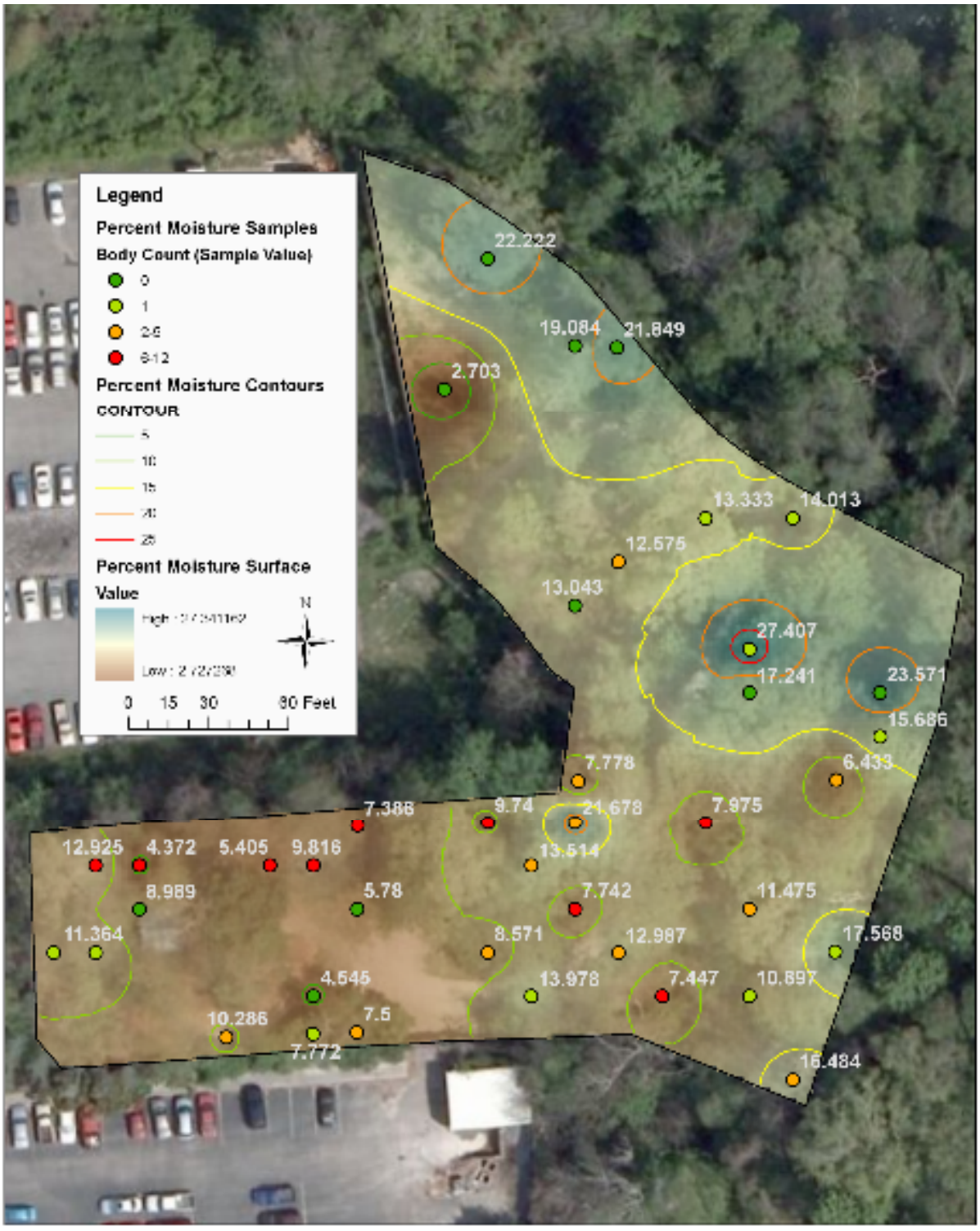

Figure D-2. Distribution of moisture content percentage across UT ARF.

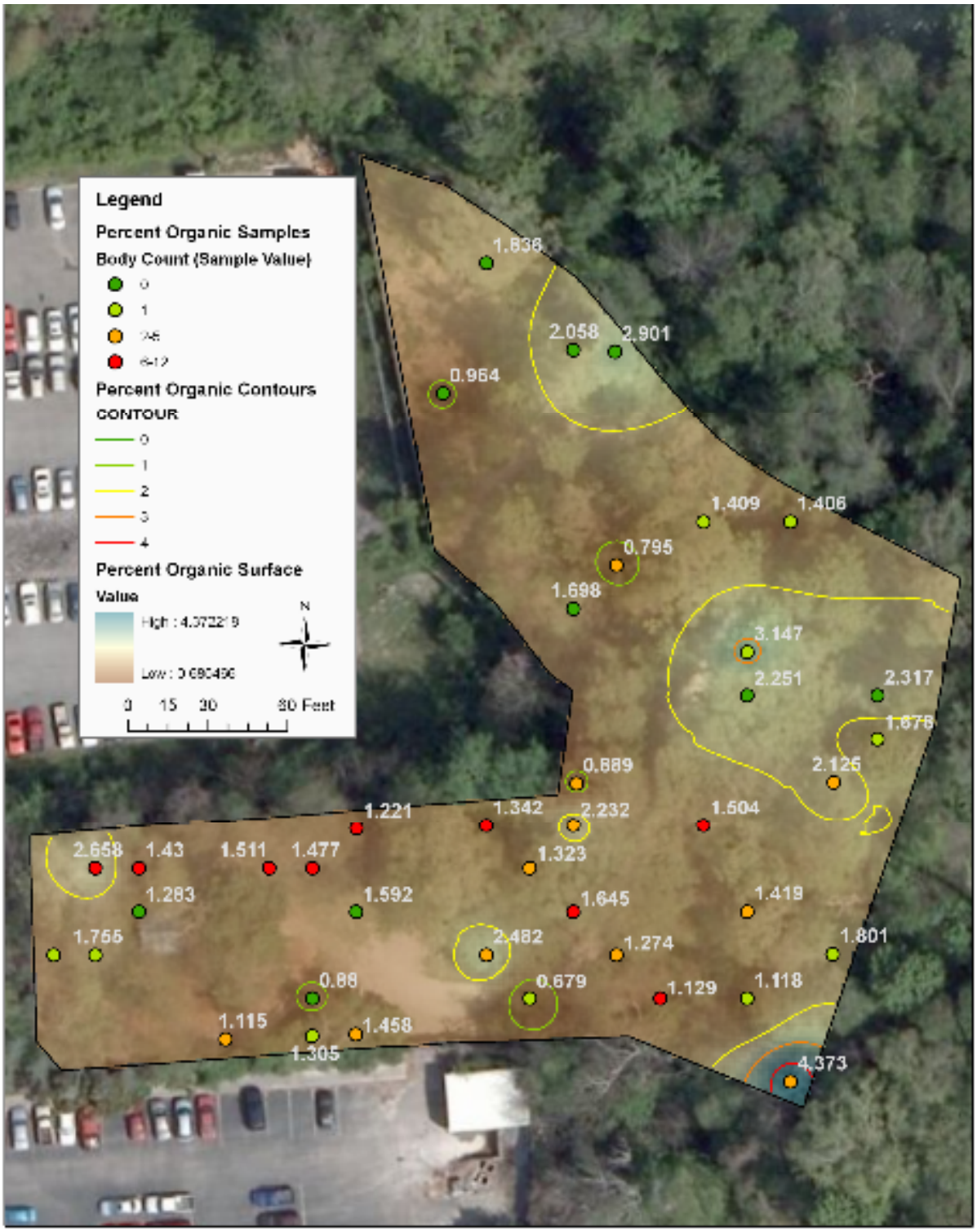

Figure D-3. Distribution of organic content values across UT ARF. Measure determined by loss on ignition.

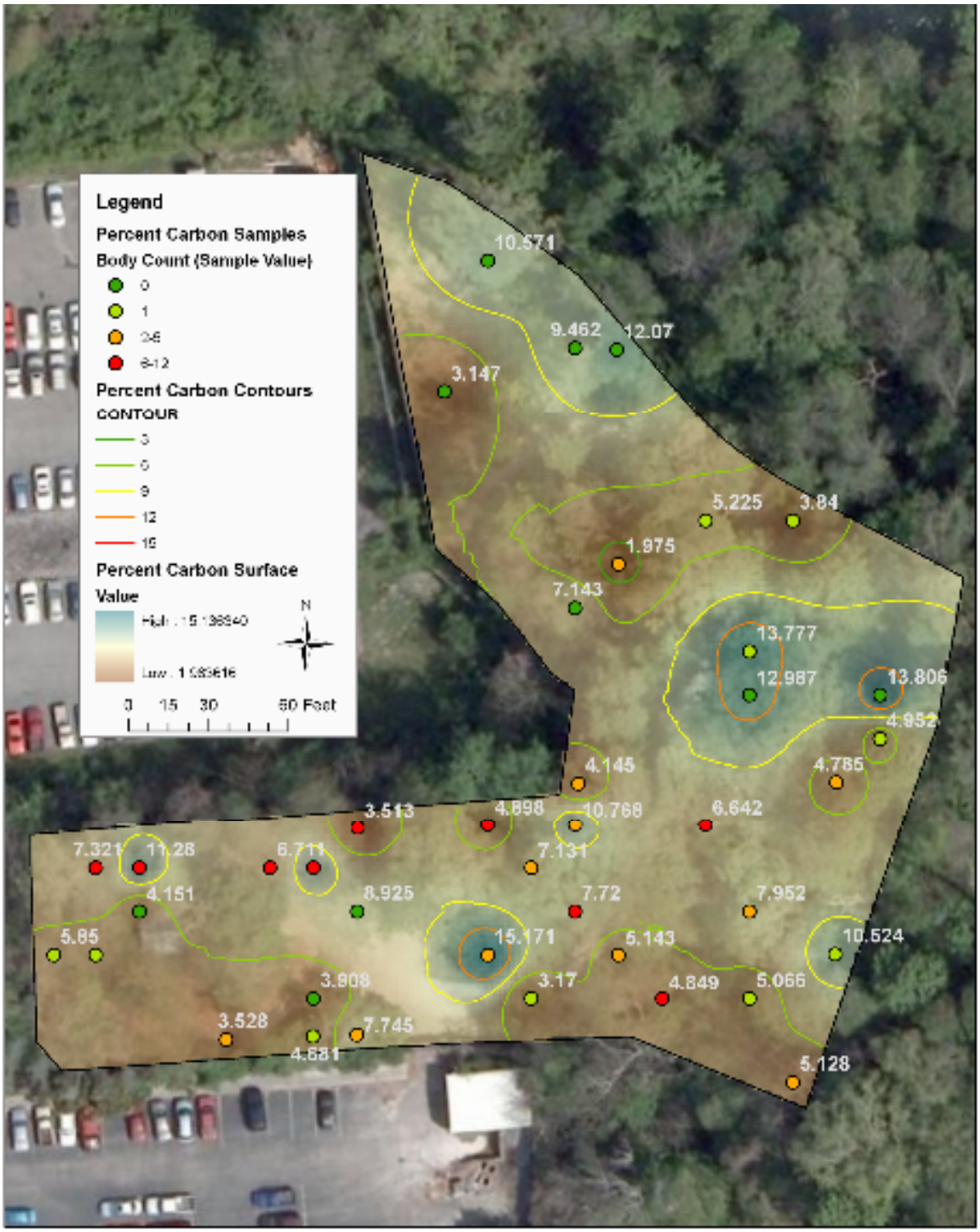

Figure D-4. Distribution of total carbon percent g^{-1} soil across UT ARF.

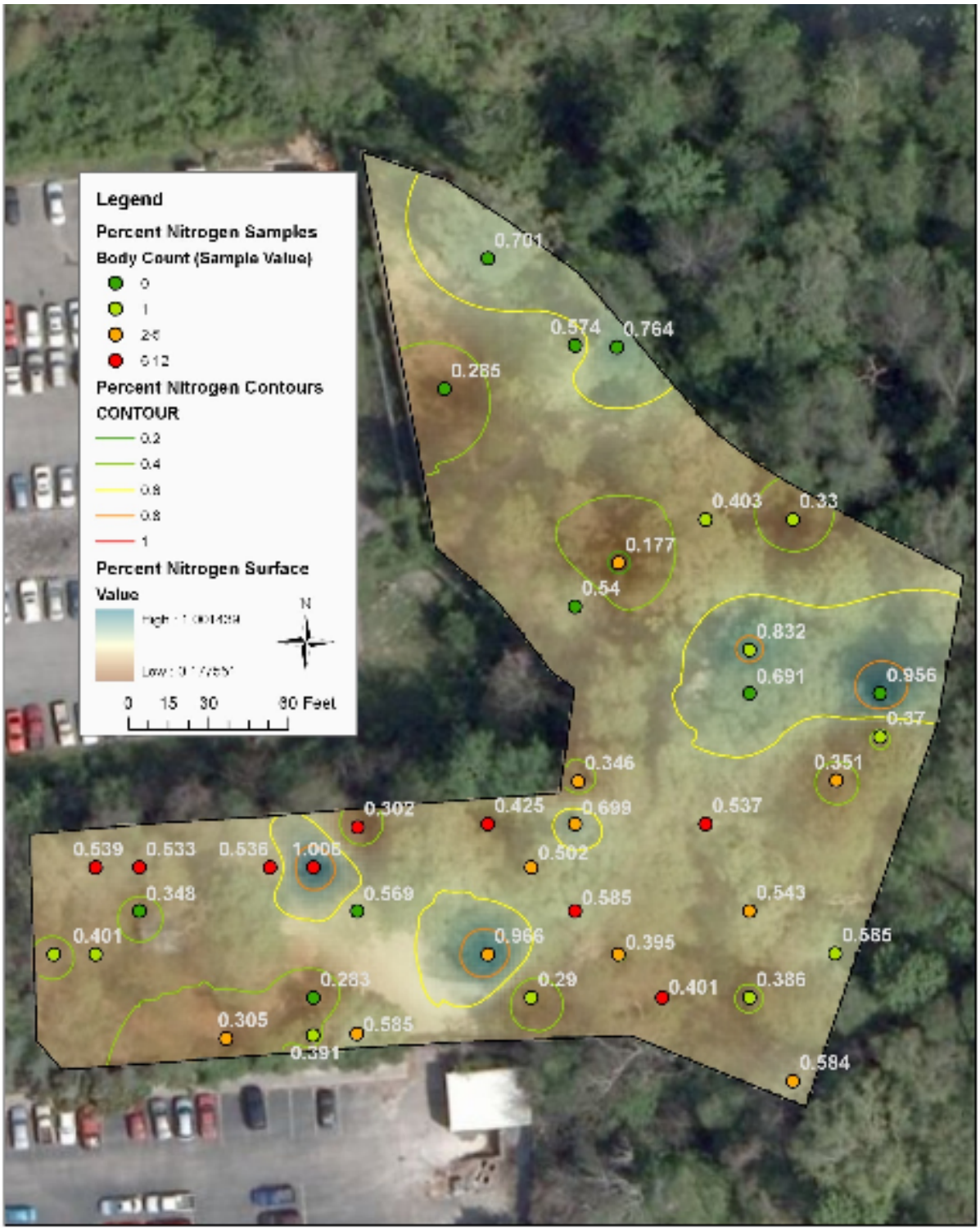

Figure D-5. Distribution of total nitrogen percent g^{-1} soil across UT ARF.

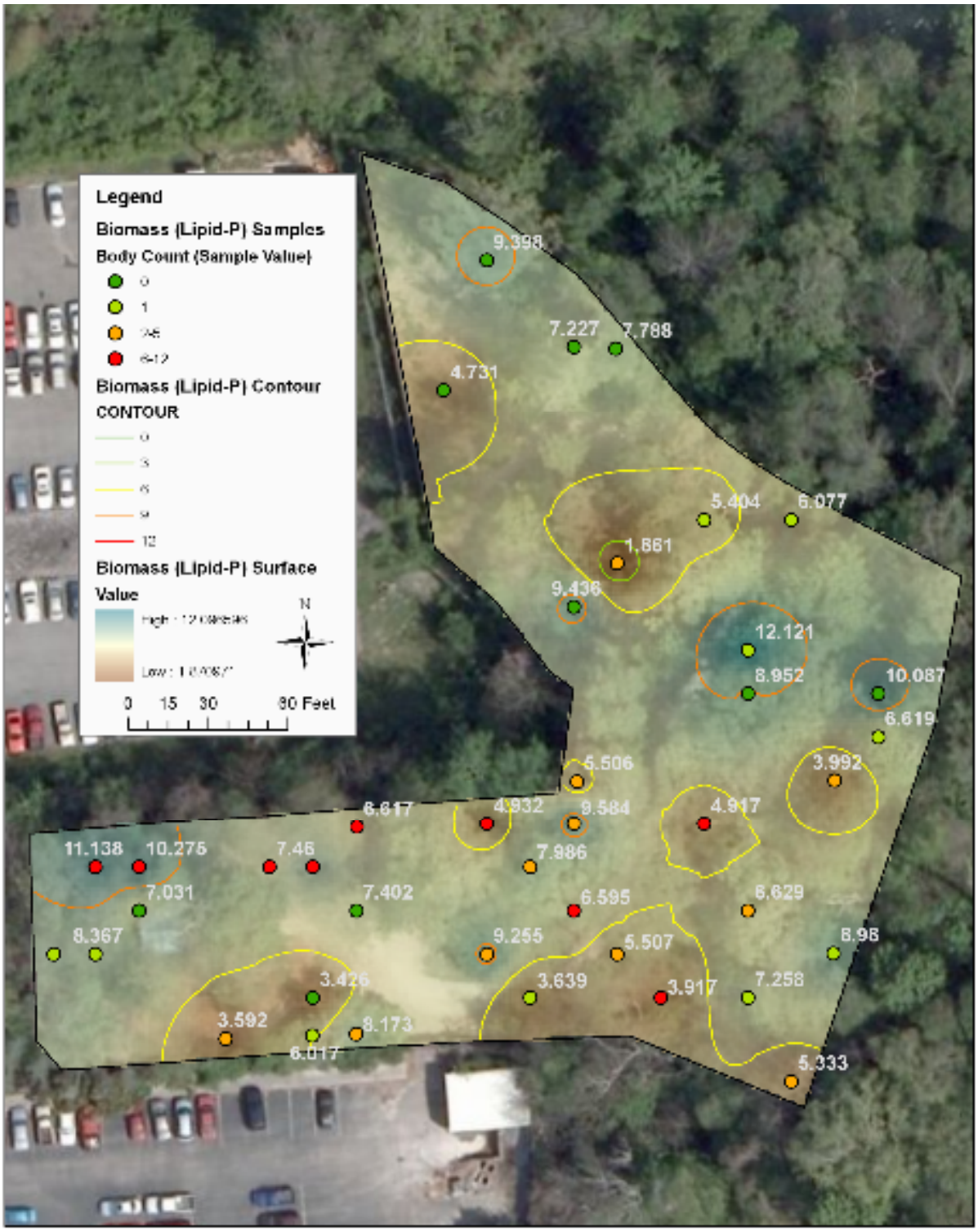

Figure D-6. Distribution of lipid-P values (µg μL^{-1}) across UT ARF.

APPENDIX E:

Statistical results of for abiotic environmental data series.

Table E-1. Mann-Whitney U test for differences in soil pH values among ARF bins [a].						
	None	**Low**	**Middle**	**High**	**Negative**	**Active**
None		28.000	45.500	34.000	0.000	8.000
Low	.182		47.000	28.000	9.500	20.000
Middle	.554	.418		39.000	10.000	25.000
High	.888	.315	.521		8.000	12.000
Negative	***.000***	***.001***	***.000***	***.003***		46.500
Active	***.000***	***.002***	***.002***	***.002***	.172	

[a] significant differences between bins with p-values less than an alpha of 0.05 are underlined.

Table E-2. Mann-Whitney U test for differences in soil moisture content (%) among ARF bins [a].						
	None	**Low**	**Middle**	**High**	**Negative**	**Active**
None		41.000	36.000	17.000	.000	55.000
Low	.780		37.000	3.000	.000	42.000
Middle	.219	.140		21.000	.000	30.000
High	.074	***.000***	***.039***		.000	4.000
Negative	***.000***	***.000***	***.000***	***.000***		.000
Active	.643	.108	***.004***	***.000***	***.000***	

[a] significant differences between bins with p-values less than an alpha of 0.05 are underlined.

Table E-3. Mann-Whitney U test for differences in soil organic matter (%) among ARF bins [a].						
	None	**Low**	**Middle**	**High**	**Negative**	**Active**
None		34.000	46.000	22.000	8.000	56.000
Low	.400		58.000	36.000	11.000	67.000
Middle	.602	.923		46.000	12.500	82.000
High	.200	.762	.910		1.000	55.500
Negative	*.001*	*.002*	*.001*	*.000*		10.000
Active	.688	.886	.940	.973	*.000*	

[a] significant differences between bins with p-values less than an alpha of 0.05 are underlined.

Table E-4. Mann-Whitney U test for differences in total carbon content (%) among ARF bins [a].

	None	Low	Middle	High	Negative	Active
None		33.000	42.000	29.000	30.000	61.000
Low	.356		51.000	31.000	41.000	47.000
Middle	.422	.582		46.000	54.000	64.000
High	.541	.460	.910		26.000	47.000
Negative	.243	.529	.722	.237		43.000
Active	.926	.192	.322	.570	.122	

[a] significant differences between bins with p-values less than an alpha of 0.05 are underlined.

Table E-5. Mann-Whitney U test for differences in total nitrogen content (%) among ARF bins [a].

	None	Low	Middle	High	Negative	Active
None		35.000	46.000	31.000	24.500	43.500
Low	.447		49.500	22.000	20.000	21.000
Middle	.602	.497		45.500	28.500	39.000
High	.673	.122	.851		9.000	26.000
Negative	.095	***.023***	***.036***	***.004***		4.500
Active	.224	***.003***	***.020***	***.042***	***.000***	

[a] significant differences between bins with p-values less than an alpha of 0.05 are underlined.

Table E-6. Mann-Whitney U test for differences in the ratios of total carbon to nitrogen among ARF bins [a].

	None	Low	Middle	High	Negative	Active
None		33.000	39.000	19.000	35.000	31.000
Low	.356		59.000	28.000	26.000	39.000
Middle	.310	.974		35.000	29.000	51.000
High	.114	.315	.343		10.000	33.000
Negative	.447	.075	***.043***	***.006***		28.000
Active	***.046***	.074	.095	.127	***.013***	

[a] significant differences between bins with p-values less than an alpha of 0.05 are underlined.

Table E-7. Mann-Whitney U test for differences in lipid-phosphorus (µg g^{-1} soil) content from soil among ARF bins [a].

	None	Low	Middle	High	Negative	Active
None		38.000	38.000	27.000	13.000	54.000
Low	.604		47.000	34.500	10.000	61.000
Middle	.277	.418		46.000	30.000	79.000
High	.423	.633	.910		10.000	55.000
Negative	***.008***	***.002***	***.050***	***.006***		37.000
Active	.600	.625	.820	.973	.056	

[a] significant differences between bins with p-values less than an alpha of 0.05 are underlined.

Table E-8. Mann-Whitney U test for differences in total recovered double-stranded DNA (ng μl^{-1}) from soil among ARF bins [a].

	None	Low	Middle	High	Negative	Active
None		26.00	43.00	28.00	6.00	25.00
Low	.121		48.00	28.00	15.00	15.00
Middle	.434	.429		41.00	15.00	28.00
High	.441	.286	.589		8.00	14.00
Negative	.166	1.000	.665	.414		8.00
Active	***.017***	***.001***	***.004***	***.004***	.101	

[a] significant differences between bins with p-values less than an alpha of 0.05 are underlined.

Appendix F:

Biotic Environmental Data sets

Table F-1. Biotic Environmental Data Sets for Samples 6 through 56.											
Bacterial Orders	**6**	**12**	**14**	**15**	**33**	**38**	**41**	**43**	**46**	**47**	**56**
Acidobacteria Gp1	0	0	0	0	0	2	0	0	1	1	0
Acidobacteria Gp10	0	0	0	1	0	1	0	2	0	0	0
Acidobacteria Gp11	0	0	0	0	0	0	0	0	0	0	0
Acidobacteria Gp12	0	0	0	0	0	1	0	0	0	0	0
Acidobacteria Gp14	0	0	0	0	0	1	0	0	0	0	0
Acidobacteria Gp16	0	1	0	1	0	2	0	8	0	2	0
Acidobacteria Gp17	0	0	0	0	0	2	0	4	0	0	0
Acidobacteria Gp18	0	0	0	0	0	1	0	0	0	0	0
Acidobacteria Gp21	0	0	0	1	0	0	0	2	0	0	0
Acidobacteria Gp22	0	0	0	0	0	0	0	1	0	0	0
Acidobacteria Gp25	0	0	0	0	0	0	0	0	0	0	0
Acidobacteria Gp3	0	1	1	0	1	1	0	0	1	5	0
Acidobacteria Gp4	0	1	2	5	6	2	0	5	0	0	0
Acidobacteria Gp5	1	1	7	1	0	12	0	2	0	1	3
Acidobacteria Gp6	3	22	35	20	2	0	0	14	8	8	7
Acidobacteria Gp7	0	1	0	0	0	0	0	0	0	0	0
Holophagales	0	0	0	0	0	0	0	0	0	0	0
Acidimicrobiales	0	7	3	3	8	6	7	3	2	6	2
Actinomycetales	75	41	59	39	16	31	0	55	16	36	5
Bifidobacteriales	1	0	0	0	0	0	0	0	0	0	0
Coriobacteriales	0	0	3	3	4	1	0	7	1	0	0
Nitriliruptorales	0	6	3	4	2	2	1	4	0	6	0
Rubrobacterales	0	0	1	0	2	0	0	0	0	0	0
Solirubrobacterales	1	7	8	4	3	9	0	9	0	6	0
Thermoleophilales	1	6	3	3	0	2	0	5	0	2	0
Aquificales	0	0	0	0	0	0	0	1	0	0	0
Bacteroidetes *inc sed.*	0	0	0	0	1	0	0	1	0	0	0
Bacteroidales	0	0	0	0	0	0	2	1	0	0	0
Flavobacteriales	4	1	10	5	1	2	0	1	2	1	3
Sphingobacteriales	20	18	34	22	11	9	5	20	2	7	1
Caldisericales	0	0	0	0	0	1	0	0	0	0	0
Chlamydiales	0	0	4	0	0	0	0	0	0	0	0
Anaerolineales	0	4	0	0	2	0	0	0	0	0	0
Caldilineales	0	0	0	0	0	0	0	0	0	0	0
Chloroflexales	0	0	0	0	1	1	0	0	0	0	0
Herpetosiphonales	0	1	1	1	1	2	0	0	0	0	0
Dehalogenimonas	0	1	3	0	0	0	0	0	0	0	0
Sphaerobacterales	1	0	0	0	1	0	0	1	0	1	0

Table F-1 continued.											
Bacterial Orders	**6**	**12**	**14**	**15**	**33**	**38**	**41**	**43**	**46**	**47**	**56**
Thermomicrobiales	0	1	0	0	0	0	0	1	0	0	0
Chloroplast	0	0	0	0	1	0	0	0	0	0	0
Deferribacterales	0	0	0	0	0	0	0	0	0	0	0
Deinococcales	0	0	4	0	1	0	0	0	0	0	0
Dictyoglomales	0	0	0	0	0	0	0	0	0	0	0
Bacillales	0	1	0	1	1	2	0	2	0	1	0
Clostridiales	0	3	3	1	2	1	0	0	0	0	1
Halanaerobiales	0	0	0	0	0	0	0	0	0	1	0
Natranaerobiales	0	0	0	0	0	1	0	1	0	1	0
Thermoanaerobacterales	1	0	0	0	0	0	0	0	0	0	0
Erysipelotrichales	0	0	0	0	1	0	0	0	0	0	0
Gemmatimonadales	5	3	7	1	5	4	0	3	2	3	0
Ktedonobacterales *inc sed.*	0	0	0	0	0	1	0	0	0	0	0
Nitrospirales	0	0	0	0	0	0	0	0	0	0	2
OP10_*inc sed.*	0	0	0	0	1	0	0	1	0	0	0
OP11_*inc sed.*	0	0	0	0	0	0	0	0	0	0	0
Planctomycetales	0	0	9	0	0	0	0	0	0	1	0
Alphaproteobacteria *inc sed.*	1	5	3	1	0	0	3	4	1	2	2
Caulobacterales	1	7	5	7	4	4	0	5	3	4	3
Kiloniellales	0	0	0	0	0	0	0	0	0	0	1
Kordiimonadales	0	0	0	0	0	0	0	0	1	0	0
Rhizobiales	19	15	45	28	7	17	14	25	12	27	13
Rhodobacterales	2	3	5	2	1	1	1	0	0	1	0
Rhodospirillales	4	0	4	1	3	1	1	2	1	1	0
Rickettsiales	0	0	0	0	0	1	1	1	0	0	0
Sphingomonadales	8	6	18	12	10	8	4	5	7	11	10
Burkholderiales	2	7	8	5	5	3	0	5	0	3	0
Hydrogenophilales	0	0	0	0	1	2	0	0	0	0	0
Methylophilales	0	0	0	0	0	0	0	0	0	0	0
Neisseriales	0	0	0	1	0	0	0	0	0	0	0
Nitrosomonadales	4	0	0	0	2	3	0	0	0	0	0
Rhodocyclales	1	1	1	2	2	4	0	3	1	0	2
Bdellovibrionales	0	0	2	1	1	1	0	0	0	0	0
Desulfarculales	0	0	1	6	0	1	0	0	0	1	0
Desulfobacterales	1	2	0	2	0	1	0	1	1	0	0
Desulfovibrionales	0	1	1	1	4	1	0	0	0	1	1
Desulfurellales	0	0	0	1	0	0	0	0	0	0	0
Desulfuromonadales	0	0	0	0	1	0	0	0	0	0	0

Table F-1 continued.											
Bacterial Orders	**6**	**12**	**14**	**15**	**33**	**38**	**41**	**43**	**46**	**47**	**56**
Myxococcales	1	8	13	14	4	8	3	9	6	3	7
Syntrophobacterales	0	0	0	1	1	0	0	0	0	0	1
Campylobacterales	0	2	0	0	2	0	0	1	1	0	0
Nautiliales	0	0	0	0	0	0	1	0	0	0	0
Aeromonadales	0	0	0	0	0	0	0	0	0	0	0
Alteromonadales	1	0	2	0	1	0	0	0	0	0	0
Cardiobacteriales	0	0	0	0	0	0	0	0	1	0	0
Chromatiales	1	0	0	1	0	2	0	0	2	0	0
Enterobacteriales	2	1	5	1	0	1	0	1	2	3	0
Legionellales	0	2	2	0	0	1	0	0	1	0	0
Methylococcales	0	0	0	0	0	0	0	0	0	0	0
Oceanospirillales	0	0	2	0	0	0	0	0	0	0	1
Pseudomonadales	2	0	15	0	0	0	0	1	0	1	0
Thiotrichales	0	0	0	1	0	0	0	0	0	1	0
Vibrionales	0	0	0	0	0	0	0	0	0	0	0
Xanthomonadales	41	3	11	3	1	0	2	0	3	3	0
Spirochaetales	0	0	0	0	0	0	0	0	0	0	0
Synergistales	0	0	0	0	0	0	0	0	0	0	0
Thermodesulfobacteriales	0	1	0	0	0	0	0	0	0	0	0
TM7 *inc sed.*	5	0	2	2	1	0	0	1	0	0	0
Spartobacteria *inc sed.*	0	0	0	0	0	0	0	0	0	0	0
Subdivision3 *inc sed.*	1	0	0	0	0	0	0	0	0	0	0
Verrucomicrobiales	0	0	0	0	0	0	0	0	0	0	0
WS3 *inc sed.*	0	0	0	0	0	0	0	0	0	0	0
Gammaproteobacteria *inc sed.*	0	0	0	0	0	0	0	1	0	0	0
Unknown	0	0	0	0	0	0	0	0	0	0	0

Table F-2. Biotic Environmental Data Sets for Samples 59 through 97.											
Bacterial Orders	**59**	**64**	**68**	**73**	**78**	**82**	**87**	**88**	**91**	**92**	**97**
Acidobacteria Gp1	3	0	0	0	0	0	0	0	0	0	0
Acidobacteria Gp10	5	3	0	1	1	1	0	10	0	2	0
Acidobacteria Gp11	1	0	0	0	0	0	0	0	0	0	0
Acidobacteria Gp12	0	0	0	0	0	0	0	0	0	0	0
Acidobacteria Gp14	0	0	0	0	0	0	0	0	0	0	0
Acidobacteria Gp16	18	1	0	1	1	3	0	3	1	2	3
Acidobacteria Gp17	1	0	0	0	0	0	0	1	1	0	0
Acidobacteria Gp18	0	0	0	0	0	0	0	0	0	0	0
Acidobacteria Gp21	0	1	0	0	0	0	0	0	0	0	0
Acidobacteria Gp22	2	0	0	0	0	0	0	0	0	0	0
Acidobacteria Gp25	1	0	0	0	0	0	0	0	0	0	0
Acidobacteria Gp3	5	1	0	0	0	0	1	0	0	0	1
Acidobacteria Gp4	6	1	1	1	0	2	0	0	0	0	0
Acidobacteria Gp5	17	3	0	3	0	1	0	0	0	0	0
Acidobacteria Gp6	48	12	6	5	11	20	3	12	2	1	10
Acidobacteria Gp7	0	0	0	1	0	0	0	0	0	0	1
Holophagales	0	0	0	0	0	0	0	0	0	0	0
Acidimicrobiales	19	12	8	2	3	5	2	6	6	0	8
Actinomycetales	105	29	25	19	23	36	12	60	56	29	46
Bifidobacteriales	0	0	0	0	0	0	0	0	0	0	0
Coriobacteriales	13	3	2	2	2	2	0	3	1	0	4
Nitriliruptorales	17	6	4	2	0	5	1	3	1	1	12
Rubrobacterales	0	0	0	0	0	0	0	0	2	0	0
Solirubrobacterales	38	8	4	6	2	4	0	17	4	1	3
Thermoleophilales	19	1	1	3	4	8	0	4	5	4	4
Aquificales	0	1	0	0	0	0	0	0	0	0	0
Bacteroidetes *inc sed.*	1	0	0	0	0	0	0	0	0	0	0
Bacteroidales	0	0	0	0	0	0	0	0	0	0	0
Flavobacteriales	6	7	1	5	1	0	2	19	9	2	4
Sphingobacteriales	61	0	8	9	6	8	0	47	10	8	0
Caldisericales	0	0	0	0	0	0	0	0	0	0	0
Chlamydiales	1	0	0	0	0	0	0	0	0	0	0
Anaerolineales	1	0	0	0	0	0	0	4	0	0	0
Caldilineales	1	0	0	0	0	0	0	0	0	0	0
Chloroflexales	0	0	0	0	0	0	0	0	0	0	0
Herpetosiphonales	0	0	0	0	1	0	0	1	0	1	0
Dehalogenimonas	1	0	0	0	0	0	0	0	0	0	0

Table F-2 continued.											
Bacterial Orders	**59**	**64**	**68**	**73**	**78**	**82**	**87**	**88**	**91**	**92**	**97**
Sphaerobacterales	2	3	0	0	1	0	0	4	2	1	8
Thermomicrobiales	1	0	0	0	0	0	0	0	0	0	0
Chloroplast	0	0	0	1	0	0	0	0	0	0	0
Deferribacterales	0	0	0	1	0	1	0	0	0	0	0
Deinococcales	0	1	0	0	1	0	0	1	0	0	1
Dictyoglomales	0	0	0	0	0	0	0	0	1	0	0
Bacillales	4	0	2	0	0	0	0	0	0	1	0
Clostridiales	5	1	0	1	0	3	1	2	1	2	0
Halanaerobiales	3	0	0	0	0	0	0	0	0	0	0
Natranaerobiales	1	0	0	0	0	0	0	1	1	0	0
Thermoanaerobacterales	3	1	1	0	1	2	0	3	1	0	1
Erysipelotrichales	0	0	0	0	0	0	0	1	0	0	0
Gemmatimonadales	0	2	3	5	0	3	0	1	1	0	2
Ktedonobacterales *inc sed.*	1	0	0	0	0	0	0	1	0	1	1
Nitrospirales	1	0	0	0	0	0	0	0	0	0	0
OP10_*inc sed.*	3	0	0	0	0	0	0	0	0	0	1
OP11_*inc sed.*	1	0	0	0	0	0	0	0	0	0	0
Planctomycetales	2	1	0	0	0	0	0	1	2	0	0
Alphaproteobacteria *inc sed.*	5	4	0	1	0	4	1	8	0	0	3
Caulobacterales	19	8	3	1	1	5	2	6	0	2	7
Kiloniellales	0	0	0	0	0	0	0	0	0	0	0
Kordiimonadales	0	0	0	0	0	0	0	0	0	0	0
Rhizobiales	94	51	21	13	21	32	14	38	18	11	28
Rhodobacterales	0	1	0	0	0	2	0	8	6	0	1
Rhodospirillales	11	5	2	1	2	3	2	4	5	0	5
Rickettsiales	0	0	0	0	0	0	0	0	0	1	0
Sphingomonadales	32	9	13	5	5	5	4	33	19	16	10
Burkholderiales	20	2	3	3	0	1	0	25	4	10	16
Hydrogenophilales	2	0	1	0	0	0	0	1	1	1	1
Methylophilales	1	0	0	0	0	0	0	1	0	0	0
Neisseriales	0	0	0	0	0	0	0	2	1	0	1
Nitrosomonadales	3	0	0	1	0	0	0	3	3	7	1
Rhodocyclales	9	3	0	2	0	4	0	2	0	2	1
Bdellovibrionales	2	1	0	1	0	1	0	7	2	1	1
Desulfarculales	5	1	0	1	0	1	0	1	2	3	0
Desulfobacterales	1	1	1	0	0	1	0	4	1	0	2
Desulfovibrionales	3	0	1	0	0	0	1	3	0	1	0
Desulfurellales	1	0	1	0	0	0	0	0	0	0	0

Table F-2 continued.											
Bacterial Orders	**59**	**64**	**68**	**73**	**78**	**82**	**87**	**88**	**91**	**92**	**97**
Desulfuromonadales	3	1	0	0	0	0	0	1	1	0	0
Myxococcales	18	10	5	6	3	5	4	15	5	5	7
Syntrophobacterales	3	1	0	2	0	2	1	9	1	0	0
Campylobacterales	2	0	0	1	0	2	0	3	2	0	0
Nautiliales	1	0	0	0	0	0	0	0	0	0	0
Aeromonadales	0	0	0	0	0	0	0	1	1	0	0
Alteromonadales	0	0	1	0	0	0	0	0	0	0	0
Cardiobacteriales	0	0	0	0	0	0	1	0	0	0	0
Chromatiales	7	0	0	2	0	0	0	6	0	0	0
Enterobacteriales	1	2	0	1	5	1	0	1	1	0	1
Legionellales	3	2	0	0	0	0	0	1	1	1	0
Methylococcales	0	0	0	0	0	0	0	0	1	0	0
Oceanospirillales	0	0	0	0	0	0	1	0	0	0	1
Pseudomonadales	1	0	1	1	0	0	0	3	5	0	1
Thiotrichales	2	0	0	3	0	0	0	2	0	0	0
Vibrionales	0	0	0	0	0	0	0	0	0	0	0
Xanthomonadales	22	6	6	3	2	1	1	10	7	14	7
Spirochaetales	0	0	0	0	0	0	0	0	0	0	0
Synergistales	0	0	0	0	0	0	0	0	0	0	0
Thermodesulfobacteriales	1	1	0	0	2	0	0	0	0	0	0
TM7 *inc sed.*	9	1	0	0	0	1	0	7	5	1	4
Spartobacteria *inc sed.*	2	0	1	0	0	2	0	0	0	0	0
Subdivision3 *inc sed.*	0	0	0	0	0	3	0	0	0	0	0
Verrucomicrobiales	0	0	0	0	0	0	0	0	0	0	0
WS3 *inc sed.*	0	0	0	0	0	0	0	0	0	0	1
Gammaproteobacteria *inc sed.*	14	0	0	3	0	1	0	1	0	0	2
Unknown	0	0	0	0	0	0	0	0	0	0	0

Table F-3. Biotic Environmental Data Sets for Samples 113 through 156.									
Bacterial Orders	**113**	**116**	**118**	**121**	**130**	**136**	**146**	**153**	**156**
Acidobacteria Gp1	0	0	0	0	0	0	0	0	0
Acidobacteria Gp10	0	0	0	0	0	0	0	0	1
Acidobacteria Gp11	0	1	0	0	0	0	0	0	0
Acidobacteria Gp12	0	0	0	0	0	0	0	0	0
Acidobacteria Gp14	0	0	0	0	0	0	0	0	0
Acidobacteria Gp16	0	7	2	0	0	0	0	0	0
Acidobacteria Gp17	0	0	0	0	0	0	0	0	0
Acidobacteria Gp18	0	0	0	0	0	0	0	0	0
Acidobacteria Gp21	0	0	1	0	0	0	0	0	0
Acidobacteria Gp22	0	0	0	0	0	0	0	0	1
Acidobacteria Gp25	0	0	0	0	0	0	0	0	0
Acidobacteria Gp3	0	1	3	0	0	0	0	0	1
Acidobacteria Gp4	3	3	1	0	0	0	0	1	0
Acidobacteria Gp5	1	0	0	0	0	0	0	4	0
Acidobacteria Gp6	8	4	2	3	4	0	4	17	3
Acidobacteria Gp7	0	0	0	0	0	0	0	1	0
Holophagales	0	0	0	0	1	0	0	0	2
Acidimicrobiales	2	10	3	2	1	1	2	3	5
Actinomycetales	24	137	38	15	8	17	31	40	21
Bifidobacteriales	0	0	0	0	0	1	0	0	0
Coriobacteriales	1	5	4	0	0	1	1	3	3
Nitriliruptorales	3	20	6	2	0	1	1	9	1
Rubrobacterales	0	0	0	0	0	0	0	0	0
Solirubrobacterales	4	6	1	5	0	1	1	10	1
Thermoleophilales	1	13	1	4	0	0	0	4	0
Aquificales	0	1	0	0	0	0	0	0	0
Bacteroidetes *inc sed.*	0	0	0	0	0	0	2	1	0
Bacteroidales	0	0	0	0	0	0	0	0	0
Flavobacteriales	6	2	2	1	0	1	1	8	3
Sphingobacteriales	8	15	3	8	0	1	7	13	0
Caldisericales	0	0	0	0	0	1	0	0	0
Chlamydiales	0	0	0	0	0	0	0	1	0
Anaerolineales	0	0	0	0	0	0	0	0	0
Caldilineales	0	0	0	0	0	0	0	1	1
Chloroflexales	0	0	0	0	0	0	0	0	0
Herpetosiphonales	0	0	0	0	0	0	0	0	0
Dehalogenimonas	0	2	0	0	0	0	0	0	0
Sphaerobacterales	1	1	3	0	0	0	0	0	0

Table F-3 continued.									
Bacterial Orders	**113**	**116**	**118**	**121**	**130**	**136**	**146**	**153**	**156**
Thermomicrobiales	0	0	0	0	0	0	0	0	0
Chloroplast	0	0	0	0	0	0	0	0	0
Deferribacterales	0	0	0	0	0	0	0	0	0
Deinococcales	0	0	0	0	0	0	0	0	0
Dictyoglomales	0	0	0	0	0	0	0	0	0
Bacillales	0	0	1	0	0	0	0	0	2
Clostridiales	2	1	0	2	0	1	0	3	0
Halanaerobiales	0	0	0	0	0	0	0	0	0
Natranaerobiales	0	1	2	0	0	0	0	0	0
Thermoanaerobacterales	2	5	0	0	0	0	0	2	1
Erysipelotrichales	0	0	0	0	0	0	0	0	0
Gemmatimonadales	0	1	1	1	2	0	1	4	0
Ktedonobacterales *inc sed.*	0	0	0	0	0	0	0	0	0
Nitrospirales	1	0	0	0	0	1	0	0	0
OP10_*inc sed.*	0	1	0	0	0	0	0	0	0
OP11_*inc sed.*	0	0	0	0	0	0	0	0	0
Planctomycetales	0	0	1	0	0	0	0	0	0
Alphaproteobacteria *inc sed.*	1	0	3	1	0	0	4	6	1
Caulobacterales	5	4	5	3	1	4	4	14	4
Kiloniellales	0	0	0	0	0	0	0	0	0
Kordiimonadales	0	0	0	0	0	0	0	0	0
Rhizobiales	13	41	16	20	10	11	16	36	15
Rhodobacterales	0	0	0	0	1	0	0	0	1
Rhodospirillales	1	2	1	2	0	1	2	4	1
Rickettsiales	0	0	0	0	0	1	0	0	0
Sphingomonadales	4	9	5	4	4	6	5	15	4
Burkholderiales	4	14	7	6	0	7	0	6	3
Hydrogenophilales	0	2	0	1	0	1	0	1	1
Methylophilales	0	0	0	0	0	0	0	0	0
Neisseriales	0	3	0	1	0	0	0	5	1
Nitrosomonadales	0	0	0	1	1	1	0	3	0
Rhodocyclales	1	3	1	1	0	0	1	5	1
Bdellovibrionales	1	1	0	0	0	0	0	0	0
Desulfarculales	0	1	0	0	0	0	0	1	0
Desulfobacterales	0	2	0	0	0	1	1	0	0
Desulfovibrionales	0	0	1	2	0	0	0	1	0
Desulfurellales	0	0	0	0	0	0	0	2	0
Desulfuromonadales	0	0	0	0	1	0	0	0	0

Table F-3 continued.									
Bacterial Orders	**113**	**116**	**118**	**121**	**130**	**136**	**146**	**153**	**156**
Myxococcales	7	10	3	2	2	7	1	10	6
Syntrophobacterales	0	4	1	0	1	0	0	2	2
Campylobacterales	0	0	0	0	0	0	0	1	0
Nautiliales	0	0	0	0	0	0	0	0	0
Aeromonadales	0	1	0	0	0	0	0	0	0
Alteromonadales	0	0	0	0	0	2	1	0	0
Cardiobacteriales	0	0	0	0	0	0	0	0	0
Chromatiales	0	2	1	1	0	2	0	4	0
Enterobacteriales	0	2	3	1	2	0	2	3	4
Legionellales	0	0	1	0	0	0	0	0	0
Methylococcales	0	0	0	0	0	0	0	0	0
Oceanospirillales	0	0	0	0	1	0	0	0	1
Pseudomonadales	9	5	1	0	1	0	0	6	0
Thiotrichales	0	0	1	0	0	0	0	2	0
Vibrionales	0	0	0	0	0	0	1	0	0
Xanthomonadales	11	12	6	2	3	7	3	10	1
Spirochaetales	0	0	0	0	0	0	0	0	0
Synergistales	0	0	0	1	0	0	0	0	0
Thermodesulfobacteriales	0	0	0	0	0	0	0	1	0
TM7 *inc sed.*	0	5	0	0	0	0	0	3	0
Spartobacteria *inc sed.*	0	0	0	0	0	0	0	0	0
Subdivision3 *inc sed.*	0	0	0	0	0	0	0	0	0
Verrucomicrobiales	0	0	0	0	0	0	0	0	0
WS3 *inc sed.*	0	0	0	0	0	0	0	0	0
Gammaproteobacteria *inc sed.*	1	0	0	0	0	0	0	2	0
Unknown	0	0	0	0	1	0	0	0	0

Table F-4. Biotic Environmental Data Sets for Samples 164 through 250.									
Bacterial Orders	**164**	**172**	**186**	**201**	**203**	**227**	**238**	**239**	**250**
Acidobacteria Gp1	0	0	0	0	0	0	0	0	0
Acidobacteria Gp10	0	3	0	1	0	0	0	0	1
Acidobacteria Gp11	1	0	0	0	0	1	0	0	0
Acidobacteria Gp12	0	0	0	0	0	0	0	0	0
Acidobacteria Gp14	0	0	0	0	0	0	0	0	0
Acidobacteria Gp16	0	0	0	0	0	0	0	0	0
Acidobacteria Gp17	0	3	0	0	0	0	0	1	0
Acidobacteria Gp18	0	0	0	0	0	0	0	0	0
Acidobacteria Gp21	1	0	0	0	0	0	0	0	0
Acidobacteria Gp22	0	0	0	0	0	0	0	0	0
Acidobacteria Gp25	1	1	0	0	0	0	0	0	0
Acidobacteria Gp3	0	0	0	0	0	1	0	0	0
Acidobacteria Gp4	0	0	0	0	0	0	0	0	0
Acidobacteria Gp5	0	2	2	1	0	2	0	0	1
Acidobacteria Gp6	12	10	9	10	4	5	4	9	10
Acidobacteria Gp7	0	0	0	0	0	0	0	0	0
Holophagales	0	0	0	0	0	0	0	0	0
Acidimicrobiales	0	4	3	3	4	1	3	3	5
Actinomycetales	25	43	11	17	6	11	19	12	37
Bifidobacteriales	0	0	0	0	0	0	0	0	0
Coriobacteriales	1	2	0	0	2	0	1	0	3
Nitriliruptorales	4	6	2	1	1	3	2	2	9
Rubrobacterales	0	0	0	0	0	0	0	0	0
Solirubrobacterales	0	4	1	1	1	0	4	0	0
Thermoleophilales	0	0	0	1	2	0	0	0	1
Aquificales	0	0	0	0	0	0	0	0	1
Bacteroidetes *inc sed.*	0	0	1	0	0	0	0	0	0
Bacteroidales	0	0	0	0	0	0	0	0	0
Flavobacteriales	0	3	2	2	1	2	0	1	3
Sphingobacteriales	1	7	5	3	0	0	0	2	1
Caldisericales	1	0	0	0	0	0	0	0	0
Chlamydiales	0	0	0	0	0	0	0	0	0
Anaerolineales	0	1	0	0	0	0	0	0	0
Caldilineales	0	0	0	0	0	0	1	0	0
Chloroflexales	0	0	0	0	0	0	0	0	0
Herpetosiphonales	0	0	0	0	0	0	0	0	0
Dehalogenimonas	0	0	0	0	0	0	0	0	0
Sphaerobacterales	0	0	0	0	0	0	0	0	0

Table F-4 continued.									
Bacterial Orders	**164**	**172**	**186**	**201**	**203**	**227**	**238**	**239**	**250**
Thermomicrobiales	0	0	0	0	0	0	0	0	0
Chloroplast	0	0	0	0	0	0	0	0	0
Deferribacterales	0	0	0	0	0	0	1	0	0
Deinococcales	0	0	0	0	0	0	0	0	0
Dictyoglomales	0	0	0	0	0	0	0	0	0
Bacillales	0	2	0	0	0	0	0	0	2
Clostridiales	1	2	1	0	0	0	1	0	2
Halanaerobiales	0	0	0	0	0	0	0	0	0
Natranaerobiales	0	0	0	0	0	0	1	1	0
Thermoanaerobacterales	0	0	0	0	1	0	0	1	2
Erysipelotrichales	0	0	0	0	0	0	0	0	0
Gemmatimonadales	2	0	0	5	0	2	0	0	0
Ktedonobacterales *inc sed.*	0	0	0	0	0	0	0	0	0
Nitrospirales	0	0	0	0	0	0	0	0	0
OP10_*inc sed.*	0	0	0	0	0	0	0	0	0
OP11_*inc sed.*	0	0	0	0	0	0	0	0	0
Planctomycetales	0	2	0	0	0	0	0	0	0
Alphaproteobacteria *inc sed.*	1	6	2	1	0	1	3	0	8
Caulobacterales	9	4	2	3	1	1	0	3	2
Kiloniellales	0	1	0	0	0	0	0	0	0
Kordiimonadales	0	0	0	0	0	0	0	0	0
Rhizobiales	24	33	16	13	3	16	23	15	25
Rhodobacterales	0	0	0	0	1	0	0	0	1
Rhodospirillales	1	6	2	0	3	2	1	1	4
Rickettsiales	0	0	1	0	0	0	0	0	0
Sphingomonadales	9	15	8	8	2	4	3	6	4
Burkholderiales	2	3	1	6	0	0	1	1	0
Hydrogenophilales	1	0	0	0	1	0	0	0	0
Methylophilales	0	0	0	0	0	0	0	0	0
Neisseriales	0	2	0	0	0	0	0	0	0
Nitrosomonadales	0	1	0	1	1	0	0	0	0
Rhodocyclales	1	1	2	2	0	0	0	1	0
Bdellovibrionales	1	0	0	0	0	1	0	0	0
Desulfarculales	0	0	0	0	0	0	0	0	0
Desulfobacterales	1	0	0	1	0	0	0	0	1
Desulfovibrionales	3	3	0	2	0	2	0	1	1
Desulfurellales	0	0	0	0	1	1	0	0	2
Desulfuromonadales	0	0	0	0	0	0	0	0	1

Table F-4 continued.									
Bacterial Orders	**164**	**172**	**186**	**201**	**203**	**227**	**238**	**239**	**250**
Myxococcales	11	8	3	6	2	3	4	2	1
Syntrophobacterales	1	1	0	0	0	1	0	1	2
Campylobacterales	0	1	0	0	0	2	0	0	2
Nautiliales	0	1	0	0	0	0	0	0	0
Aeromonadales	0	0	0	0	1	0	0	0	0
Alteromonadales	0	0	0	0	0	0	2	0	0
Cardiobacteriales	0	0	0	0	0	0	0	0	0
Chromatiales	2	0	1	2	0	0	1	0	0
Enterobacteriales	0	2	0	2	0	1	1	0	4
Legionellales	0	0	0	0	0	0	0	0	0
Methylococcales	0	0	0	0	0	0	0	0	0
Oceanospirillales	1	0	0	0	0	0	0	0	0
Pseudomonadales	2	1	2	4	1	1	1	0	1
Thiotrichales	0	0	0	1	0	0	0	0	0
Vibrionales	0	0	0	0	0	0	0	0	0
Xanthomonadales	0	0	4	0	3	1	4	0	1
Spirochaetales	0	1	0	0	0	0	0	0	0
Synergistales	0	0	0	0	1	0	0	0	0
Thermodesulfobacteriales	2	0	0	0	0	0	0	0	0
TM7 *inc sed.*	0	0	0	0	0	0	0	0	0
Spartobacteria *inc sed.*	0	0	0	0	0	0	0	0	0
Subdivision3 *inc sed.*	0	0	0	0	0	0	0	0	0
Verrucomicrobiales	1	0	0	0	0	0	0	0	0
WS3 *inc sed.*	0	0	0	0	0	0	0	0	0
Gammaproteobacteria *inc sed.*	0	0	0	0	0	0	0	0	0
Unknown	0	0	0	0	1	1	0	1	0

Appendix G:

Abundance of identified bacterial taxonomic orders that contributed to the top 75% of all bacterial orderd identified.

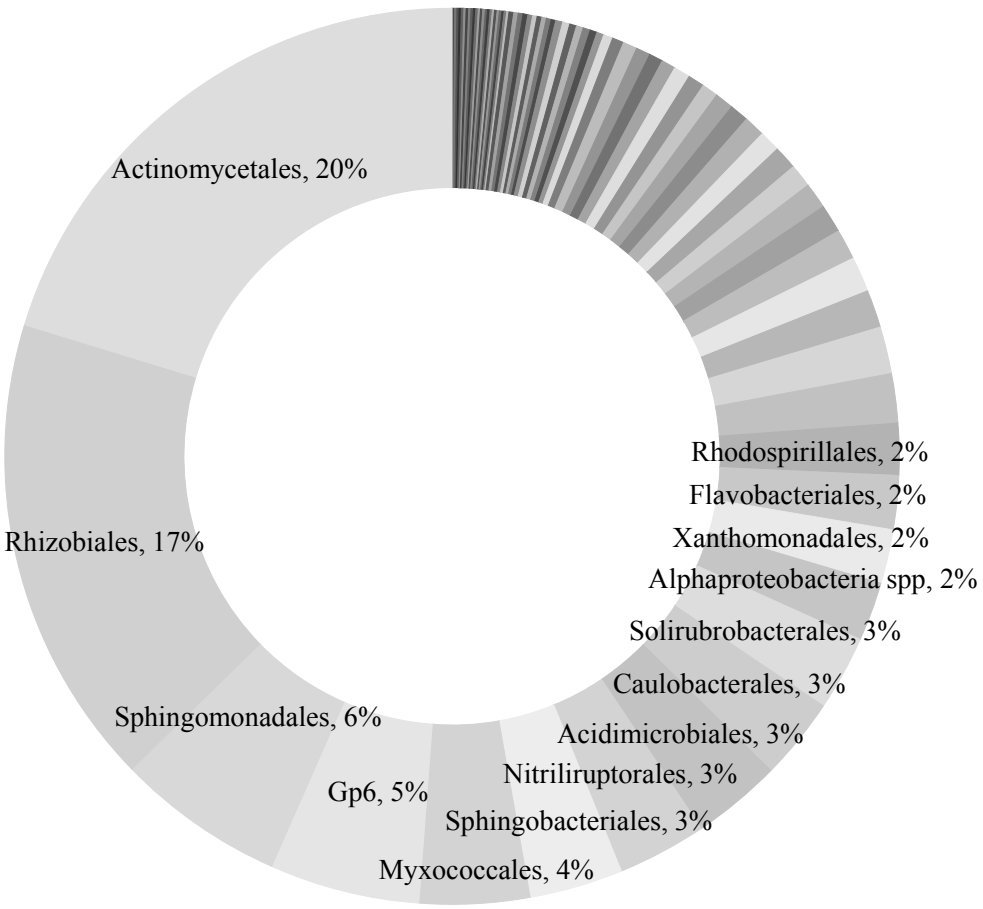

Figure G-1. Abundance chart of identified bacterial orders from ARF samples with no record of human decomposition (None).

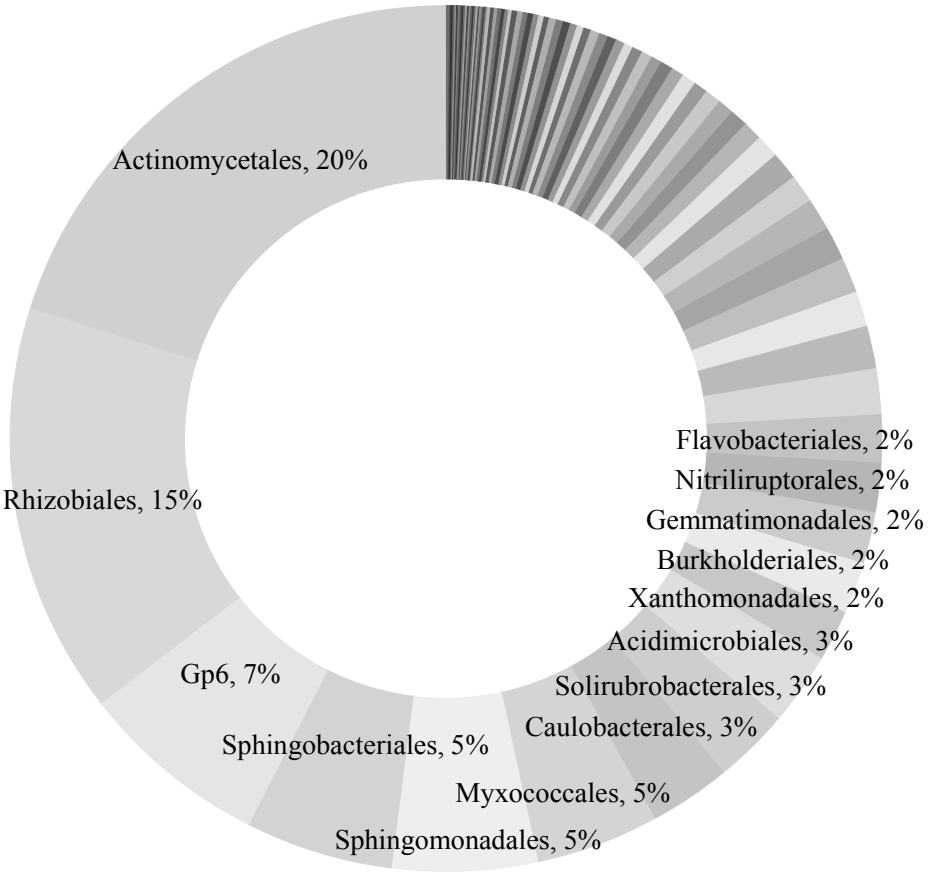

Figure G-2. Abundance chart of identified bacterial orders from ARF samples with low frequency use of human decomposition (Low).

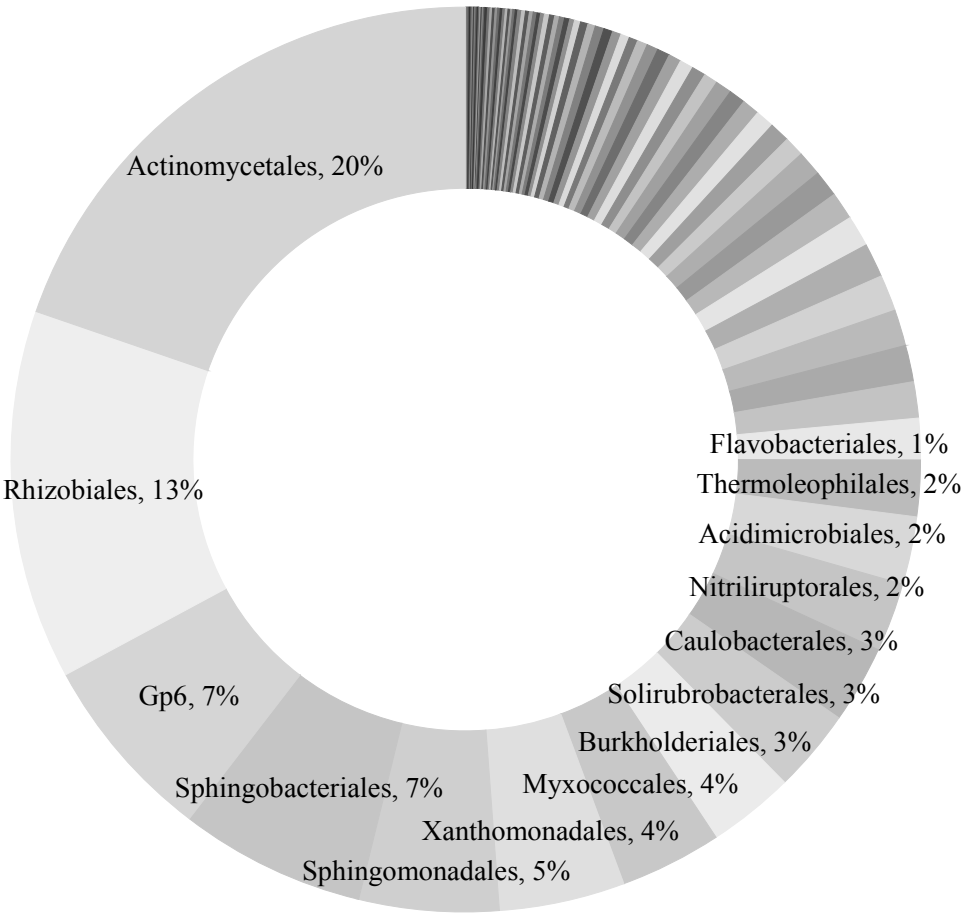

Figure G-3. Abundance chart of identified bacterial orders from ARF samples with medium use for human decomposition (Middle).

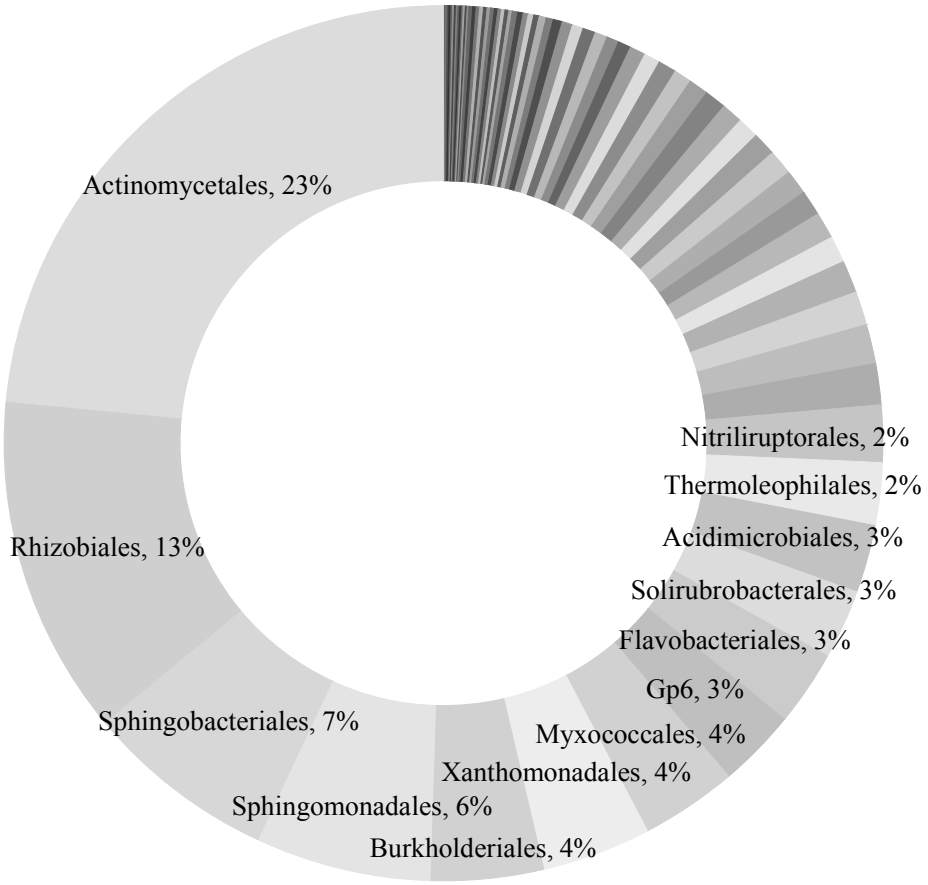

Figure G-4. Abundance chart of identified bacterial orders from ARF samples with medium use for human decomposition (High).

VITA

Franklin Edward Damann was born in Baton Rouge, LA on 20 February 1975, and for better or worse, is a product of public education in Louisiana, graduating from Baton Rouge Magnet High School in 1993. Franklin remained in Baton Rouge and completed his Bachelor of Arts (1998) and Master of Arts (2000) in Anthropology from Louisiana State University. His Master's research investigated the presence of *Mycobacterium leprae* by PCR from skeletal remains of *Dasypus novimcintus* (Nine-banded armadillo). This research was conducted under the direction of Robert Tague and researchers from the Gillis W. Long Hansen's Disease Center in Baton Rouge.

In early March 2001 Franklin accepted a postgraduate fellowship with the Central Identification Laboratory (CIL) and moved to Hawaii to work as a forensic anthropologist. In August 2004, he moved to Knoxville and started the PhD program in the Department of Anthropology at the University of Tennessee. Soon thereafter he moved back to Hawaii and the CIL. In 2007 Franklin returned to the mainland and has since been employed with the Armed Forces Institute of Pathology National Museum of Health and Medicine in Washington, DC.